The Dissertation Committee for Ajay Seth
certifies that this is the approved version of the following dissertation:

A Neuromusculoskeletal Tracking Method for Estimating Muscle Forces in Human Gait from Experimental Movement Data

Committee:

Marcus G. Pandy, Supervisor

Kenneth R. Diller, Supervisor

Lawrence D. Abraham

Jonathan B. Dingwell

David G. Hull

Glenn Y. Masada

A Neuromusculoskeletal Tracking Method for Estimating Muscle Forces in Human Gait from Experimental Movement Data

by

Ajay Seth, B.A.Sc., M.A.Sc.

DISSERTATION

Presented to the Faculty of the Graduate School of

The University of Texas at Austin

in Partial Fulfillment

of the Requirements

for the Degree of

DOCTOR OF PHILOSOPHY

THE UNIVERSITY OF TEXAS AT AUSTIN

May 2007

I dedicate this dissertation to my wife, Olga. I could not have succeeded without her unwavering love and encouragement.

Acknowledgments

I would like to begin by thanking my graduate adviser, Professor Marcus Pandy, for his invitation to work with him at the University of Texas at Austin and his continuous support. I am also indebted to the Biomedical Engineering Department at UT and particularly to Professor Kenneth Diller for graciously taking on a supervisory role and providing additional support during the challenging final stages of this dissertation.

Warm appreciations go out to my dissertation committee: Professors Lawrence Abraham, Jonathan Dingwell, David Hull and Glenn Masada for their patience, accomodating spirit and insightful inquiries. In particular, I would like to recognise Professor Dingwell for taking me under his wing at ISB 2005 and being an invaluable sounding-board in the preparation of this dissertation.

Finally, I have to thank members of the BME department staff, namely: Dr. Jack Hart, Heidi Fagerlund, Joni Burks, Majid Vadiei and Maggi Fitch who were invaluable in navigating the bureaucratic 'red tape'. Your kindness and thoughtfulness does not go unnoticed.

A Neuromusculoskeletal Tracking Method for Estimating Muscle Forces in Human Gait from Experimental Movement Data

Publication No. _____

Ajay Seth, Ph.D.

The University of Texas at Austin, 2007

Supervisors: Marcus G. Pandy
Kenneth R. Diller

The research results contained in this dissertation relate to a novel approach to estimating individual muscle forces in human movement by exploiting typical experimental observations acquired in movement laboratories. A neuromusculoskeletal model is made to move as observed and exert the same forces on the environment as recorded in the laboratory. Electrical activity of muscles can also be used to guide the solution process such that in the end, the muscle activity of the model is in better agreement with these recordings while still producing the desired movement.

The innovation of this process is the efficient combination of inverse and forward analysis techniques. These classical techniques combined with nonlinear control theory form the basis of a neuromusculoskeletal tracking methodology for systematically replicating human performance in a computer model. The purpose is to capitalize on the non-invasive nature of this methodology to extract internal information about muscle forces and subsequent bone and soft-tissue loads during human movement. This information is sought by orthopedic surgeons and movement scientists alike in order to determine the function of individual muscles and to understand what interventions/treatments may be the most effective at restoring function and comfort to their patients.

This treatise has accomplished three primary objectives: 1) it provides the detailed development of a non-invasive method for estimating muscle forces that includes complete system dynamics and is

computationally tractable; 2) performs a benchmark analysis to validate the increased accuracy and computational advantages of the tracking approach, and 3) applies neuromusculoskeletal tracking to one of the most challenging problems in biomechanics, which is human gait simulation and analysis.

In reaching these objectives four principle findings were made. 1) Tracking has provided results that are superior to previous dynamic optimization methods and at 3 to 4 orders of magnitude savings in computational costs, with the relative savings increasing with model complexity. 2) When random and systematic error/noise is present in kinematic data (due to skin movement, sampling, environmental interference, and data processing techniques), then ground reaction forces are better predictors of the true movement of the system. Under these circumstances, closely tracking experimentally estimated model kinematics is insufficient to demonstrate movement accuracy and ground reaction forces must be closely duplicated to indicate accuracy. 3) Because of its relative speed, neuromusculoskeletal tracking has proven to be a powerful validation tool since poor results or even tracking failure occurs if the model is not adequately representative of the subject data. Therefore, models must be evolved until the desired accuracy is obtained. 4) Controller weightings can further improve simulation accuracy by tracking certain reference data (such as ground reaction forces) more closely than others (i.e. motion of the toes). However, obtaining the set of weightings that balance tracking accuracy across multiple references is not a trivial task especially when there are a large number of reference signals to consider. Although improvements in tracking accuracy can be obtained by the optimization of weightings, they may not justify the high computational cost.

Table of Contents

List of Figures

List of Tables

Chapter 1

Introduction

Accurate knowledge of muscle forces is essential for understanding muscle function and for determining skeletal loading during human movement. Direct recording of muscle forces *in vivo* is currently infeasible, and so measurements of body-segment kinematics, ground reaction forces, and muscle activity are often used, in conjunction with mathematical models, to estimate muscle forces non-invasively (*Pandy* (2001)).

The application of general physical principles results in tremendous complexity such that, until recently, it was a formidable task to evaluate or even formulate the equations resulting from Newton's laws of motion for systems having more than a couple of joints and a few actuators. That, however, is rapidly changing thanks mainly to computer modeling tools (SIMM-DynamicPipeline, SD/Fast, ADAMS, Pro-Engineer, etc...) which can automatically generate and solve the equations-of-motion for systems with arbitrary numbers of segments, joints and actuators. In fact, the specific kinematic constraints, such as the knee joint, can readily be implemented so that models can mimic the motion of these joints that have been shown to translate and are not simple hinges (*Freeman and Pinskerova* (2005)). Similarly complex muscle paths can be specified to mimic the musculoskeletal geometry of individual patients from MRI and advances in ultrasound imaging (*Huang et al.* (2005)).

The fundamental question that still remains for these models to be of clinical utility, however, is how will they be controlled? That is, how to actuate these models via net joint moments (i.e. torques) or muscle generated forces such that they do something useful. At this point it is not model fidelity/complexity that is the limiting factor - it is systematically controlling these models to make them

do what we want. What we want is to replicate human performance with the model so that we can "poke and prod" the model for internal loads due to muscles and movement without requiring any invasive procedures for the subject. Ultimately, we wish to predict the outcome of treatment and intervention on patient performance using these models. Towards this end, a powerful approach emerged over a decade ago that employed optimization to vary the signals to individual muscles until the model minimized a performance based index (*Pandy et al.* (1992)). This approach was based on a robust methodology for solving nonlinear optimal control problems in general (*Goh and Teo* (1988)). Although this approach has been successful at replicating the salient features of gait (*Anderson and Pandy* (2001a);*Neptune et al.* (2001)) large-scale optimization has one major limitation: it requires vast computational resources in terms of facilities and/or time. Either supercomputers must be employed (*Anderson and Pandy* (2001a)) or control parametrization must be grossly oversimplified (i.e. common drive to multiple muscles and on-off control,*Neptune et al.* (2001)) in which case solutions still required many days to several months. In both cases it was impossible to show that convergence was achieved and their simulations did not closely replicate individual subject performance, particularly with respect to ground reaction forces. Earlier approaches based on inverse dynamics from the kinematics and ground reaction forces in the laboratory are generally discounted for providing inaccurate joint torques (see review, *Zajac et al.* (2003)). Furthermore, static optimization techniques used to estimate muscle forces from the results of inverse dynamics have been criticized for lacking dynamics representing muscle physiology and for not being able to optimize a performance index that spans the entire performance period. Despite these criticisms, inverse dynamics and static optimization remain widely used particularly in clinical applications (e.g. *van Drongelen et al.* (2006); *Favre et al.* (2005); *Granata et al.* (2005); *Heller et al.* (2001)) primarily because it remains the most time-effective means of getting quantitative muscle force data from patient performance.

The obvious question, which is at the core of this dissertation, is whether we can combine the accuracy of synthesis from forward dynamics with the efficiency of inverse dynamics and static

optimization? The advantage of the inverse approach is that it utilizes the experimental data directly, so no search is required for a viable solution, which is the bulk of the cost of using forward dynamics via optimization methods. Are there not similar problems where dynamical systems are required to produce a desired behavior? Posed this way it becomes clear that manufacturing and control systems engineers have been solving similar problems to make manipulators follow optimal paths (*Bobrow et al.* (1985)) or to control airplanes on autopilot. The methods in these examples may not be predictive, but they could allow us to utilize more realistic dynamical models of the human neuromusculoskeletal system to reproduce human performance as observed in a motion laboratory, without employing exhaustive search techniques.

1.1 Specific Aims

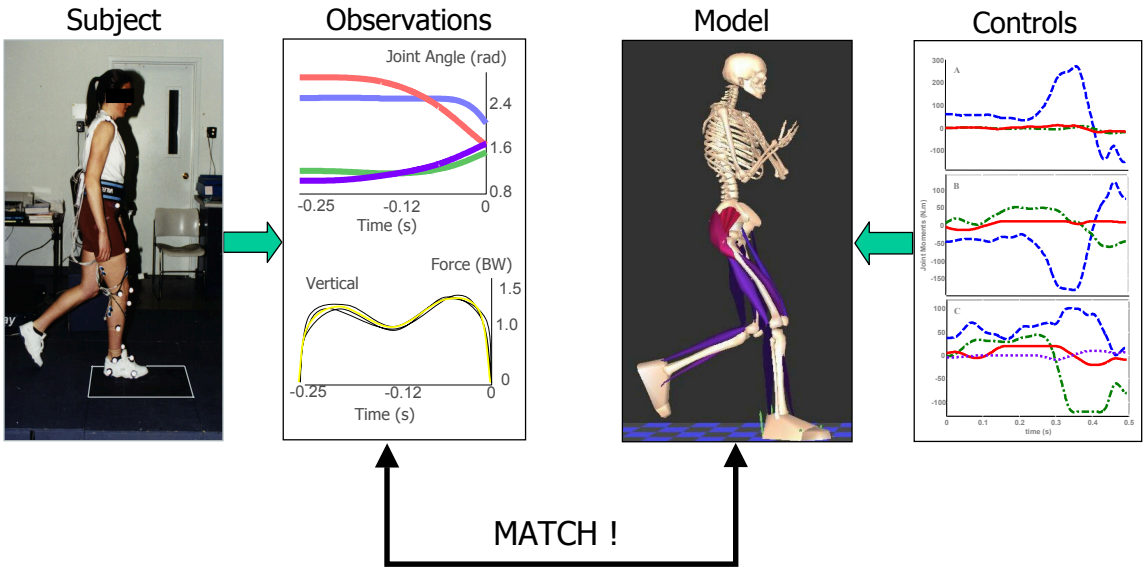

Figure 1.1: Primary objective of dissertation research.
Schematic of the primary dissertation objective to control musculoskeletal models such that the performance of the model matches that of the subject.

Although simple models have their place in our understanding of biomechanics, both *Pandy* (2003) and *Zajac et al.* (2004) caution that simple models lacking adequate degrees of freedom and

muscle actuators may in fact provide misleading results. It is essential that a suitable model replicate the observed performance of an individual subject/patient before the model can be trusted to explain the movement behavior of that patient. The primary objective is to replicate complex coordinated human movements such as gait using computer models (Fig. 1.1). It is unrealistic, however, to expect a model with rigid segments, mechanistic joints, approximated ground contact dynamics and simplified muscle representations, etc... to be identical to human performance in every respect. Therefore, the purpose of this dissertation is to develop a new method that yields forward simulations of human movement that are closer to subject performance than is currently possible, without prohibitive computational costs. With this in mind, three specific aims were set forth:

1. Combine forward and inverse techniques into a single computationally efficient method- a neuromusculoskeletal tracking (NMT) method to dynamically determine individual muscle forces from human movement data

2. Perform a comparison of the NMT method against forward and inverse dynamics methods using maximum height jumping as the benchmark task

3. Apply the NMT method to quantify individual muscle forces in human gait from a forward dynamics musculoskeletal model scaled to an individual subject, by tracking experimental gait data collected from the same subject

1.2 Dissertation Overview

This dissertation is divided into four parts which discuss the goals of musculoskeletal modeling in general and the three specific aims of this work. We begin with some background on the problem of estimating human kinetics using musculoskeletal models and include the motivation for the present research in the context of current and previous approaches (Chapter 2). The second part describes a novel neuromusculoskeletal tracking methodology for human motion analysis that includes the synthesis

of ground contact forces and the dynamic distribution of muscle forces using common neuromuscular models (Chapter 3). The third part targets the validity of the NMT approach by comparing its solution with both the inverse dynamics and forward dynamics methods using a dynamic optimization solution as a benchmark. The same model is then used to track maximum height jumping using experimental subject data collected in a motion capture laboratory. Combined they provide the proof of concept for the efficacy of the NMT method (Chapter 4). The fourth part addresses the practical application of the NMT method for the analysis of human gait (Chapter 5). Additional adaptations to the NMT method necessary to track gait data are provided and the results of tracking human gait are presented.

Chapter 2

Background

2.1 Motivation

Walking is an incredibly important part of an individual's sense of well-being, independence and ability to interact with the world around them on a day to day basis. Unfortunately, the proportion of the population suffering from some form of mobility loss is increasing significantly in keeping pace with an aging population (*Stalenhoef et al.* (2002)). Over 30% of all unintentional deaths in the elderly (65+yrs) in 2000 were a result of accidental falls (*injury report forms* (2000)). Furthermore, sedentary lifestyles are contributing increasingly to adult onset diabetes (with 13-49% increase in rheumatologic manifestations over normal (*Crispin and Alcocer-Varela* (2003)), hypertension, obesity and frailty which all have deleterious consequences on locomotor performance. Factoring gross increases in motor vehicle and recreational accidents as well as the increasing rates of survivability from severe injuries and chronic diseases, a significant proportion of the population suffers some form of gait disorder.

Consequently, the study and understanding of locomotor performance is vital in developing regimens and treatments to prevent and remedy these disorders. Unlike the study of physics, chemistry or mathematics, however, the study of human movement is not only much younger, but it lies on the boundary of many of these traditional disciplines. As a result, generalized laws of human motion do not yet exist even though one realizes that the human system must obey physical laws. The application of general physical principles results in tremendous complexity such that, until recently, it was a formidable task to evaluate or even formulate the equations resulting from Newton's laws of motion for systems having more than a couple of joints and a few muscles. Although applying physical laws would provide models that could test cause and effect relationships, the difficulty of doing so has lead

us to focus mainly on observation and expert knowledge for understanding and treating gait disorders. Naturally, those dealing with actual patients, namely clinicians, have come to rely heavily on observation and adopt case-based methods as the primary tool for assessment and prescription of treatment. A collection of observational methods and movement reconstruction techniques are the basis of gait analysis today. These data are complimentary to physical assessment (providing anthropometry, tissue health, identifying inflammation, etc...) and patient interviews (identify regions of pain/numbness and level of performance). What is desperately required are the analytical tools that can provide quantitative information about performance particularly of internal loads due to muscles.

2.1.1 Gait Analysis

Gait analysis includes observations from kinematic markers that locate the position of key landmarks (such as bony processes, spines, estimates of joint centers and segment/system center of mass (COM) locations) as they move in time and space. In addition, force plate data yields information about the interaction kinetics of the body and environment, which is the amount of force (magnitude and in what direction) the body imparts on the ground and how the ground reacts to accelerate the body. Finally, electromyography (EMG) is used to detect the electrical activity, of select muscles, at surface or indwelling (needle) electrode sites. Electrical activity is detectable in or on muscles as a result of the summation of action potentials from individually depolarizing muscle fibers, which leads to their contraction and ultimately to muscle tension production (*Duchene and Goubel* (1993)). Marker kinematics, force plate and muscle EMG are sampled and recorded on a computer simultaneously in the gait analysis laboratory. This provides a record for a subject or patient that describes: 1) the motion of the limb segments and the whole body COM, 2) the net system-environment kinetics resulting in the acceleration of the COM and 3) electrical activity of a subset of muscles involved in producing those kinetics. A more complete review of the data collection technology is provided by *Lee and Pollo* (2001). These data are compared explicitly (via statistical correlation/confidence) to nominal data sets or implicitly by the

expertise of the clinician. Clinicians are expert experimentalists who have developed their own internal rule systems through years of training and experience with numerous patterns of these data, in order to correlate features of observed patient performance with specific disorders as well as possible treatments.

In fact, much of the clinical evaluation of gait function is based on keen observations made fifty years ago. *Saunders et al.* (1953) defined six determinants of human gait, which transformed a conceptual model of compass gait (two straight legs pinned together to form a hip) into a multi-articular coordinated and fluid movement that is observed in normal human gait. They described the determinants as necessary adaptations in order to produce an energy efficient upright bipedal gait, in which each determinant played a role in increasing "efficiency" by smoothing out the trajectory of the whole body COM. They suggested that vertical motion of the COM contributes to inefficiency due to the work necessary to repeatedly lift it against gravity. Thus, they equated vertical and lateral excursions with greater metabolic cost and were the first to hypothesize that energy is a quantity that is minimized effectively in normal human gait.

In contrast, models from 1939 to the present day have gradually shown that these determinants do not effectively reduce the vertical travel of the COM and that some vertical motion of the COM is, in fact, more efficient when considering the mechanics of the system interacting with its environment. Briefly, the COM rise first helps to decelerate the body at mid stance and enables the swing leg to swing forward, and subsequently the COM lowers transforming potential to kinetic energy that translates the COM forward onto the now heel striking leg (previously the swing leg) (*Elftman* (1939)). This interplay of kinetic and potential energy transfer is an important feature of human gait, which is ignored by the classical "determinants" of gait. Current models (*Croce et al.* (2001);*Gard and Childress* (1997)) show that these determinants are intriguing observations rather than the basis for human locomotion. They present a case that the determinants have more practical implications for avoiding the scuffing of the swing leg and provide the necessary mechanical degrees-of-freedom to produce clearance over a

variety of surfaces and potential obstacles. *Kerrigan* (2001) suggests that there is some confusion today between the function and the aesthetics (fluidity and apparent ease) of walking especially in the clinical assessment of gait.

In spite of the limitations of observation-based analyses, gait analysis is an influential tool in the decision making process for clinicians and surgeons. Having the same surgeon performing pre and post analyses per patient-case, a recent study by *Cook et al.* (2003), found gait analysis altered the decision in 40% of the cases in the type or level of operation recommended after clinical gait assessment. This study strongly demonstrates how the availability of additional information takes precedence over the intuition of the surgeon (or clinician) in making critical decisions. Even so, interpretation of analysis data and their relative importance differs significantly between practitioners based on their training and expertise. Specifically, *Watelain et al.* (2003) observed a diverse group of practitioners studying the same group of hemiplegia patients. They found that: 1) neurologists always tried to localize lesions (i.e. identify region of nerve damage) in the spinal cord and used data to enforce or refute candidate locations of a lesion, 2) physical and rehabilitation medicine specialists relied heavily on quantitative assessment via biomechanical analysis (kinematics and kinetic abnormalities) to assert the effectiveness of intervention, and 3) physiotherapists were qualitatively the most descriptive, relying heavily on physical assessment results over gait analysis data and manually identified muscles and joints affected in order to define the degree of functional loss and to recommend therapies they felt would minimize additional losses. For the most part, the varying assessments were complimentary and reflect the multiple facets of the disorder, but there were also more than a few contradictions about which muscles were affected, especially for muscles where no electromyographical data was available. Second, there were discrepancies as to what some muscles were or were not doing, which affected lesion location decisions and assistive recommendations alike. Interestingly, physical assessment was the deciding factor in these cases, basing muscle function on anatomical position and voluntary contractions.

It can be gathered from the discussion thus far that current clinical gait assessment is both necessary and uncertain in providing information to treat gait disorders. Uncertainty is due to the ambiguity between function and kinematics, where features of the latter have been imbedded as "determinants" in gait assessments over the last 50 years. Supplying multiple (physiological, neurological and mechanical) interpretations does not appear to contribute significantly to the indecision. The indecision arises from a lack of information upon which to make definitive conclusions, especially about muscle function. Models are providing the tools to test and define the boundaries between form and function and are forcing a reassessment of the classifications of gait function in general. However, it has been difficult to obtain information from models that clinical practitioners could use to effectively diagnose and treat individual patients.

The synthesis of gait using mathematical/computer models to elucidate how the human motor system actuates the body has had a rapidly evolving history from the control of double pendulum legs with prescribed pelvis trajectory and ground reaction forces (*Chow and Jacobson* (1971)) to a single mass autonomous body with massless legs (*Townsend and Seireg* (1972)) to multi-body models used to predict ground reaction forces during particular phases of the gait cycle (*Pandy and Berme* (1988a)). It is only more recently, however, due mainly to the availability of computing resources and automated formulation of multi-body dynamics that more highly articulated and realistic models have developed that have also included muscle actuators (*Davy and Audu* (1987); *Bobbert and van Ingen-Schenau* (1988); *Anderson and Pandy* (2001a); *Neptune et al.* (2001)). In this regard the computer modeling framework for bone segments and musculoskeletal geometry (*Delp and Loan* (1995)) from cadaveric specimen digitizing (*Delp* (1990)) and *in vivo* imaging (*Osborne et al.* (1995)) has been and will continue to be invaluable.

Quantifying individual muscle forces from patient specific models (i.e. using imaging to model techniques) would go a long way in demystifying muscle coordination and function during gait. It would, in effect, provide a common thread between practitioners because muscle function is a direct consequence

of neural stimulation and thus can be used to localize or test hypotheses about lesions; it can be used to explain why net joint torques (and thus kinematics) are abnormal, and, finally, it can either support or contradict the qualitative description of muscles and joint tissues that are physically assessed to be affected. The question is not whether that data will be useful, but how to systematically and accurately extract muscle information from increasingly more sophisticated models.

2.2 Methods to Quantify Muscle Forces

The determination of muscle forces has been an area of active research with two principle approaches: electromyography and biomechanical modeling. First, those dealing directly with patients having gait disorders, such as physiotherapists, neurologists and clinical biomechanists, rely on clinical gait assessment methods (described earlier), which include video (marker positions), force-plate and electromyography (EMG) as the primary "views" of patient performance. The EMG of a selected muscle does elucidate (electrically at least) the role a muscle plays especially relative to other participating muscles. The limitations of this approach are that there is an insufficient number of surface muscles that can be detected reliably given the varying anatomy of muscles and adipose tissue composition of different individuals (*Duchene and Goubel* (1993)). Besides the fact that indwelling electrodes are very invasive, these electrodes are much more localized thereby reflecting the activation of a few fibers in close proximity of the needle electrode and may not reflect the total level of muscle activity (*G.Rau et al.* (2004)). Furthermore, quantifying the contribution of a muscle from its EMG in terms of force is tenuous since the total activation of the muscle is not obtainable, and even the local measure can vary based on electrode positioning and contact quality. Even if EMG were reliable and representative of total muscle activity, the effects of electromechanical delay, muscle length and muscle contraction velocity on force production would still have to be accounted for before drawing any conclusions about muscle force (*Patla et al.* (1982); *Duchene and Goubel* (1993)). Furthermore, the contribution of a muscle to coordinate movement of the body would remain elusive due to the complex interactions of articulated

multi-body systems known as dynamic coupling (*Zajac and Gordon* (1989)). Because of these difficulties, biomechanical models have come to the forefront in human performance research, specifically to target what is going on inside the body to produce observed performances.

Biomechanical models use the principles of mechanics to describe the multi-body dynamics of articulating rigid bodies analogous to joints and bones, the deformation of tissue within and surrounding a joint as well as the properties of muscles as nonlinear actuators. These elements are combined to replicate through simulation the movements/behavior observed *in vivo*. These models provide the advantage of systematic repeatability, enabling hypothesis testing and answers to "what if?" scenarios. Moreover, they are perfectly observable in that every aspect of the model's performance is directly known or can be calculated unlike its human counterpart where muscle forces are not directly measurable.

2.2.1 Inverse and Forward Dynamics

Biomechanical models can be categorized into inverse dynamics and forward dynamics models. Inverse dynamics refers to the solution of algebraic equations for the joint torques (forces) that result from the substitution of system kinematics (positions, velocities and accelerations estimated from observations) into the equations of motion. Forward dynamics is the application of forces (or torques) to evaluate the instantaneous acceleration of the system, in which case the equations of motion describe a set of ordinary differential equations. Integrating the second order system forward in time yields the velocity and positions of system coordinates (angles, translations) throughout the performance period to generate a forward (in time) simulation of human performance.

An inverse dynamics technique that does not require the system equations of motion to be described explicitly is a link segment analysis that only requires the applied forces at any end of the linkage (series of segments interconnected by joints) to be known and uses Newton-Euler formulations to evaluate internal forces and moments sequentially through the linkage, away from the known end, until all forces are evaluated (*Bresler and Frankel* (1950); *Winter* (1990);*Hof* (1992)). Unfortunately, inverse

dynamics alone can only be used to determine the actuating torques (forces) per degree-of-freedom that produced the observed motion. An additional decomposition scheme is required in order to decompose these torques into individual muscle forces, since multiple muscles have their forces contributing to the net muscle dependent torque about the joints that they span.

Typically, an inverse dynamics model that determines the net joint torques (due to muscles) from observed kinematics (i.e. from a link-segment analysis) fails to drive the system to replicate those kinematics when the torques are applied to an equivalent forward model. Since torques from direct inverse dynamics do not provide the proper actuation, any decomposition of these torques will inherit this inaccuracy. It has been shown that torques calculated by the double differentiation of sampled positions suffer from two distinct problems. The first is due to discrete sampling of kinematic data such that even if the accelerations are accurate (i.e. determined directly from a forward model), applying sampled (discrete) torques will not replicate the performance of continuous torques, unless sufficient dimensionality is restored by adequate interpolation of the discrete torques (*Risher et al.* (1997)). The second and more significant problem is based on the quality of the position data that includes the effects of non-rigid movement of skin and underlying non rigid tissues such as muscles and tendons, which have been shown to have considerable effects on movement estimates (*Reinbolt et al.* (2005); *Sangeux et al.* (2006); *Benoit et al.* (2006)). This adds a systematic noise component to the position recording and can result in configurations that are either impossible for the rigid model to attain or require very large velocities and accelerations to satisfy the transitions from one observed state to the next. Although low-pass filtering is useful at removing higher frequency "chatter", it cannot remove skin deflections that are synchronized with the movement, which are arguably greater in magnitude than random movement noise. This error in positions is amplified by differentiation techniques to produce observed velocities and further exacerbated by double differentiation to produce system accelerations. The inconsistency in the dynamic equations occurs when accelerations of the center of mass (COM) are not identical to those evaluated from the total (external) ground reaction forces. Given the inaccuracies in the position

data, it is difficult to imagine any real case where these two evaluations of COM acceleration would be equivalent.

An alternative to the link-segment/recursive solution to the inverse dynamics problem, is to recognize that both accelerations and ground reaction forces contribute to the torque computations simultaneously and that the inverse system of equations for system torques is, in fact, over-determined. That is, there are more joint acceleration and ground reaction force inputs to the inverse dynamics problem than torque outputs. That is why the recursive approach results in residual forces- to decouple the ground reaction forces from the angular accelerations. Therefore, a pseudo-inverse method can be applied to solve the problem in a least-squares sense and assigning individual acceleration and ground reaction force inputs different weightings. When weightings are related to their measurement error *Kuo* (1998) demonstrated up to a 30% reduction in torque estimate error over typical Newton-Euler formulations across varying noise and bias errors.

A forward model simply means that the multi-body system and muscle model dynamics (when included) are integrated simultaneously forward in time to produce a simulation. Forward simulation models are widely considered more accurate in predicting joint torques (*Chow and Jacobson* (1971)) and muscle forces (*Pandy* (2001); *Zajac et al.* (2003)) because they must synthesize the motion according to known (or hypothesized) dynamics. The synthesis models discussed earlier (*Chow and Jacobson* (1971); *Townsend and Seireg* (1972); *Pandy and Berme* (1988a); *Davy and Audu* (1987) ...) are all examples of early forward dynamics models where the motion is synthesized via the forward integration of the equations of motion. In particular, musculoskeletal model estimated muscle forces must satisfy excitation-to-activation dynamics, force-length, and force-velocity characteristics of physiological muscles in actuating the forward model (*Davy and Audu* (1987); *Bobbert and van Ingen-Schenau* (1988); *Pandy et al.* (1990); *Anderson and Pandy* (2001a); *Kaplan and Heegard* (2001); *Neptune et al.* (2001); *Jonkers et al.* (2002); *Buchanan et al.* (2004)). Therefore, these models will be dynamically constrained from

exhibiting unrealistic changes in muscle forces and from exceeding a muscles capacity to produce force at various lengths and contraction speeds.

On their own, both inverse and forward dynamic models are unable to provide information about individual muscle forces and require optimization to either optimally decompose joint moments from inverse dynamics into muscle forces, or to determine the set of inputs to muscle models to synthesize motion in a forward dynamics model.

2.2.2 Static Optimization

Because there are redundant actuators in the sense that there are more muscles spanning a joint then degrees-of-freedom of the joint, torques from an inverse dynamics analysis cannot be directly decomposed into their constituent muscle contributions. Consequently, the necessary forces to generate the torques are distributed amongst individual muscles in an optimal way. That is, at a given instant with known muscle moment-arms, the muscle forces generate the necessary torque and minimize a cost function involving the muscle forces. Static optimization refers to the fact that the optimization is for a single instant in time independent of any other instant because there are no dynamic (time-dependent) effects being modeled. For example forces can go from near maximal in one instant and in the next produce very little force, although this could not happen in reality because muscle activation decays gradually according to a deactivation time constant (*Zajac* (1989)).

The most common approaches are to minimize a function of total muscle force (*Penrod et al.* (1974); *Pedotti et al.* (1978)) or muscle stress (muscle force over its cross-sectional area) or some exponent (i.e. quadratic) thereof (*Crowninshield and Brand* (1981)) at each instant. The drawbacks to this approach are that it relies heavily on the accuracy of the observed kinematics implicit in inverse dynamics; it neglects muscle activation and contraction dynamics, and performance indices evaluated over the entire performance period (such as total effort or metabolic energy consumption) cannot be applied. The main advantage is that estimates of muscle forces (with virtually an unrestricted number) from a model can be

determined in a relatively short amount of time (i.e. often in minutes), which is appropriate for clinical applications.

The pseudo-inverse approach to inverse dynamics can also be applied to map muscle forces directly to system accelerations (*Yamaguchi et al.* (1995)) for the purpose of generating a forward simulation. In this case, each muscle's induced acceleration resulting from a unit of stress is used to determine the amount of muscle force to generate the desire system acceleration (not torques) which are then integrated forward in time. The unknowns at each time step are the relative amount of stress assigned to each muscle to achieve the measured accelerations directly. At each instant the sum of squared muscle stresses is minimized. Although computationally efficient and producing a multi-body forward dynamics simulation, it remains limited to the square of muscle stresses as a static performance index, cannot include muscle dynamics, and has no way of dealing with the synthesis of ground reaction forces in the forward simulation.

2.2.3 Dynamic Optimization

The problem, therefore, becomes one of determining either the muscle excitations necessary to control the muscle models or the joint torques directly that in turn drive the musculoskeletal model to synthesize the desired motion. The most direct approach is solve an optimal control problem that determines the controls that minimize a performance index relating the output of the forward model with some desired behavior.

Unfortunately, the nonlinear multi-body dynamics as well as the nonlinearities in musculotendinous mechanics result in a highly nonlinear optimal control problem that cannot, in general, be solved analytically using optimal control theory. Rather, the dynamic optimal control problem is recast using some form of control parameterization (*Goh and Teo* (1988)) to find the optimal controls.

2.2.3.1 Large-Scale Parameter Optimization

Large-scale parameter optimization is a general method for solving optimal control problems with arbitrary dynamics and constraints (*Pandy et al.* (1992)). Specifically, system dynamics (constraints of the optimal control problem) are implicitly satisfied by performing a forward simulation (integration) to evaluate a performance index. Controls are discretized and the nodal values (at the discrete times) become the parameters to be optimized.

Performance indices can be any function of any of the variables of the musculoskeletal system such as metabolic energy (as hypothesized in walking, *Saunders et al.* (1953); *Chow and Jacobson* (1971); *Waters and Mulroy* (1999);*Anderson and Pandy* (2001a)) or some combination of criteria, which may include minimizing the differences with experimentally observed data (*Neptune et al.* (2001); *Higginson et al.* (2006)). We see in the first case, in particular, the powerful ability to predict human movement according to an overriding perhaps evolutionary goal. In the latter case, the minimization of differences between model and experiment attempts to obtain increased simulation accuracy with respect to a known performance by posing the inverse problem as a dynamic optimization problem.

Parameter optimization problems can be solved using a variety of search techniques. Derivative based methods are the most computationally efficient and rely on the variation of the performance index with respect to the control parameters to descend upon the minimum. Curvature information also provides information about convergence to a minimum (opposed to a local max or a saddle point). A well established derivative based method is sequential quadratic programming (SQP, *Powell* (1978); *Storen and Hertzberg* (1995)) which approximates the objective function surface along the gradient by a quadratic using a second order Taylor series expansion. The SQP algorithm has been readily employed in solving the dynamic optimization problem as describe by*Pandy et al.* (1992) to predict the performance of a musculoskeletal model to meet a specific performance objective such as minimizing metabolic energy (*Anderson and Pandy* (2001a); *Davy and Audu* (1987)) or to maximize jump height (*Anderson and*

Pandy (1999); *Bobbert and van Ingen-Schenau* (1988); *Pandy et al.* (1990)).

A major difficulty in employing derivative based methods is that they can only to descend into the minimum along the steepest path without knowing if the minimum which it has reached is in fact the global minimum. Therefore, the starting point on the objective surface, determined by an initial guess at the controls, is critical to finding the global solution. Due to the nonlinear dynamics, the probability of local minima are high, and an initial guess must be along a direct ascent from the global minimum to insure that the minimum is reached. Because of the sensitivity to initial conditions and the difficult task of determining a feasible set of initial controls, the use of stochastic methods have increased in popularity.

Neptune et al. (2001); *Higginson et al.* (2006) have employed a simulated annealing algorithm (*Ingber* (1993)) which includes stochastic processes that permits the current configuration (set of parameters) to increase in energy (cost), based on a probabilistic distribution, in order to cool to an even lower energy state, which parallels the slow cooling of molten material (rock, steel) that enables the formation of large highly organized lattices (crystalline structure) in the resultant solid. Similarly, a genetic algorithm (GA) optimization can be employed, which uses evolutionary principles of survival of the fittest, genetic recombination and random mutation to evolve a population of solutions until it is dominated by a single solution (genetic sequence) (*Holland* (1992)). Because of its exploratory nature, the GA is able of finding the globally optimal solution with greater reliability (*Srinivas and Patnaik* (1994)), which has been demonstrated to hold true for difficult musculoskeletal control problems in biomechanics (*Seth* (2000);*van Soest and Casius* (2003)). In particular, *Seth* (2000) formulated and applied a hybrid GA-SQP to predict the optimal muscle controls in human upper-limb tasks, with greater computational efficiency obtained by the maturation of chromosomes (solution) through multiple SQP iterations which exploits locally smooth regions of the objective surface.

These and other approaches that introduce random perturbations in solutions are much less

likely to converge to the nearest local minimum and therefore are, in general, more robust than gradient methods. However, the computing costs are also much larger, since surface curvature information is not as readily exploited for the sake of more exploratory behavior. Although this may not be the case if costly external numerical differentiation is required in a gradient based approach (*Anderson and Pandy* (2001a)). Because the search space is proportional to the power of the number of design variables, reducing the set of control parameters is often necessary to obtain solutions in tractable time. For example, *Neptune et al.* (2001) parameterize muscle controls by on and off times only, thus only requiring $2m$ parameters for m muscles, opposed to $2nm$ parameters, if n time nodes were used to discretize the controls.

Even applying efficient gradient based methods with good initial guesses, which are the nodal values at discrete time intervals for each muscle, dynamic optimization requires an enormous amount of computing capacity if analytical gradients are unavailable. For example, three months of computing on a parallel processing super-computer (*Anderson and Pandy* (2001a)) was required to reach a viable solution (where convergence was not established) given a good initial guess. Albeit the model was highly complex and comparable to human capabilities, in terms of the number of joints (23 degrees of freedom), number of muscles (54 musculotendinous actuators), ground contact interaction and the influence of ligaments. Nonetheless, months of super-computing is impractical for synthesizing the performance of a single patient in a clinical setting.

2.2.3.2 An Optimal Muscle Control Sub-problem

A major source of musculoskeletal system nonlinearities is a result of the multi-body dynamics and the nonlinear coupling of actuator forces to the acceleration of all degrees of freedom by virtue of the the mass matrix (in the typical joint formulation of multi-body dynamics, 3.4). Therefore, theoretically it is not unreasonable to decouple the muscle control problem from the multi-body dynamics problem similar to the two step inverse dynamics and static optimization approach.

To confront the criticism of the static optimization method in tandem with the inverse approach, *Menegaldo et al.* (2006) defined an optimal muscle control sub-problem that included activation and contraction dynamics and used parameter optimization to solve for discretized muscle excitations (controls) to reproduce desired torque profiles. They showed that even with the same number of muscles producing identical torques (from a previous forward simulation) that individual muscle controls could be obtained in hours and not days. One reason for the performance improvement is that each muscle control has a summative effect (i.e. linear) on one or two joint torques and the force-length and force-velocity relationships (*Hill* (1938)) that modulate muscle force capacity are smooth and do not vary significantly with small changes in states or time. Therefore, gradient based methods can take larger steps and converge more quickly not to mention the integration of muscle dynamics, alone, is also faster.

Although a relatively simple and effective approach to obtain more dynamically accurate muscle forces from inverse dynamics, this approach ignores the inherent inaccuracies associated with an inverse dynamics analysis. Unless torques from inverse dynamics can be demonstrated to reproduce an observed movement, one has to be wary of any conclusions about muscle function drawn from an analysis of these torques.

2.2.3.3 Direct Collocation

A predecessor of the LSPO method is the direct collocation approach to solving the optimal control problem. Unlike, LSPO the system dynamics (constraints) are not satisfied implicitly through forward integration of the dynamical equations, but are enforced as explicit constraints on the optimal control problem itself. Unknowns are comprised of viable states and controls at discrete intervals (nodes) in time.The unknown controls and states are varied via optimization until the performance is minimized and the dynamic constraints (defining transition from node to node) are satisfied (*Kaplan and Heegard* (2001)).

Although a far more complex optimization problem is born in terms of the number of unknowns

(number of states and controls multiplied by the number of discrete nodes), direct collocation can be significantly faster than LSPO. Primarily, direct collocation does not require the numerical integration of the dynamical equations to evaluate the performance index. For a given set of controls and states, the evaluation of the performance index requires one function call where LSPO requires many calls to the system dynamical equations to integrate the equations forward in time to make one evaluation of performance. Even the most efficient implementations would require on the order of seconds to integrate the musculoskeletal dynamics of similar complexity to the model of (*Anderson and Pandy* (1999)). In contrast, direct collocation would require milliseconds. The system dynamics are explicit in the constraints of the optimization problem and in effect describe the permissible transition from node to node. For the pedaling model presented by *Kaplan and Heegard* (2001) analytical derivatives of the performance index and constraints with respect to the states and controls were also available. This is highly advantageous since since numerical evaluation would require on the order of the number of design variables in function calls to evaluate the gradient at just one point. Analytical derivatives result in a single function call. Furthermore, second order derivatives were also available in analytical form, thus precise knowledge of local curvature was available to the optimization again based on a single function call.

For the general problem of neuromusculoskeletal control in biomechanics, direct collocation presents serious limitations due to the sheer number of design variables and the reliance on analytical derivatives. Because of the large number of unknowns that include muscle and kinematics states, analytical derivatives are virtually required, otherwise the algorithm will become bogged down in numerically differentiating the performance index and constraints with respect to each state and control at every node. For kinematically constrained planar models (i.e. few independent degrees of freedom and so fewer kinematic states, as the case was in the cycling example by *Kaplan and Heegard* (2001)) where the movement is well defined and initial guesses at viable states is also feasible with relatively few muscles, this is an efficient approach. However, for more complex unconstrained 3D models (as in

gait) where contact dynamics and additional muscle dynamics and states (regarding metabolic energy, for example) are included, then analytical derivatives will be extremely difficult to obtain even with the most sophisticated symbolic mathematics software.

2.2.3.4 Difficulties Applying Dynamic Optimization Methods

Initial conditions for derivative based methods are difficult to determine without *a priori* knowledge of the solution, particularly in the direct collocation case, which requires both viable controls and corresponding system states. The solution to the optimal control problem (i.e. dynamic optimization) can provide forward simulations that are predictive (except for 2.2.3.2), which is a very powerful aspect of this approach. Unfortunately, model predictions have not closely matched individual subject data and it is difficult to determine the source of discrepancy either from modeling inaccuracy, invalid assumptions, and/or an inability to converge to the global solution.

Despite their high computational cost, large scale parameter optimizations have been able to generate muscle actuated forward simulations of human locomotion (i.e. *Bobbert and van Ingen-Schenau* (1988); *Anderson and Pandy* (1999, 2001a); *Neptune et al.* (2001); *Higginson et al.* (2006)...) where ground interaction is involved that have resembled human performance. Particularly in the more recent studies, the analysis of clinical gait disorders using these methods have provided novel insights. Nonetheless, attention must be drawn to the inability of these models to sufficiently replicate ground reaction forces, thus far. To say that a muscle, such as soleus, maybe activated prematurely based on a model of a hemiparesis subject lacks credibility when the model also exceeds the vertical ground reaction force by over 40% of body weight at heel-strike compared to experiment (*Higginson et al.* (2006)). It may very well be that soleus is activated early, but it is equally (if not more) likely that the increase is soleus activation corresponds to the excessive ground reaction force produced by the model. Similar conclusions are drawn by *Neptune et al.* (2001) about the function of ankle plantar-flexors in normal gait being dominant in support and forward propulsion (as a proportion of the ground-reaction force),

however the model also produces 200% of the ground reaction force at heel-strike. Is it possible that the perceived dominant role of ankle plantar-flexors corresponds with the error in the model? These questions will remain until models are able to more closely replicate observed ground reaction forces.

2.2.4 EMG Driven Models

Several studies (*Olney and Winter* (1985); *White and Winter* (1993); *Cholewicki et al.* (1995); *Jonkers et al.* (2002); *Lloyd and Besier* (2003); *Buchanan et al.* (2004)...) have combined EMG analysis with musculoskeletal modeling to provide EMG-driven muscles (models) in order to produce the net joint torques evaluated by dynamometer or via inverse dynamics. Given the variability in EMG measurements and processing techniques, EMG inputs to muscle models must be "scaled" to individual recordings such that the transformation from EMG to muscular torques is consistent with measurements/calculations of net joint torques (*Staudenmann et al.* (2006)). Although modeled muscle activity is naturally in agreement with recorded EMG, it has not been clearly shown that the resultant output muscle forces remain in agreement with EMG considering the optimization of muscle parameters that is required in order for muscles to reproduce desired joint moments. The combined data processing and muscle parameter tuning, in fact, can prove to be less reliable than conventional static optimization techniques (*Heintz and Gutierrez-Farewik* (2006)).

In addition to the complex art of transforming EMG signals to forces, there are two additional limitations that make the use of EMG driven models alone incapable of being used clinically to analyze the majority of lower extremity muscles during gait. *Buchanan et al.* (2005) describe the state of the art of EMG driven models and compare muscle moments estimated from the ankle to those of dynamometer measurements and from an inverse dynamics analysis of gait. What is troubling is that they model four muscles that span the ankle where there are a dozen, yet four EMG signals to four muscle models identically produce the ankle moment. Even more problematic is that other joints, particularly the hip have many more muscles that lay deeper and under other muscles, where EMG from primary muscles

cannot be measured with surface electrodes. Particularly in the case of of iliacus and psoas muscles, which are important hip flexors, various surface electrode placement were unable to estimate peak EMG consistently below an error of 20% of MVC for a variety of tasks compared to indwelling electrodes (*McGill et al.* (1996)). The second issue is the use of inverse dynamics as the validation of the modeled muscle moments without validating that the moments would adequately actuate a representative model to produce experimental kinematics and ground reaction forces. Since inverse dynamics defines the target joint torques, this approach suffers from the same inaccuracies plaguing inverse dynamics.

It may prove more clinically applicable to employ hybrid methods combining EMG and optimization (*Cholewicki et al.* (1995)) so activity of muscle models closely resemble corresponding measured muscle EMG when available and resolving the contributions of unmeasured (undetected) muscles via optimization.

2.2.5 Movement Data Tracking

To mitigate errors introduced by acceleration estimates *Runge et al.* (1995) used linearization and optimal control methods to produce a solution for standing postural control by employing feedback of tracking errors in postural joint angles. The errors themselves provided information about how the system should accelerate to determine the appropriate joint torques for a linear system. Similarly, *Seth et al.* (2003), tracked upper limb kinematics during dynamic upper-limb tasks using the method of computed torques, borrowed from robotics (*Spong and Vidyasagar* (1989)), to obtain the joint torques that would replicate arm-motions in a forward simulation. Unlike *Runge et al.* (1995), the method of computed torques continuously linearizes the model about the current state not just the initial state, and thus enables much more complex behavior.

Computed muscle control (CMC, *Thelen et al.* (2003); *Thelen and Anderson* (2006)) is the most recent technique to track available movement data. CMC is also based on the method of computed torques, which essentially uses the inverse dynamics equations to linearize a forward dynamics model, at

which point a linear feedback controller is used to drive differences between the model and experimental kinematics to zero (or close to it) during a forward simulation. CMC goes further to decompose computed torques into individual muscle forces by using static optimization to obtain "desired" activations, which linear excitation-to-activation dynamics can track. This was a simple yet powerful development in the efficient computation of muscle forces that include activation dynamics. Nonetheless, two shortcomings standout when compared to dynamic optimization. First, how a forward model of gait synthesizes ground-reaction forces is not yet addressed and second the differences between model and human that lead to tracking inconsistencies are ignored by the tracking itself and compensated by a residual elimination algorithm (REA, *Thelen and Anderson* (2006)). Because the model does not produce reaction forces, CMC must apply ground reaction forces as external loads in the inverse dynamics calculations even though they may not reflect achievable forces given the position and velocity of the contact foot at that time. For example, an error of 3°in hip flexion angle is sufficient to misplace the foot by $4cm$, which may result in the foot not being in contact with the ground where experiencing a reaction force would be impossible.

These inconsistencies combined with errors in acceleration estimates (from experiment) result in residual forces when performing a bottom-up recursive Newton-Euler analysis upon the model. That is, an additional force at the top of the linkage is required in order for the sum of forces including the ground forces acting on the feet to result in the observed acceleration, given the inertia of the model. In order to "force" the model to be consistent (i.e. no residual force) with both kinematics and ground reaction forces, REA alters the kinematics of certain degrees of freedom (like pelvis translation and back angles) such that residuals are eliminated in the inverse analysis. Unfortunately, it cannot be shown that the model can generate these accelerations and corresponding reaction forces, since the GRFs are prescribed. That is to say the accelerations, while consistent with the experimental GRFs have virtually nothing to do with the forward model. As an illustrative thought exercise, assume the model used to track experimental data has half the mass and inertia of the subject. Using REA, greater

accelerations can be assigned to the pelvis and back (which have the greatest effect on COM acceleration and thus GRFs) and in effect cancel the effects of having the wrong inertia. The limbs are then "free" to match the experimental joint kinematics, since the leg does not have to push to accelerate the pelvis because the pelvis kinematics are being assigned by REA. Of course, it is impossible for a person of half the mass to produce the same GRFs, yet applying REA could theoretically achieve that result. It is preferable to avoid acceleration estimates altogether and allow the model kinematics and ground reaction forces to vary from experiment given the differences between model and subject. If the model grossly misrepresents the subject, then tracking should fail to reproduce subject performance closely. The amount of discrepancy between model and subject performances should be indicative of the real differences that exist between the two. Consequently, the goal then becomes to develop models that are more and more representative of the subject. CMC would give the illusion that a 20 degree-of-freedom rigid linkage was able to produce virtually identical kinematics and ground-reaction forces. It should be clear from the above thought exercise that CMC results applied to the same forward model with ground contact would fail to reproduce the desired performance.

2.3 Simulation Accuracy

Whereas the power of large-scale optimizations to predict human performance is not in question, the utility to generate subject specific simulations comparable to experimental data is both extremely time consuming and lacks sufficient specificity. As a minimum, for a model to be "reasonably" trustworthy it should fall within one or two standard deviations of the experimental data in ground reaction forces and motion of the major degrees-of-freedom from trials from a single subject. In particular, a peak ground reaction force error of 10% in ground reaction force should translate to 10% or less in muscle force error for any muscle contributing to the ground reaction force at that instant. This amount or error is reasonable in that it should not change any conclusions about muscle function for that subject especially if forces are within the standard deviation boundaries. Similarly, a 10% error in a back extension,

hip flexion, knee extension, or ankle dorsiflexion angle should result in less than 10% in muscle length differences of primary movers and similarly not significantly impact conclusions about muscle function.

Standard deviation information across multiple subjects is an inadequate measure of performance, since it acts only to broaden the range of possible solutions without any assurance that the average is representative of any subject in particular. A model should be tested against a single typical (median) trial for a single patient and closeness measured directly to that and other trials from that subject. This is contrary to the notion of statistical significance, but significance is only relevant in drawing conclusions about performance across a population or to make general statements about function. Significance is not a relevant measure of how well a model represents a subject. It is quite a different question altogether to ask how well a model and simulation can reproduce the observed performance of a subject. Since this treatise is focused on how well a model can replicate human performance, discussions of accuracy will be confined to comparison with standard deviation of performance from trials of the same subjects and a '10% rule' in peak forces and joint angles for the movement trial that is being tracked.

2.4 Criteria for Muscle Force Estimation Methods

Based on the discussion of previous methodologies and their limitations, the measure for a successful methodology for estimating individual muscle forces from experimental data can be summarized by the following five criteria:

1. Muscle moments produce a forward dynamics simulation, where:
2. Simulated kinematics and especially ground reaction forces follow within the standard deviations of experimental data
3. Muscle forces satisfy neuromuscular dynamics

4. Simulated muscle activity is in qualitative agreement with EMG of recorded muscles

5. All computations can be performed on the order of minutes

Chapter 3

Neuromusculoskeletal Tracking (NMT)

3.1 The Tracking Problem

The first aim is to develop a computational neuromusculoskeletal tracking method to dynamically determine individual muscle forces from human movement data. The control of a dynamical system so that it follows a desired or specified trajectory is known as tracking. When experimental data about human movement is available, determining the actuation of a musculoskeletal model to follow the experimental data as closely as possible defines a tracking problem. This differs from the inverse dynamics problem, which provides estimates of joint torques without verification that the torques in fact actuate the model to produce the same performance from which they were calculated.

The formulation of the tracking problem as a large-scale parameter optimization (LSPO) problem (i.e. *Neptune et al.* (2001); *Higginson et al.* (2006)) although valid, suffers from the same computational intractability as the predictive case. The LSPO method cannot distinguish between a performance index that is tracking or predicting - the method simply varies the model controls until convergence to a minimum is achieved. Using the desired performance to influence the control problem directly, is a far more efficient approach to the tracking problem.

Seth et al. (2003)and *Thelen et al.* (2003) have shown that it is possible to use kinematics to compute torques based on inverse dynamics and to employ feedback of the tracking error to correct torques and obtain the desired performance. More recently, *Thelen and Anderson* (2006) have demonstrated the tracking of human gait kinematics with ground reaction forces (GRFs) as known external forces applied to the feet at the center of pressure. In this case, additional forces from translational and

rotational spring-dampers were applied at discrete instants at the point of contact to ensure the point remained stationary until the next time step. It was not shown whether the model would produce the same GRFs with a suitable contact model and the same muscle moments.

The question is whether it is possible to include GRFs into the tracking set in addition to kinematics? Just as the model produces kinematics and we can infer controls from errors in tracking kinematics, could GRFs be synthesized and the errors from this stream of data also be used to obtain better estimates of the controls? Second, if nonlinear skeletal dynamics could track experimental motion to generate net actuation more accurately, would it also not be possible to apply the same approach to enable dynamic models of muscles to track the necessary joint torques?

The answers to these questions are yes. But, before delving into the methods let us review the data that is being tracked and what essential information that each provides in directing the tracking solution using a neuromusculoskeletal model. The fundamental components of neuromusculoskeletal modeling are also briefly reviewed.

3.1.1 Kinematic data

Video-graphic markers are used to identify the spatial positions of landmarks and points of interest on the body, such as bony processes, condyles and spines, as well as estimated joint centers and the location of the center of mass of segments. Captured at discrete intervals, they describe the spatial trajectory of these points through time. The generalized coordinates (segment positions and joint angles that define the state) of a model are determined by inverse kinematics techniques, which yield the joint motion, such as knee extension, hip flexion, ankle dorsiflexion, etc ... which are typically used in human motion analysis.

An inverse kinematics analysis attempts to map marker positions to joint coordinates that posture the model such that the corresponding (to the markers) fixed locations on the rigid segments of the model are in close agreement with the marker coordinates. Model segment dimensions, joint

axes and the fixed points representing marker positions can be optimized in combination with the joint coordinates in a two step process (*Reinbolt et al.* (2005)) to minimize differences. However, the fixed positions of a model, in general, cannot precisely match the spatial marker coordinates when there is relative skin/muscle movement and the model is rigid with differences with actual bone translation and rotation differing by as much as 22mm and 15° in the lower extremity (*Sangeux et al.* (2006)). Therefore, skin movement error is included in the estimated rigid body motion affecting joint angle estimates and their derivatives.

The generalized speeds and accelerations that form a complete set of model kinematics are estimated by numerical differentiation of the generalized coordinates computed from inverse-kinematics. Thus, both random noise and skin movement artifacts are amplified by differentiation. Low pass filtering of position data can attenuate high frequency noise, but skin motion which occurs at roughly the same frequency as the body's movement, remains. Therefore, random and bias noise are introduced at virtually every step in acquiring a complete set of generalized kinematics for a model representing a subject's performance.

3.1.2 Kinetic data

Ground reaction forces (GRFs) and moments from a force-plate provide another independent view of system center of mass (COM) acceleration. In addition, center-of-pressure (cop) which defines the effective point of application of contact forces, provides vital position data independent of marker kinematics. GRF and cop data are more accurate measures than kinematic data and provide more reliable information about the acceleration of the COM and placement of the feet, because no differentiation of the data is necessary and there are no skin movement artifacts.

Consequently, one would not expect accelerations estimated from kinematic data to be consistent with the accelerations of the COM determined from the GRFs. Therefore, any method that purports to obtain precise kinematic tracking with identical experimental GRFs is highly suspect without a method

of systematically altering the kinematics to enforce consistency (i.e. Residual Elimination Algorithm, *Thelen and Anderson* (2006)).

GRFs, on one hand, provide additional constraints on acceleration estimates of individual joints (from kinematics) that can direct the solution of actuation forces/moments. This was made obvious by the pseudo-inverse approach (*Kuo* (1998)) where increasing the influence of GRFs in a least-squares sense had the greatest effect on improving torque estimates (*Cahouet et al.* (2002)). Where this approach improves the inverse analysis, on its own it fails to demonstrate the accurate synthesis of GRFs by the model to ensure that similar forces are being exerted by the model.

3.1.3 Neuromusculoskeletal modeling

The neuromusculoskeletal model can be broken into two categories: 1.) multi-body and contact dynamics that reflect the body as a linkage of rigid-segments, which make up a skeleton; and 2) tissue mechanics such as muscles and ligaments that produce internal forces actively and/or passively. Rigid segments are connected via joints that constrain the movement of one segment relative to another, such as revolute (pin), ball-and-socket, and slider joints which limit how the system can move as a whole. The use of ideal joints (which can provide infinite reaction forces to maintain joint integrity) cannot represent the complete reality of possible joint separation at high loads, but they can reflect the degrees-of-freedom observed under average loading conditions. In some cases, as in the knee, translations of the tibia with respect to the femur (*Freeman and Pinskerova* (2005)) can be assumed to be small relative to displacements of the segments and changes in muscle length and thus have been ignored in models used to study whole body movement and coordination as assumed by many studies (i.e. *Davy and Audu* (1987); *Yamaguchi* (1990); *Anderson and Pandy* (2001a); *Neptune et al.* (2001); *Jonkers et al.* (2002); etc...). The inclusion of ideal joints also reduces the set of system coordinates (independent variables that can fully describe the motion of the system) and provides for a reduced set of equations of motion. Thus written in terms of joint coordinates alone the equations of motion have the form,

$$M\ddot{q} = \Im(q, \dot{q}, t)$$

where the mass matrix, M, describes how the accelerations of the generalized coordinates, q, are coupled in their contribution to the total acceleration of the system. The generalized coordinates and their speeds $(q, \dot{q})$ are together considered the states of the multi-body dynamics. $\Im$ is the combined effect of all the forces acting on the system including contributions from centripetal and Coriolis (velocity dependent) accelerations and any applied or reactionary loads. To limit the range of motion of any coordinate, q, passive ligament forces (torques) are applied such that they resist motion as the coordinates exceed physiological ranges. Viscous damping is often included to reflect the passive resistance of fluid filled joint capsules to rapid movements. Expressing the state dependent passive ligament forces, L, separately, the equations of motion become:

$$M\ddot{q} = \Im(q, \dot{q}, t) + L(q, \dot{q})$$

Multi-body models are either assumed to be rigidly affixed to a ground body or "free-floating" where specific points or surfaces on the multi-body system are constrained from passing through another surface, such as the surface of the ground in walking. Since we are concerned primarily with locomotion, the inclusion of contact dynamics is critical to the synthesis of whole body movement. A survey of the literature yields a common form for models of contact in the modeling and simulation of human gait (i.e. *Anderson and Pandy* (2001a); *Neptune et al.* (2001); *Zajac et al.* (2002); *Wojtyra* (2003)). These models use the location and velocity of predefined points on the foot to determine the amount of resistive force experienced by each point with respect to a constraint (ground) surface, for example, by the amount of surface penetration and the speed in to or away from the surface. Consequently, they have the form $S(q, \dot{q})$ since the position and velocity of the points on the feet are functions of the generalized coordinates and their speeds, like spring-damper units. These forces are not instantaneous consequences

of applied loads and accelerations (as a rigid constraint) but are compliant and exhibit state dependent dynamics, such that they contribute another term to the system dynamics:

$$M\ddot{q} = \Im(q, \dot{q}, t) + L(q, \dot{q}) + S(q, \dot{q})$$

Forces generated by muscles pull segments together having equal but opposite effect, which is a muscle generated moment according to each muscle's moment-arm about the joint(s) it spans. In fact, the moments on each body can be represented by a single joint rotational force (torque) due to that muscle. The torque experienced at a joint is the net effect of each muscle spanning that joint. With applied muscle torques at every spanned joint, the equations of motion can be further expanded into its constituent contributors, such that:

$$M\ddot{q} = \Im(q, \dot{q}) + L(q, \dot{q}) + S(q, \dot{q}) + T\tau \tag{3.1}$$

where τ are the applied torques, and T is a matrix relating them to the acceleration of each coordinate. Since muscles do not span every degree of freedom, such as the translations of the whole system, T often includes zero rows indicating there are fewer applied torques than generalized coordinates.

The neuromuscular system is another dynamical system that is coupled to the skeletal dynamics above, as the source of applied torques in Eq. 3.1. The neuromuscular dynamics describe several physiological processes that influence control and force production. These include: 1) how neural drive is transformed to muscle activation, which can be described as the state of muscle (fiber) depolarization and calcium release, 2) how activation causes muscle contractile force, and 3) muscle force dependence on fiber length and shortening speed (*Hill* (1938)).

A common model of excitation (a normalized value representing the amount of neural drive) to activation dynamics is the first order linear model described by *Zajac* (1989), and nonlinear dynamics, such as that formulated by *Pandy et al.* (1990) have not been shown to generate significantly different

responses. Contraction dynamics, which include the passive muscle elasticity and active cross-bridge formation range from the highly complex partial differential constitutive equations of *Hatze* (1977) to the lumped parameter phenomenological models (*Glantz* (1977);*Zajac* (1989);*Pandy et al.* (1990) and *Anderson and Pandy* (1999)). The lumped models include length and velocity dependence of the muscle contractile unit by employing the phenomenological curves by *Hill* (1938), which were observed from single frog muscle fiber experiments. Nonetheless the lumped parameter models are more tractable and can provide comparable muscle forces with constitutive muscle models if the details of muscle contraction mechanisms are not of interest (*Winters and Stark* (1987); *Winters* (1990)).

The activation and contraction dynamics can be described by a series of first-order equations:

$$\dot{x} = \mathcal{A}(x,\, l^{MT}(q),\, ^{MT}(q,\dot{q}),\, u) \tag{3.2}$$

where the muscle states x may vary somewhat from model to model, but invariably include muscle activation and either the normalized muscle force itself or an internal state of the contractile unit such as fiber length from which the musculotendinous force can be computed from the corresponding length/strain in the tendon . The complete musculotendinous lengths and shortening velocities (l^{MT}, v^{MT}) are defined by the musculoskeletal geometry and are dependent on the kinematics states. The muscle excitations, u, are the independent inputs (controls) to the muscle models. The output of the system are the resultant musculotendinous forces:

$$f = F^{MT}(x)$$

The musculoskeletal geometry of the model also determines how the muscle forces act upon the joints they span and can be quantified as a single linear transformation by the instantaneous moment-arm, r, such that

$$\tau_{j,m} = r_{j,m}(q) \cdot f_m$$

where subscripts j and m denote the joint and the spanning muscle. We can resolve all the torques from all muscle forces using a moment-arm transformation matrix, $\Upsilon(q)$, such that the complete neuromusculoskeletal dynamics can be described compactly by one set of ordinary differential equations:

$$\begin{aligned} M\ddot{q} &= \Im(q,\dot{q}) + L(q,\dot{q}) + S(q,\dot{q}) + T \cdot \Upsilon(q) \cdot F^{MT}(x) \\ \dot{x} &= \mathcal{A}(x,\, l^{MT}(q),\, v^{MT}(q,\dot{q}),\, u) \end{aligned} \tag{3.3}$$

In the development of a neuromusculoskeletal tracking methodology, we assume this general form of the system equations as our starting point. The general structure of the equations and the linearity of certain terms are exploited by the NMT method. Any biomechanical model that can be described in this general form are candidates for neuromusculoskeletal tracking and therefore includes a majority of the models in use today.

3.2 Neuromusculoskeletal Tracking Overview

The inverse dynamics and static optimization approach is efficient because it does two things: 1) It employs experimental data so that it does not have to search for a solution for the net actuation of a model, and 2) the resolution of muscle forces is handled as a separate optimization that no longer includes the nonlinearities of the multi-body system. The primary shortcomings (as discussed in the background) are: 1) Inverse dynamics neglects the inherent error in kinematic data and does not provide appropriate signal dimensionality, and 2) SO excludes neuromuscular dynamics and time dependent performance indices in the resolution of muscle forces.The neuromusculoskeletal tracking approach, aims to maintain the advantages while overcoming the shortcoming by introducing the dynamics in the solution process at each stage.

Subsequently, the NMT method can also be divided into to computational stages.

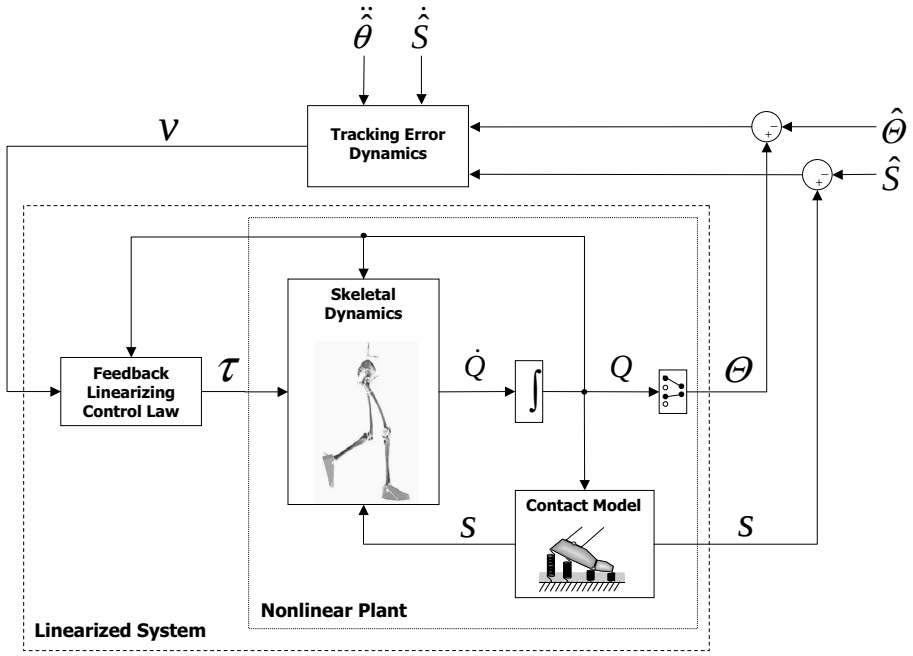

Figure 3.1: NMT Stage 1: Skeletal motion tracking methodology.
Skeletal dynamics (nonlinear plant) is characterized by joint torque inputs, τ, states, Q, with selected kinematics, Θ, and contact forces, s, as outputs. Linear system controls, ν, are determined from errors between skeletal outputs and their observed values ($\hat{\Theta}, \hat{s}$)

3.3 Stage 1: Skeletal-motion Tracking

Stage 1, uses feedback linearization (*Slotine and Li* (1991)) to eliminate the nonlinearities associated with the skeletal dynamics (Fig. 3.1), akin to the computed torques method (*Spong and Vidyasagar* (1989)). However, we include ground-contact dynamics to increase the accuracy of the computed torques method. Several forward dynamics models of human gait (*Anderson and Pandy* (2001a), *Neptune et al.* (2001), *Wojtyra* (2003)) describe contact by $s = S(q, \dot{q})$ where s contains the components of the GRFs and the coordinates of the point of application (i.e. center of pressure) which is a function of the position and velocities of the model. In this case, the S can be considered an output transformation of the kinematic states q and $\dot{q}$ without the introduction of additional variables to describe the contact forces.

The specific formulation of the equations either in absolute or relative (joint) coordinates does not alter the general approach. For the purpose of developing the skeletal motion tacker we assume the equations of motion for skeletal dynamics have the form:

$$\ddot{q} = M^{-1} \left[\Im(q, \dot{q}, t) + S(q, \dot{q}) + T\tau \right] \tag{3.4}$$

where $q = [q_1, q_2, \ldots, q_{nq}]^T$are the generalized coordinates; M is the system mass matrix; $\Im$ is the set of generalized forces due to gravity, centripetal and Coriolis effects as well as any passive forces (i.e. due to ligaments); S represents the ground contact model; and T is the coefficient matrix relating applied joint torques, τ, to applied generalized forces (torques). In first-order form, Eq. 3.4 becomes:

$$\dot{Q} = F(Q) + G(Q)\tau \tag{3.5}$$

$$y = [\theta, s]^T \tag{3.6}$$

where $Q = [q, \dot{q}]^T$, $F = [\dot{q}, M^{-1}(\Im + S)]^T$, and $G = [0_{nq \times n\tau}, M^{-1}T]$. The system output, y, is composed of a subset of model generalized coordinates, θ, and outputs of the contact model, s. In general, s can include any aspect of ground contact that will be compared to experimental measurements, which may include: fore-aft, vertical and medio-lateral forces, components of the ground moment and center-of-pressure coordinates, accounting for ns outputs. In order to establish adequate control of the system, each degree of freedom must be represented in y, otherwise that coordinate will not be adequately controlled. That does not mean that every coordinate must appear, rather, that $rank(\frac{\partial y}{\partial Q}) \geq nq$. In addition, the order of the feedback linearized system must be at least that of the nonlinear system.

To apply feedback linearization, an explicit relationship must be found between the outputs and the controls (joint torques, τ). Differentiating the kinematic outputs, θ, twice with respect to time yields:

$$\ddot{\theta} = \frac{\partial \theta}{\partial Q}\left[\frac{\partial \theta}{\partial Q}F\right]F + \frac{\partial \theta}{\partial Q}\left[\frac{\partial \theta}{\partial Q}F\right]G\tau \tag{3.7}$$

Eq. 3.7 is identical to the corresponding accelerations of the generalized coordinates in Eq. 3.4. Similarly, differentiating the ground-force output, s, once with respect to time gives:

$$\dot{s} = \frac{\partial s}{\partial Q}F + \frac{\partial s}{\partial Q}G\tau \tag{3.8}$$

Note if some components of s are only dependent on the generalized positions, q, then second order equations similar to Eq. 3.7 are required to ensure control efficacy for these outputs.

Introducing a new control variable,$\nu = [\ddot{\theta}, \dot{s}]^T$, such that,

$$\nu = \begin{bmatrix} \frac{\partial \theta}{\partial Q}\left[\frac{\partial \theta}{\partial Q}F\right] \\ \frac{\partial s}{\partial Q} \end{bmatrix} F + \begin{bmatrix} \frac{\partial \theta}{\partial Q}\left[\frac{\partial \theta}{\partial Q}F\right] \\ \frac{\partial s}{\partial Q} \end{bmatrix} G\tau \tag{3.9}$$

and solving for the joint torques yields:

$$\tau = \left[\begin{bmatrix} \frac{\partial \theta}{\partial Q} \left[\frac{\partial \theta}{\partial Q} F \right] \\ \frac{\partial s}{\partial Q} \end{bmatrix} G \right]^{-1} \left\{ \nu - \begin{bmatrix} \frac{\partial \theta}{\partial Q} \left[\frac{\partial \theta}{\partial Q} F \right] \\ \frac{\partial s}{\partial Q} \end{bmatrix} F \right\} \tag{3.10}$$

Equation 3.10 is the feedback linearizing control law that transforms the nonlinear system defined by Eq. 3.5 and Eq. 3.6 into the linear system,

$$\begin{bmatrix} \ddot{\theta} \\ \dot{s} \end{bmatrix} = \nu \tag{3.11}$$

This linear system controls, ν, is determined by the linear feedback of tracking errors of sufficient order and with appropriate gains to reject tracking errors:

$$\nu = \begin{bmatrix} \ddot{\hat{\theta}} - 2\lambda_\theta(\dot{\theta} - \dot{\hat{\theta}}) - \lambda_\theta^2(\theta - \hat{\theta}) \\ \dot{\hat{s}} - \lambda_s(s - \hat{s}) \end{bmatrix} \tag{3.12}$$

The resultant control, ν, is dependent on the observed kinematics,$\hat{\theta}$, and force-plate data, $\hat{s}$ and the model outputs $(\theta, \dot{\theta}, s)$. Interestingly, if s is empty and $\theta = q$, then the above formulation reduces identically to the method of computed torques. Note, if the number of kinematic references (positions and velocities) plus the number ground contact signals being tracked are less than the order of the multi-body system Eq. 3.5 (i.e. $2 \times nq$) there may be uncontrolled dynamics of the system and the tracking of the missing generalized coordinate may be required. Because error dynamics must be faster than the frequency of the observations to ensure tracking stability, the poles of the critically damped system, λ, should be selected to be roughly 5 times greater than the maximum frequency of the respective observation.

The inverted matrix of the system's feedback linearizing control law Eq. 3.10 is known as the decoupling matrix since at each instant it represents a linear map from the FBL control parameter, ν, to joint torques. In general, the decoupling matrix is non-square as it relates $n\theta$+ns tracking references to $n\tau$ joint torques. Because there are more equations than unknowns, the joint torques, τ, in Eq.3.10

are evaluated in a weighted least-squares sense. Weighting more reliable observations more heavily in a least-squares approach has been shown to improve the accuracy of inverse dynamics calculations significantly*Kuo* (1998). A similar least-squares approach is employed to determine the decoupling matrix for the skeletal motion tracker. Unlike *Kuo* (1998), however, the skeletal motion-tracker includes ground-contact dynamics instead of enforcing a pinned constraint, so that the model can make and break contact with the ground.

Because each reference signal influencing the FBL control is measured on grossly different scales (i.e. fractions of radians versus 100's of Newtons and cm of cop movement) it is critical to scale the the respective rows so that influence is not skewed by virtue of differing units. Each row in ν and the decoupling matrix (prior to inversion) is scaled by the mean absolute rate of change of the corresponding experimental measurements (i.e. $\left|\ddot{\hat{\theta}}\right|$and $\left|\dot{\hat{s}}\right|$) to maintain a well conditioned system of equations that are close to unity. The mean is selected opposed to the maximum to reduce the possibility of poor scaling due to large but erroneous acceleration estimates.

System Jacobians are computed numerically to emphasize a general approach.

3.4 Stage 2:Neuromuscular Tracking

Neuromuscular tracking, Stage 2, determines the optimal muscle excitations and muscle forces necessary for the neuromuscular system (Fig. 3.2) to generate the joint torques calculated in Stage 1. Because the nonlinearities due to skeletal dynamics are separated from the problem of determining muscle activity, the dynamic optimization problem for muscle excitations can be greatly simplified without over simplifying neuromuscular dynamics.

The neuromuscular system is characterized by muscle contraction dynamics and muscle activation dynamics, for example *Zajac* (1989), which relate muscle excitations, u, to musculotendinous forces, F^{MT}. The complete neuromuscular dynamics (i.e. Eq. 3.2) can be described as a system suitable for

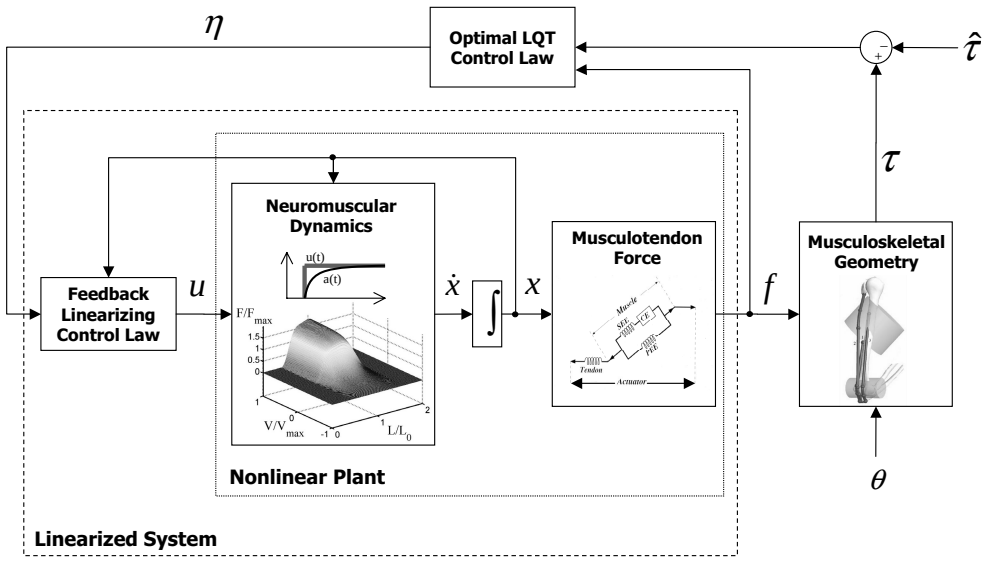

Figure 3.2: NMT Stage 2: Neuromuscular tracking methodology.
Stage 2: Neuromuscular dynamics (nonlinear plant) relate excitations, u, to muscle states, x, and muscle force outputs, f. A linear quadratic tracker (LQT) determines the optimal controls, η, based on torque tracking error, $\tau - \hat{\tau}$, and muscle forces, f. $\hat{\tau}$are known torques from Stage 1.

feedback linearization:

$$\dot{x} = A(x) + B(x)u \tag{3.13}$$

$$f = F^{MT}(x) \tag{3.14}$$

where, contains the neuromuscular system states of muscle activations and normalized forces or muscle fiber lengths; and the output, f, contains only the musculotendinous forces as a function of x. Differentiating the output vector, f, once, and defining a new control vector, η, yields the feedback-linearizing control law:

$$u = \left[\frac{\partial F^{MT}}{\partial x}B\right]^{-1}\left\{\eta - \frac{\partial F^{MT}}{\partial x}A\right\} \tag{3.15}$$

and the corresponding linear system:

$$\dot{f} = \eta \tag{3.16}$$

$$\tau_m = \Upsilon f \tag{3.17}$$

where the outputs of the feedback-linearized system are the joint torques, τ_m, and $\Upsilon(\theta)$ is the matrix of muscle moment arms, transforming muscle forces to torques as a function of joint angles, θ. Alternatively, if neuromuscular torques, τ_m, are treated directly as the outputs, with $\zeta = \dot{\tau}_m$, one obtains the following linearizing control law:

$$u = \left[\Upsilon \frac{\partial F^{MT}}{\partial x} B\right]^{-1} \left\{\zeta - \dot{\Upsilon} f - \Upsilon \frac{\partial F^{MT}}{\partial x} A\right\} \tag{3.18}$$

where the torque error feedback, $\zeta = \dot{\hat{\tau}} - \lambda_\tau(\tau - \hat{\tau})$ is sufficient to obtain muscle excitation which will follow known (i.e. stage 1) torques, $\hat{\tau}$. Unfortunately, there is no way we can influence how excitations are allocated using this approach, since the algorithm "chooses" which muscles to excite according $\Upsilon \frac{\partial F^{MT}}{\partial x}$ which indicates which muscle(s) are most effective at controlling the torque at any given instant.

Therefore, we return to the muscle force based FBL system Eqs. 3.16 and 3.17 to determine the individual muscles controls, η, such that muscle forces satisfy more physiological criteria. One physiological performance criterion used to analyze human movement is muscle "effort" which is defined as the integral of rate of change of muscle forces, $\dot{f}$, (*Pandy et al.* (1995)) over the performance period. It is also necessary to minimize torque-tracking error to ensure muscles accurately reproduce the torque required to drive the skeletal system. We can define the equivalent performance index:

$$J = \frac{1}{2}\left(\tau(t_f) - \hat{\tau}(t_f)\right)^T P \left(\tau(t_f) - \hat{\tau}(t_f)\right) + \frac{1}{2}\int_0^{t_f} \left[\left(\Upsilon f - \hat{\tau}\right)^T Q \left(\Upsilon f - \hat{\tau}\right) + \eta^T R \eta\right] dt \tag{3.19}$$

where P is the weighting matrix for the tracking error at the final time, t_f; Q is the weighting matrix for the continuous tracking error; and R is the weighting matrix for the continuous muscle effort. $\hat{\tau}$denotes the set of reference joint torques obtained from skeletal motion tracking. When muscle force rates, η, are normalized by peak isometric force, the time integral of their squared sum defines muscular effort, which has the same units as squared stresses in the static sense. Effort, however, is a cumulative value evaluated over the entire task period. *Pandy et al.* (1995) used a similar performance index to estimate the muscle forces required to rise from a chair.

The performance index, Eq. 3.19, provides the general structure of the linear optimal control problem and it can be readily adapted to implement a variety of criteria. For example, the force output is transformed to torques to minimize torque error, but the output transform, Υ, could also include the identity matrix to output the muscle forces themselves. In this case the minimization of the sum of squared muscle forces (identical to that used in static optimization) could also be employed but would be evaluated over the entire performance period. In theory, this would allow for periods of high muscle forces in exchange for longer periods of lower to no muscle forces, which would make more practical sense in movement than minimizing forces at every instant. Nonetheless, these performance indices may still be inadequate to estimate muscle forces in all activities. Therefore, it is important to note that while the structure of the optimization problem may be restrictive, the quantities that are minimized are virtually unlimited and depend on what outputs the neuromuscular dynamics provide. It is possible to include metabolic energy dynamics as long as they can be expressed in the same form as Eq. 3.13. Therefore, activation and energy are candidate outputs (Eq. 3.14) and the sum of squared energy terms can be minimized and/or activation can be compared to desired activity patterns (i.e. from EMG) so that the redundancy problem is resolved in better agreement with observed EMG data. This is demonstrated in a benchmark analysis using the NMT method,4.

The linearized system (Eqs. 3.16 and 3.17) and the performance index (Eq. 3.19) describe a

linear-quadratic tracking (LQT) problem. LQT solution methods are well established in the optimal control literature (e.g., *Bryson and Ho* (1969); *Lewis and Symros* (1995)) and involve solving the system Ricatti matrix and adjoint equations for the affine feedback control law, η, as a function of f and $\hat{\tau}$. The optimal muscle excitations are subsequently evaluated from Eq. 4.4, and the neuromuscular system (Eqs. 3.13 and 3.14) is then integrated forward in time to produce the required muscle forces. The weighting matrices, Q and R, are chosen to obtain sufficiently low tracking error while minimizing effort. For completeness, the steps for solving the optimal LQT problem are presented below.

For the sake of generality, the output transformation matrix of the FBL system, which contains the moment arm matrix, Υ, above is described by C to indicate that addition outputs can be readily included. The resultant Ricatti matrix equation for the neuromuscular LQT system is

$$-\dot{W} = -WR^{-1}W + C^T QC \tag{3.20}$$

where $W(t_f)$=$C^T PC$ is the final time value for the Ricatti matrix. The adjoint for the closed-loop system yields the differential equation for tracking the torque reference signal,

$$-\dot{\gamma} = -(R^{-1}W)^T\gamma + C^T Q\hat{\tau} \tag{3.21}$$

where $\gamma$is the 'command' signal as a function of the reference torques, $\hat{\tau}$. Integrating backwards from the final time, t_f, yields $W(t)$ and $\gamma(t)$ necessary to evaluate the affine feedback control law,

$$\eta = -(R^{-1}W)^T f + R^{-1}\gamma \tag{3.22}$$

Minimizing torque-tracking error at the final time, in particular, is generally not a priority, therefore $P = [0]$. Joint torque-tracking errors can be treated independently but if they are of equal importance, then Q is $K_q I_{n\tau \times n\tau}$. Because R is the weighting for the rate of force production squared,

η, it should be normalized by the squared peak isometric force of the corresponding muscle, otherwise larger muscles are unduly penalized. Biarticular muscles can be further scaled by $\frac{1}{2}$ or other fraction to encourage the re-distribution of loading sharing to these muscles (i.e. less cost).

3.5 Simulink^{TM} Implementation

The NMT methodology was implemented in MATLAB's Simulink environment (product of The MathWorks Inc.) so that various musculoskeletal models can be simulated and controlled interchangeably without requiring the reimplementation of the control scheme. The requirements of the musculoskeletal model are as follows:

1. The neuromuscular dynamics and skeletal motion dynamics must be separable and implemented such that they can be called as independent routines
2. Models can be implemented in MATLAB or as C, ADA, or Fortran languages that include the S-function interface (included with Simulink), which can be added to legacy code (models) in order to compile and link these models into Simulink as an S-function block.
3. The skeletal dynamics (block) must be in the form of Eq. 3.4 and take the current kinematic states, Q, as input and return:
   (a) the system mass matrix matrix (or its inverse)
   (b) the generalized force vector (that includes the effects of contact and ligamentous forces/moments)
   (c) the ground reaction forces and center-of-pressure generated by the model
4. A separate function for computing contact model outputs (GRFs and cop) is also required and compiled into MATLAB as a mex-function. This enables the efficient computation of numerical Jacobians of the GRFs with respect to Q, without the additional overhead of evaluating the whole model.

Once the skeletal and muscle models are compiled for MATLAB as Simulink S-functions they are linked into the NMT framework. An example of the Simulink model for stages 1 and 2 of the NMT method are presented below describing the interaction of the controller with the model.

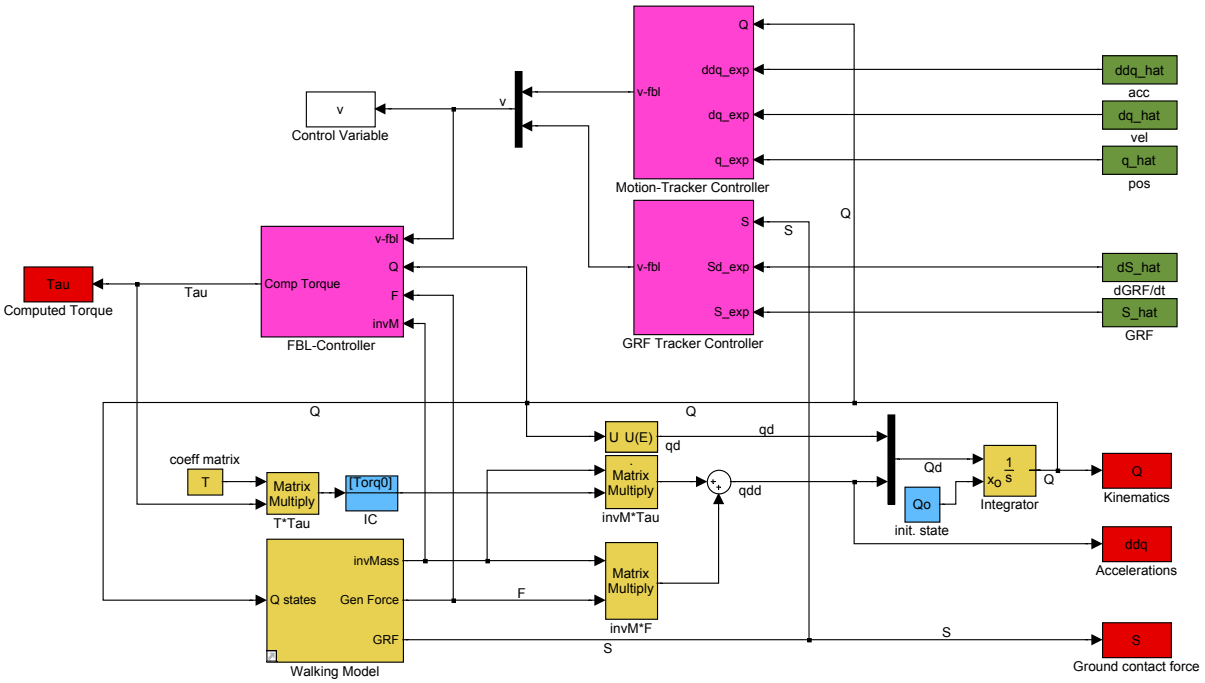

Figure 3.3: Simulink model of stage 1 of NMT method.
Skeletal motion tracker takes experimental kinematic and GRF inputs (green). Inputs are compared with current model kinematics and contact forces by the motion and GRF feedback controllers to determine the controls, v, to the forward dynamics model that is linearized by the FBL controller (all control elements in magenta). The FBL law returns torques which are the outputs of the inverse system (red) and are fed forward into the skeletal model (forward dynamics model elements in gold). Forward simulation produces the kinematic states and GRFs as system outputs (also in red).

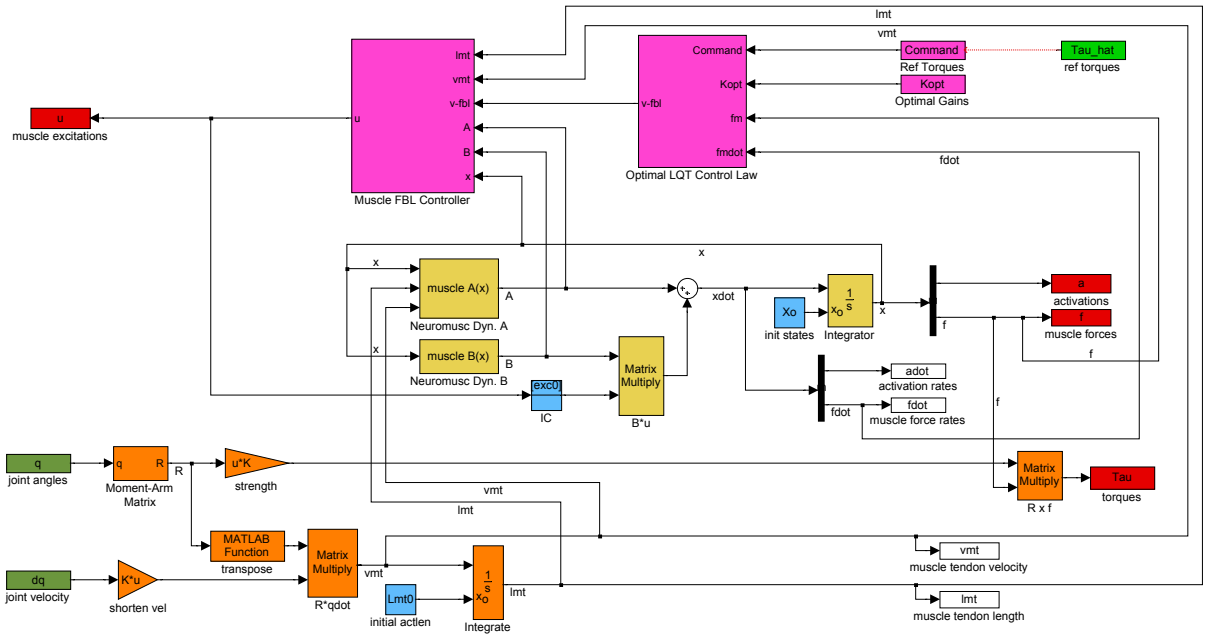

Figure 3.4: Simulink model of stage 2 of NMT method.

Optimal gains and command signals for the neuromuscular LQT system are computed offline (red line) based on reference torque inputs (green). Optimal torque tracking controller and FBL law are depicted in magenta. Output of the FBL controller are the neural excitations, u (red). These are the inputs to the neuromuscular dynamics (gold) along with kinematics from stage 1 (green). Orange elements represent the geometrical and strength transformations for moment arms, muscle lengths and shortening velocities. Muscle activations, forces and net muscular torques are outputs of the forward model (also in red).

Chapter 4

NMT Benchmark Study

The second aim of the dissertation is to compare the performance of the NMT and the inverse dynamics (IVD) methods to estimate muscle moments using a known solution from a dynamic optimization (LSPO) "gold standard" as the source of the data for analysis. Applying the IVD and tracking methods on experimental data may provide different answers, but it would be difficult to ascertain with certainty which method was more accurate, without *a priori* knowledge of the actual motion. Furthermore, muscle forces and excitations estimated from the NMT method are compared to the actual muscle forces (from dynamic optimization) to assess how accurately the NMT could uncover the muscle forces used to actuate the model.

In particular, jumping was chosen because this particular task embodies features that make tracking difficult: it is a highly dynamical task; one that is characterized by rapid muscle force production; relatively unconstrained joint motion, and nonlinear ground contact dynamics. Therefore deficiencies in the linearization approach should be most apparent for this task. Furthermore, jumping is symmetric and therefore is more tractable in solving the dynamic optimization problem.

4.1 Comparison Methods

A planar musculoskeletal model of the human body comprising 4 segments, 6 degrees-of-freedom, and 9 lower-limb muscles was used to simulate vertical jumping (4.1). LSPO was employed to determine the discretized muscle excitations (20 nodes per muscle) that maximized jump height, subject to the model beginning from a static squatting position (*Pandy et al.* (1990); *Anderson and Pandy* (1999)). An

adaptive simulated annealing (ASA) algorithm (*Ingber* (1993)) was used to increase confidence that the solution obtained was a global maximum for the redundant biomechanical system. The ASA algorithm terminated after 100 objective function evaluations with no improvement in performance. The ASA solution served as the initial guess (u_g in Fig. 4.2) to a sequential quadratic programming routine, which then ran until convergence was achieved.

The resulting muscle forces, joint torques, segment angles, and ground-contact forces defined the "actual" performance. Segment angles and ground forces were sampled at frequencies of 120 Hz and 1080 Hz, respectively, to correspond with typical motion-capture and force-plate recordings. Gaussian noise was added with a standard deviation of 1°, 2°, 3° and 5° for the HAT, thigh, shank, and foot segment angles, respectively, while 2% of body weight was used for ground force/moment noise. In order to simulate non-random noise, such as skin movement and other measurement artifacts, signal bias was also added to the data with peak magnitudes equivalent to the noise standard deviations. The ground-moment acting on the foot segment (due to the distance of the center-of-pressure from the foot center-of-mass) was biased by up to 20% of the peak moment to simulate possible errors due to measurement offsets and foot model inaccuracies. Bias was not present at time t =0 because the initial posture of the model could always be chosen to match the observed posture, and the foot springs could be adjusted to match the initial ground forces. No ground force bias was present at lift-off because the ground force must be zero at that time. The noise-contaminated segment angles and ground forces/moment, which simulated raw data recorded from a motion-capture experiment, were low-pass filtered using cut-off frequencies of 10 Hz and 50 Hz, respectively. These data served as the input "observations" to the NMT method as well as an IVD analysis.

4.1.1 Computing Muscular Joint Torques

Stage 1, of the NMT method was matched against inverse dynamics to compute the resultant muscle torques required to produce the observed kinematics and ground reaction forces. For both

approaches the observed position data ($\hat{\theta}$) was differentiated twice after low-pass filtering, to provide velocity ($\dot{\hat{\theta}}$) and acceleration ($\ddot{\hat{\theta}}$) estimates of the model segments. The skeletal dynamics of the model, including contact, were linearized according to the feedback linearization (FBL) control developed earlier (Eq. 3.10). Contact dynamics were identical to that of *Anderson and Pandy* (1999), which are a function of the kinematics of five points on the sole of each foot. Since the contact model is velocity dependent, it was only necessary to differentiate the contact model outputs, s, once to obtain s as a function of the torques, τ, to establish the FBL law. Only the joint angles were tracked since the precision of foot translations would be insufficient to accurately evaluate the ground forces with contact model. For example, errors of half a centimeter result in differences of over 100N in contact force. Control of the translational degrees-of-freedom of the model was achieved through the additional tracking of horizontal (s_1), vertical (s_2) ground reaction forces and sagittal plane reaction moment (s_3).

The skeletal motion tracking poles, λ, which define gains on the feedback errors, were selected initially by multiplying the filter cut-off frequencies of each measurement by five. Doubling, tripling, and quadrupling the pole values associated with ground forces successively improved ground force tracking accuracy, but multiplying by a factor of 5 resulted in no further improvement. The least-squares weightings were assigned according to the accuracy of each measurement, such that HAT angle and ground forces were each assigned a value of 1, while thigh, shank and foot angles were assigned progressively less weights. Ignoring foot rotations reduced tracking error even further, as did the doubling of ground-force weightings. The ground moment (s_3) pole was not doubled, as it had considerably more bias than did the vertical and fore-aft forces. Skeletal motion tracking parameters used to generate the results are given in Table 1. Marginal reductions in tracking error were obtained by refining these parameters even further.

An inverse dynamics analysis was performed using a matrix pseudo-inverse approach (Eq. 4.1) ignoring foot translations and without solving a weighted least squares problem for the torques.

Table 4.1: Skeletal motion tracking system poles (λ) and least squares weightings (w)

y	λ	w
θ_1	50	0.001
θ_2	50	0.7
θ_3	50	0.8
θ_4	50	1.0
s_1	1000	2.0
s_2	1000	2.0
s_3	1000	1.0

$$\tau = T^{-1}[\Im(\hat{\theta}, \dot{\hat{\theta}}) + \hat{S} - M(\hat{\theta})\ddot{\hat{\theta}}] \tag{4.1}$$

The pseudo-inverse method is more accurate than recursive Newton-Euler methods (*Kuo* (1998); *Cahouet et al.* (2002)) and does not require residual forces. The torque estimates from both the NMT and IVD analyses are presented in Fig. 4.3.

4.1.2 Elucidating Individual Muscle Forces

Stage 2 of the NMT method (3.4) was applied to estimate the muscle forces in maximum height jumping from the joint torques necessary to synthesize kinematics and ground-reaction forces that matched the "experimental" data (Stage 1).

The neuromuscular dynamics were characterized by the first order activation and contraction dynamics described by *Zajac* (1989). The neuromuscular system state, x, was comprised of activations, muscle fiber lengths and complete musculotendon lengths. Musculotendon lengths were computed by integrating the musculotendon velocities that were determined by the product of the instantaneous moment-arm, $r(\theta)$, and the joint angular velocity, $\dot{\theta}$,where the states $(\theta, \dot{\theta})$ were the forward model simulation results from Stage 1. All muscles moment arms were obtained according to the corresponding muscles from *Anderson* (1999) and splined as functions of θ.

Individual muscle controls (excitations) were determined by solving the neuromuscular LQT

problem (Eq. 3.19) for the optimal muscle force production rates, η.

In solving the neuromuscular LQT for individual muscle excitations, the torque tracking errors for hip, knee, and ankle joints for the present musculoskeletal model (4.1) were assigned equal weighting, κ_Q, such that $Q = \kappa_Q[diagonal\{1,1,1\}]$. Because R is the weighting for the rate of force production, η, squared (as in Eq. 3.19), R_i was normalized by the squared peak isometric force of the corresponding muscle. The biarticular muscles (HAMS, RF, and GAS) were initially scaled by $\frac{1}{2}$ to encourage the re-distribution of loading to these muscles, and these weightings were adjusted further to encourage loading of HAMS and RF in particular. The final weightings used for R were as follows:

$$R = \kappa_R \cdot \left[diagonal \left\{ \begin{array}{cccccccccc} \frac{1}{f^2_{gmax}} & \frac{1}{f^2_{ilpso}} & \frac{0.1}{f^2_{hams}} & \frac{0.3}{f^2_{rf}} & \frac{1}{f^2_{vas}} & \frac{1}{f^2_{bfsh}} & \frac{0.75}{f^2_{gas}} & \frac{1}{f^2_{sol}} & \frac{1}{f^2_{ta}} \end{array} \right\} \right]$$

Given the large magnitude of the maximum isometric muscle forces, $\kappa_R = 1000$ was used so that the system Ricatti matrix equation (Eq. 3.20) was adequately scaled. Accordingly, $\kappa_Q = 1500$ was found to adequately reject torque tracking errors by the neuromuscular system.

Table 4.2: Model maximum isometric forces for vertical jumping

f_{gmax}	f_{ilipso}	f_{hams}	f_{rf}	f_{vas}	f_{bfsh}	f_{gas}	f_{sol}	f_{ta}
2480 N	1627 N	2814 N	1320 N	6865 N	864 N	1651 N	2125 N	1003 N

4.2 Method Comparison Results

The LSPO algorithm required 21,000 evaluations of jump height to converge to the dynamic optimization solution, which took more than 24 hrs of CPU time. The optimal solution produced a jump height of 60.1 cm, in close agreement with earlier findings by *Anderson and Pandy* (1993), who used a similar model. The NMT method took 84 secs of CPU time (28 secs for skeletal motion tracking plus 56 secs for neuromuscular tracking) to determine continuous muscle excitation histories for jumping on the same desktop PC.

There was good agreement between the joint torques calculated by the skeletal motion tracker and the actual torques obtained from LSPO (Fig. 4.3). Small differences were evident and were attributable to the significance of random and bias noise, but these differences did not influence the ability of the skeletal motion tracker to accurately reproduce the observed segment kinematics and ground forces/moment (Figs 4.4 and 4.5). The segment kinematics produced by the skeletal motion tracker were closer to the actual kinematics than the observed quantities (Fig. 4.4) especially for ankle velocities, and the bias in the ground moment observation was practically eliminated (Fig. 4.5(B)).

The joint torques computed from an IVD analysis were significantly different from the actual torques (Fig. 4.3). Furthermore, when the IVD torques were used in a forward simulation of the model, the resulting segment kinematics and ground forces deviated from the actual trajectories (Fig. 4.4), causing the model to leave the ground early (Fig. 4.5).

Muscle excitations determined by neuromuscular tracking indicated muscle activity timings that were in agreement with the actual muscle inputs, except for those of HAMS and RF. There was better agreement between the muscle forces estimated by the neuromuscular tracker and the actual muscle forces for most of the muscles in the model (Fig. 4.6). Coordination of the hip and knee extensors and ankle plantarflexors (GMAX, VAS, SOL, and GAS), the prime movers for vertical jumping (*Pandy et al.* (1990); *van Soest et al.* (1993)), was consistent with that predicted by the parameter optimization solution, but the peak force calculated for VAS was lower in the NMT solution. The most significant difference between the two methods was related to the forces estimated for HAMS and RF. For both of these muscles, the forces computed by the NMT method were much lower than those obtained by parameter optimization. Overall, however, the NMT torques were similar to the actual torques (Fig. 4.7A), and produced segment angles and ground forces that nearly duplicated the actual values (Figs. 4.8 and 4.9), resulting in a jump height of 58.8 cm.

4.3 Tracking Experimental Jumping Data

In this section, we employ the same aforementioned model to track real experimental data to verify that previous results were not unduly favorable due to any inherent consistency of the model and the synthetic data since the data was generated using the same model. Although random and bias noise was added to the dynamic optimization solution, it was not data collected from a subject and more significant differences may exist that make tracking impossible. The same NMT methodology as above is employed, except that experimental data is used, the contact model is modified, and EMG is included in the neuromuscular tracking stage.

4.3.1 Experimental Data

The NMT method was used to track joint kinematics and GRFs measured for a subject performing a maximum-height jump beginning from a static squat. The kinematics, force plate, and muscle EMG data recorded by *Anderson and Pandy* (1999) for a single subject (age 24 yrs, weight 71.39kg, and height 1.746 m) were used as inputs to the NMT method. The 3D positions of markers affixed to the legs and torso were recorded at 60 Hz and were used to determine the position of the HAT and the relative joint angles corresponding to a planar musculoskeletal model (Fig 4.1) except generalized coordinates were described by physiological joint angles (i.e. HAT orientation, hip flexion, knee extension and ankle dorsiflexion). Model anthropometry such as segment lengths and body weight were measured from the subject, while segment masses and moments of inertia were calculated using the regression equations reported by *McConville et al.* (1980). The model was actuated by same nine leg muscles (Fig. 4.1). The musculotendinous parameters were also taken from *Anderson and Pandy* (1999).

GRFs and moments for both feet were recorded at 1000 Hz from a force plate. The joint angles

and GRFs were low-pass filtered at 10 Hz and 50 Hz, respectively. EMG signals from seven leg muscles: gluteus maximus (GMAX), hamstrings (HAMS), rectus femoris (RF), vasti (VAS), gastrocnemius (GAS), soleus (SOL), and tibialis anterior (TA), were recorded using surface electrodes. The EMG signals were rectified, enveloped, and normalized by the peak voltage recorded, except for tibialis anterior, which was not expected to reach maximal values during the jump and thus was scaled to half the peak value recorded.

4.3.2 Ground Contact Model

The original ground contact model developed by *Anderson and Pandy* (1999) was found to produce contact behavior that was unrealistic. In particular, each horizontal spring force was being compared to its vertical counterpart to determine whether slipping occurred, and if so, the horizontal component was set equal to the limit of the frictional force. In reality, however, it is the total horizontal force acting on the foot that must be compared to the total vertical force. If this ratio exceeds the coefficient of friction, the foot should slip and the resultant horizontal force must then be zero. These conditions for slipping were implemented in the current model while preserving the vertical and horizontal spring functions given by *Anderson and Pandy* (1999).

4.3.3 Skeletal Motion Tracking for Experimental Movement Data

The method of computing torques from the experimental data is identical to that used to track the synthetic jump data, above 4.1.1. The only modification was in the description of the model degrees of freedom. In the experimental case, model segmental angles were transformed into joint angles to correspond with the available experimental data, and the model was feedback linearized after this transformation. The new kinematic outputs are ankle dorsiflexion, knee extension, hip flexion and the sagittal plane orientation of the HAT, which correspond to θ_1 through θ_4, respectively. The tracking weightings are given in Table 4.3.

Table 4.3: Skeletal motion tracking system poles (λ) and least squares weightings (w) for experimental data

y	λ	w
θ_1	50	0.2
θ_2	50	0.75
θ_3	50	1.0
θ_4	50	0.9
s_1	250	2.0
s_2	250	2.0
s_3	250	0.25

4.3.4 Neuromuscular Tracking Including EMG

Because of the discrepancy between the muscle forces estimated from the dynamic optimization solution and those computed by the NMT method (Fig. 4.6), we include EMG data from available muscles into the data tracking set to test if qualitative improvements in muscle activity could be garnered by tracking EMG.

We assumed that rectified and enveloped EMG data corresponds well with the model activations. Therefore, the neuromuscular system dynamics (3.13) remained unchanged, but the outputs (3.14) now include the activation states, a.

$$\dot{x} = A(x) + B(x)u \tag{4.2}$$

$$y = \left\{ \begin{array}{c} f \\ a \end{array} \right\} \tag{4.3}$$

The resulting feedback linearizing control law is

4.4

$$u = \left[\frac{\partial y}{\partial x}B\right]^{-1} \left\{\eta - \frac{\partial y}{\partial x}A\right\} \tag{4.4}$$

where $\eta = \dot{y}$. The neuromuscular LQT can now be written as:

$$J = \frac{1}{2}\int_0^{t_f} \left[\left(C \left\{ \begin{array}{c} f \\ a \end{array} \right\} - \left\{ \begin{array}{c} \hat{\tau} \\ \hat{a} \end{array} \right\} \right)^T Q \left(C \left\{ \begin{array}{c} f \\ a \end{array} \right\} - \left\{ \begin{array}{c} \hat{\tau} \\ \hat{a} \end{array} \right\} \right) + \eta^T R \eta \right] dt \tag{4.5}$$

where the output transformation matrix, $C_{(m+7)\times 2m}$, has the moment-arm matrix as the first m rows and an additional seven sparse rows with ones corresponding to the muscle's where the processed EMG signals, $\hat{a}$, are available. The tracking error weighting matrix, Q, is used to balance between torque and EMG tracking.

Table 4.4: Neuromuscular weightings (Q) for torque and EMG tracking errors

Output	Q
τ_{ankle}	$\frac{500}{max(\hat{\tau}_{ankle})}$
τ_{knee}	$\frac{300}{max(\hat{\tau}_{knee})}$
τ_{hip}	$\frac{300}{max(\hat{\tau}_{hip})}$
a_{gmax}	1
a_{hams}	50
a_{rf}	40
a_{vas}	1
a_{gas}	10
a_{sol}	1
a_{ta}	1

$$R = \kappa_R \cdot \left[diagonal \left\{ \begin{array}{ccccccccc} \frac{1}{f^2_{gmax}} & \frac{1}{f^2_{ilpso}} & \frac{0.1}{f^2_{hams}} & \frac{0.3}{f^2_{rf}} & \frac{1}{f^2_{vas}} & \frac{1}{f^2_{bfsh}} & \frac{0.75}{f^2_{gas}} & \frac{1}{f^2_{sol}} & \frac{1}{f^2_{ta}} \end{array} \right\} \right]$$

4.4 Experimental Data Tracking Results

The NMT method used 140 s of CPU time on a Pentium 4 desktop PC to determine the continuous neural excitations to produce a muscle-driven forward simulation of jumping. Total CPU time was comprised of 43 s for skeletal motion tracking (stage 1), 92 s for neuromuscular tracking (stage 2) that included EMG, and 5 s for the complete forward simulation of the neuromusculoskeletal model. EMG tracking nearly doubled the CPU time for stage 2 from 47 s to 92 s.

The NMT method closely reproduced the joint kinematics and GRFs measured for the subject (Fig. 4.10 and 4.11), in spite of the fact that the body was modeled as a planar four-segment linkage. Although a peak discrepancy of 12° was observed for the tracking of the ankle angle, the differences between the computed and measured angles for the remaining joints were less than 4°. The model also left the ground 0.03 s earlier at 0.47 s, compared to 0.50 s for the subject. In contrast, when torques computed from inverse dynamics were used to drive the model in a forward simulation, differences between model and experiment for the knee and hip approached 40° at lift-off (Fig. 4.10), and the model left the ground 0.06 s earlier than the subject. As expected, the largest discrepancy in the GRFs was in the reaction moment (Fig. 4.11, triangles). The NMT-computed muscle torques were different from those obtained by inverse dynamics, particularly for the ankle (Fig. 4.12).

Consistent with EMG measurements, the predicted coordination of the primary extensor muscles in the model (Fig. 4.13, GMAX, VAS and SOL) was proximal-to-distal, which was also noted in earlier studies of human jumping (*Bobbert and van Ingen-Schenau* (1988); *Pandy et al.* (1990); *van Soest et al.* (1993)). These results support the validity of the muscle activations and muscle forces estimated by the NMT method.

EMG tracking affected the muscle coordination determined by the NMT method in stage 2, even though the muscular torques with and without EMG tracking were identical. As hoped, EMG tracking caused the calculated muscle activation patterns to move towards the measured EMG data (4.13). The most significant changes were seen in the activation patterns of the biarticular rectus femoris and gastrocnemius muscles. Peak activation of rectus femoris shifted to correspond with measured EMG at 0.3 s of the jump, and its peak force increased by 330 N (or 25% of the muscle's peak isometric force). Activation of gastrocnemius was reduced by nearly 50% in the model, with the first peak becoming more closely aligned with EMG, while gastrocnemius force decreased by 693 N (or 42% of the muscle's peak isometric force). Meanwhile, soleus force increased by 425 N (or 20% of the muscle's peak isometric

force) to compensate for the decrease in gastrocnemius recruitment.

4.5 Discussion of Benchmark Results

The purpose of this study was to present and demonstrate a computationally efficient and accurate method for calculating individual muscle forces during human movement, in contrast to more widely used approaches like IVD and LSPO. Forward simulation accuracy is obtained by dynamically tracking kinematics and ground forces, whereas computational speed is obtained by posing the dynamic optimization problem as an LQT problem. In this way, system dynamics are integrated once, rather than thousands of times, as is often required by LSPO (*Pandy et al.* (1992); *Anderson and Pandy* (2001a); *Neptune et al.* (2001)). The results demonstrate that the NMT method can produce estimates of muscle forces roughly 1000 times faster than LSPO.

While the concept of tracking has been used previously to estimate muscle forces from human movement data (*Davy and Audu* (1987); *Neptune et al.* (2001); *Thelen et al.* (2003); *Thelen and Anderson* (2006)), the two developments introduced by the NMT method offer distinct advantages. First, ground-force references included in skeletal motion tracking produce more accurate estimates of joint torques, which are needed in order to perform an accurate forward simulation of the movement. The results demonstrate very clearly that the joint torques computed from IVD cannot be used for this purpose (Figs. 4.3,4.4, and 4.5). Unlike IVD, the NMT method does not apply measured ground forces directly to a model; instead, it expects ground forces to be synthesized by the model in order to be compared to observed data. Synthesis improves simulation accuracy because the model must satisfy both the link-segment kinematics and ground-contact dynamics together, which reflect the reality that body motion and ground reaction forces are coupled. Many IVD analyses inadvertently decouple kinematics from ground forces by including residual forces to account for inconsistencies between input accelerations and ground forces. The NMT method does not artificially adjust input kinematics or ground forces in order to eliminate residual forces (e.g. *Thelen and Anderson* (2006)). Accordingly, the skeletal motion

tracker produced jumping kinematics that agreed more closely with the actual kinematics than with the observed data (4.4, Foot and Shank). This occurred because the model had to satisfy system dynamics and it closely tracked more accurate ground reaction forces, which were more heavily weighted than the segment kinematics. These results indicate that if the model is a good representative of the subject (in the case of synthesized data they were one and the same) then the model itself acts like dynamic filter, to obtain movement accuracy that is superior to the experimental kinematic data.

The second advantage offered by the NMT method is that it solves the muscle redundancy problem dynamically and optimizes muscle performance over the entire task period. Because neuromuscular tracking is partitioned from the nonlinearities of skeletal dynamics in the optimal control problem, more efficient LQT techniques can be exploited when solving the problem of muscle redundancy. *Thelen et al.* (2003) introduced an approach that is conceptually similar to the NMT approach, but utilizes static optimization to resolve the muscle redundancy problem. Unfortunately, static optimization cannot accommodate time-dependent performance criteria, such as total muscular effort. *Menegaldo et al.* (2006) formulated a similar minimization of torque-tracking error and muscular effort in order to dynamically determine individual muscle forces for postural control. However, the problem was solved using a general recursive optimal control solver, employing direct collocation methods, and required an average of 87 min to compute muscle forces, which tracked ideal torques obtained from a previous postural control simulation. By comparison, the neuromuscular tracker required 56 secs to track non-ideal torques computed from noisy data for a highly dynamical task.

Although the NMT method and LSPO both solved a dynamic optimization problem, the optimization problems were different, which explains why the muscle excitations and forces computed by these two methods were not identical (Fig. 4.6). Whereas LSPO maximized jump height without regard to the cost of generating muscle force, the NMT method minimized torque-tracking error and muscle effort. It is not surprising, therefore, that the NMT solution utilized less co-contraction (Fig. 4.6,

compare HAMS to VAS and RF) to satisfy the muscle effort criterion. Differences are also attributed to the different solution techniques to the optimal control problem. Nodal excitation values are optimized by LSPO and thus limit the rate of variation, whereas the NMT method can vary excitations instantaneously, consistent with neural impulses, and thereby appear to be more erratic (4.6, compare solid lines). It is important to note that neither the NMT nor the LSPO solution corresponded well to EMG data reported by *Anderson and Pandy* (1999) for HAMS and RF. Both methods, however, produced a proximal-to-distal sequence of muscle recruitment, consistent with experiment (*Bobbert and van Ingen-Schenau* (1988); *Pandy et al.* (1990); *Anderson and Pandy* (1993, 1999)).

By tracking experimental data, as well, using the same model as with simulated data, we have demonstrated that the NMT method remains effective on real data and does not require inherent consistency between subject and model to produce accurate results (Figs. 4.10 and 4.11). The philosophy behind the NMT method is one that leverages all of the available biomechanical measurements. The NMT method was developed (3) to track joint kinematics and GRFs simultaneously, but, as we have shown here (Eqs. 4.2-4.5), it can easily be extended to follow measured muscle activity (EMG) in the dynamic distribution of muscle control. The results (4.13) demonstrate both the feasibility of tracking EMG within the NMT framework and the improvements in muscle behavior towards measured EMG even in a simplistic model. Given the significant differences in muscle force estimates (i.e., -693 to +425 N) when EMG tracking was included, there is a legitimate concern that these differences could lead to different prognoses of tissue loading. Because EMG provides another independent view of movement behavior, modeled muscle activity should at least be qualitatively similar to measured EMG before muscle force estimates can be trusted. EMG tracking is an attractive option, given that EMG data has been shown to improve the quality of forward simulations of movement (*White and Winter* (1993); *Jonkers et al.* (2002); *Lloyd and Besier* (2003)).

In tracking experimental jumping data, the model reproduced the major features of the subject's

jump although differences between model and experiment were evident in the ankle kinematics and in the vertical GRF prior to lift-off (Figs. 4.10 and 4.11). These differences are not a direct shortcoming of the NMT method, but instead highlight a deficiency of the model itself. In particular, because the model (Fig. 4.1) did not have separate toes, it could not simulate rocking onto the toes during the initial phase of the jump ($<$0.3 s), which was evident in the experimental data. To compensate for a lack of separate toes, the NMT primarily manipulated the ankle to obtain the desired ground reaction forces as well as the motion of the whole body. Consequently, the differences in ankle angle between model and experiment were the most significant at up to 11°. We also attribute the slightly earlier lift-off time of the model to a lack of toes, which would have increased the duration of ground contact.

Differences were also noted between the muscle activations predicted by the model and the measured EMG, which can be explained by modeling simplifications and measurement inaccuracies. First, only 9 muscles actuated the model, whereas more than 40 muscles actuate each human leg. Second, the lumped-parameter muscle model (*Zajac* (1989)) used in this study does not fully represent the complex neural and muscular interactions present *in vivo*. Also, the parameters that govern the behavior of the muscle model (e.g., optimal muscle-fiber length, tendon rest length, muscle moment arms, etc.) were taken directly from *Anderson and Pandy* (1999) (which correspond to *Delp* (1990)) and were not specific to the subject used in this study. Third, surface EMG is predominantly a measure of voltage changes of the muscle fibers closest to the electrode. Consequently, EMG itself is not a quantitatively accurate measure of the complete muscle activity as it relates to muscle force. If EMG were accurate and reliable quantitatively, musculoskeletal models for estimating muscle force would not be necessary. Nonetheless, improvements in models to transform EMG to muscle force and joint moments are improving by combining forward dynamic muscle models and measured moments from a dynamometer or from inverse dynamics analysis (*Lloyd and Besier* (2003); *Buchanan et al.* (2004, 2005)). These developments fit nicely with the NMT method, which can accommodate these models so that they could benefit from feedback control to track torques from skeletal motion tracking instead of

inverse dynamics.

The main limitation of the LSPO approach is that it is difficult to identify the source of discrepancy between simulation and experiment, which can be the result of a deficient model, an inadequate performance criterion, or a failure to converge to the optimal solution. Any analysis to pinpoint the cause is virtually impossible due to the computational expense of reevaluating a parameter optimization solution. In contrast, a requirement of the NMT method is that the model be capable of reproducing the movement observations; otherwise, tracking simply fails or yields poor tracking accuracy. Unlike parameter optimization, this can be assessed in a matter of seconds with the NMT method. Thus, NMT can be used to quickly test the suitability of a model and/or a candidate performance criterion in estimating muscle forces for a given motor task. In fact, this was the case in the present study with regard to contact. The tracker was unable to accurately track kinematics and GRFs simultaneously until a more realistic model of ground contact was implemented.

Once a model has been validated against experiment using NMT, the same model can then be applied in the broader optimal control context (i.e., not tracking) to: 1) predict novel movements, and/or 2) determine the effect of an assumed performance criterion on the calculated values of muscle force. An NMT solution provides a valid starting point about which to vary the controls (neural excitations) in order to simulate a modified task or the same task with a modified model (e.g., incorporating the properties of muscle spasticity in a model of walking to simulate cerebral palsy gait).

Inverse dynamics and CMC (*Thelen and Anderson* (2006); *Thelen et al.* (2003)), in general, are less well suited for validating forward dynamics models because: 1) GRFs are not synthesized in either of these approaches, and 2) static optimization cannot be used to track joint moments, follow muscle EMG, and minimize effort over the task interval. Both the NMT and CMC methods require *a priori* motion data to define a tracking problem, which means that the accuracy of the muscle force estimates inevitably depends on the accuracy of kinematics and GRF measurements. However, unlike inverse dynamics and

CMC, the NMT method employs FBL to formulate an inverse of the complete model dynamics (i.e., 3.10 includes link-segment and contact dynamics), and therefore it must satisfy more conditions in a least-squares sense. Applying residual forces or a residual elimination analysis, as in the CMC method (*Thelen and Anderson* (2006)), serves to decouple contact dynamics (GRFs) from joint motion, so that each joint moment is only affected by the estimated joint angular acceleration corresponding to that joint. This has the undesired effect of enabling any model with the same dofs to track the experimental kinematics regardless of its anthropometry. Moreover, it eliminates the possibility of exploiting more accurate GRFs to improve the accuracy of model kinematics (beyond the experimental data), which our analysis using simulated data clearly demonstrated was possible by weighting GRFs more significantly than kinematics in the NMT formulation (Fig. 4.4).

Aside from requiring a priori motion data, the NMT method is limited in the system dynamics that it can represent, because FBL requires dynamics that are linear with respect to the controls and outputs that are explicit functions of the system state. This limitation restricts how contact and neuromuscular dynamics can be modeled. For example, reaction forces that are enforced kinematic constraints (e.g., rolling-without-slipping constraints) cannot be tracked in the current form of the NMT method, as these forces (i.e., Lagrange multipliers) are not explicit functions of the state only. Furthermore, muscle models that employ activation dynamics as nonlinear functions of the controls (neural excitations) cannot be directly incorporated into the NMT method.

In summary, the NMT method was used to determine the neural excitations and muscle forces needed to track measured joint angles and GRFs of a test subject performing a maximum-height jump. Including EMG in the tracking scheme garnered significant improvements in the quality of the estimated muscle activations and forces. In this regard, the NMT method is a powerful analysis tool that enables the movement scientist to leverage all available experimental data in order to deliver estimates of muscle and joint loading with increased confidence and with 3 orders of magnitude less computing time than

parameter optimization methods.

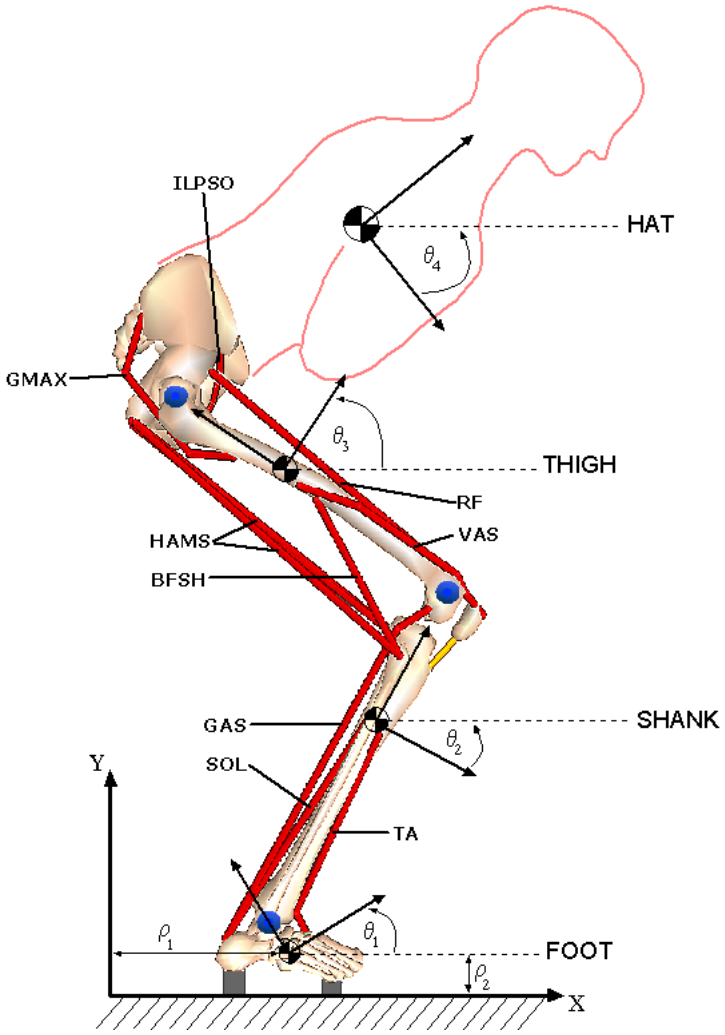

Figure 4.1: Human musculoskeletal model for simulating maximum height jumping. The model consists of 6 degrees of freedom for motion in the sagittal plane: foot, shank, thigh, and HAT angles, $\theta_1 ... \theta_4$, respectively; and foot translations, ρ_1 and ρ_2. The model includes 9 musculotendinous actuators: gluteus maximus (GMAX), iliopsoas (ILPSO), hamstrings (HAMS), biceps femoris short head (BFSH), rectus femoris (RF), vasti (VAS), gastrocnemius (GAS), soleus (SOL), and tibialis anterior (TA). Model parameters were based on data reported by *Anderson and Pandy* (1999).

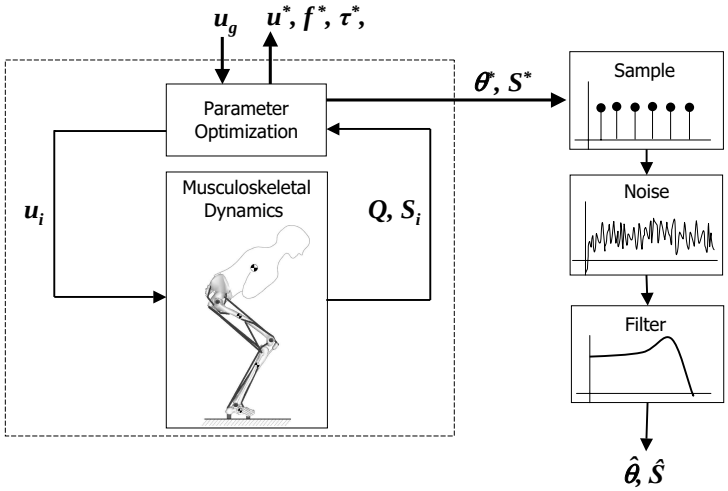

Figure 4.2: "Experimental" data synthesis methodology.
Parameter optimization was used to solve the dynamic optimization problem to maximize the vertical jump height of the musculoskeletal model (Fig. 4.1) . The controls, u^*, muscle forces, f^*, joint torques, τ^*; segment angles , θ^*, and ground-contact forces, s^*, from the optimal solution are then used to generate "experimental" observations $(\hat{\Theta}, \hat{s})$ by introducing typical sampling, noise and processing errors.

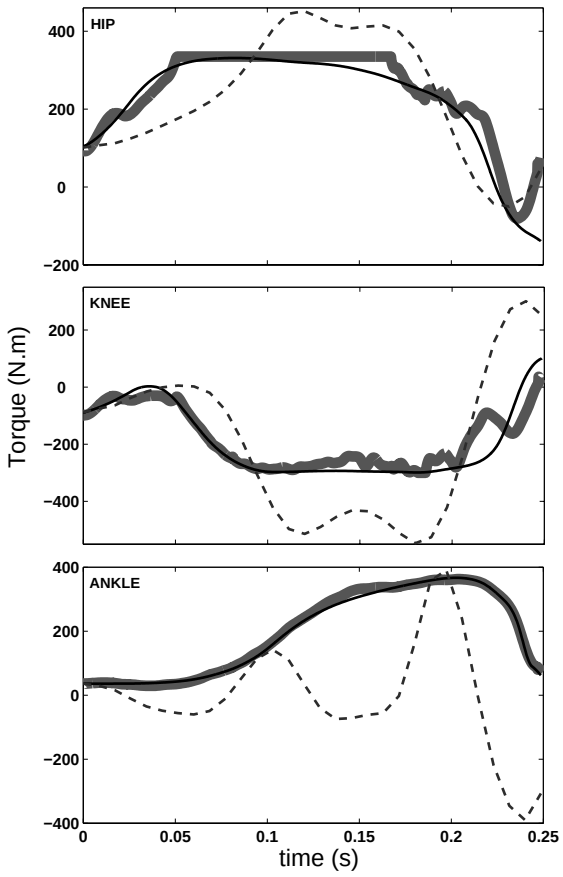

Figure 4.3: Joint torques for maximum-height jumping.
Torques computed by NMT (bold) and inverse dynamics (IVD, dashed) compared to actual torques (black thin) used to generate the simulated "experimental" observations.

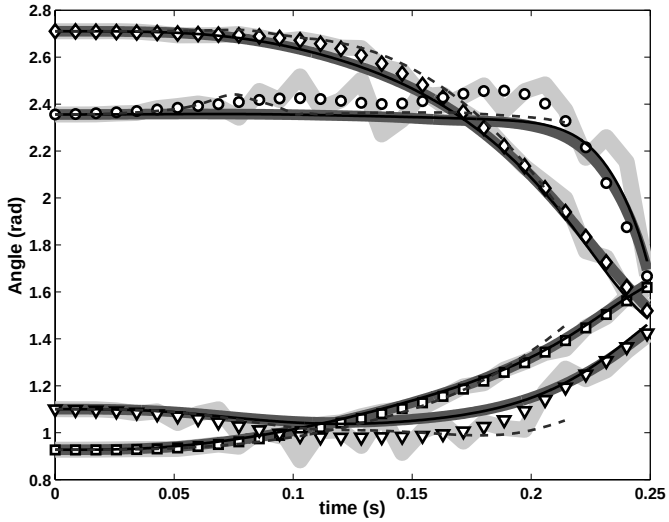

(A)

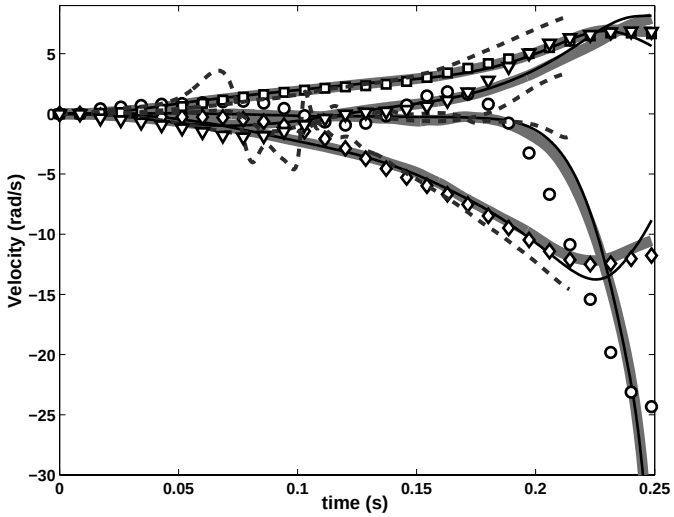

(B)

Figure 4.4: Tracking segment kinematics from maximum-height jump.
Segment angles (A) and velocities (B) obtained from skeletal motion tracking (bold) compared to filtered inputs (HAT-square, thigh-diamond, shank-triangle, foot-circle) and actual values (black thin) overlaid upon unfiltered observations (light gray). Torques obtained from inverse dynamics were applied to the model in a forward simulation to generate segment motion (dashed lines).

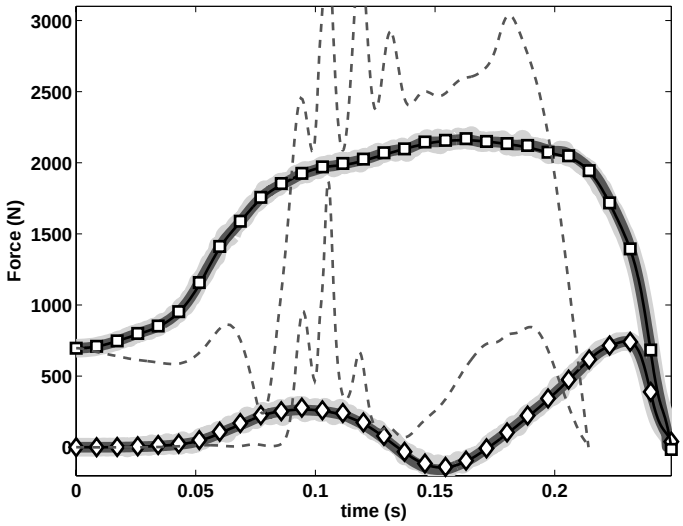

(A)

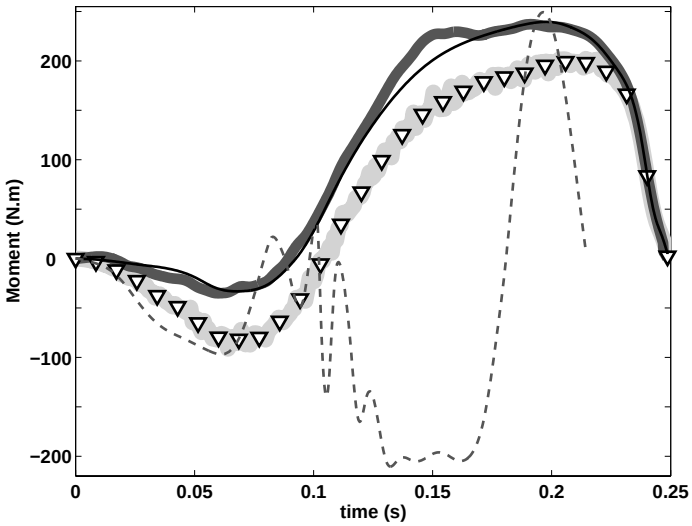

(B)

Figure 4.5: Tracking ground reaction forces and moment from maximum-height jump.
Model synthesized ground reaction forces (A) and moment (B) obtained from skeletal motion tracking (bold) compared to filtered inputs (vertical-square, fore-aft-diamond, moment-triangle) and actual values (black thin) overlaid upon unfiltered observations (light gray). Torques obtained from inverse dynamics were applied to the model in a forward simulation to generate ground reaction forces and moments (dashed lines) as well.

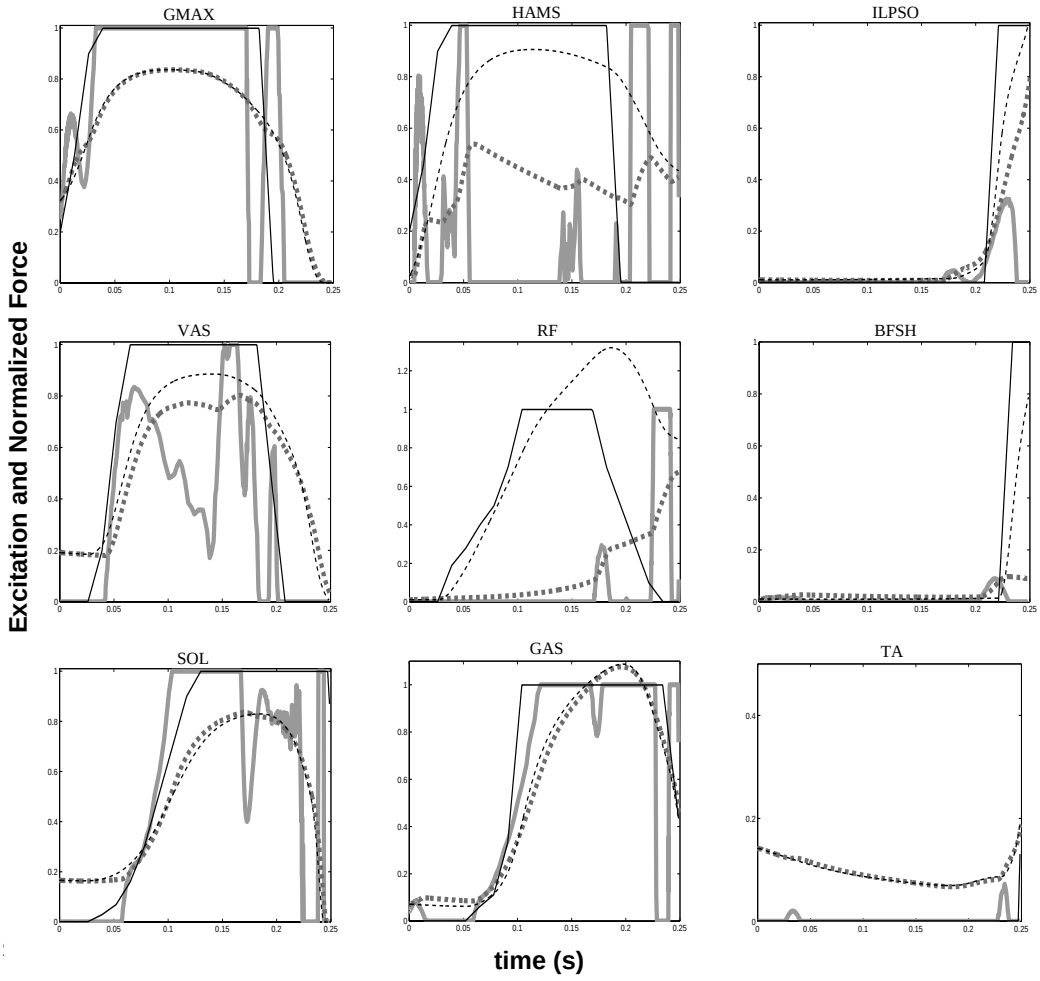

Figure 4.6: Estimated muscle activity for maximum height jumping.
Muscle excitations (gray lines) and normalized muscle forces (dashed gray) computed by the NMT method compared to muscle excitations (thin black) and normalized muscle forces (thin black dashed) determined by parameter optimization. See Figure 4.1 for muscle abbreviations.

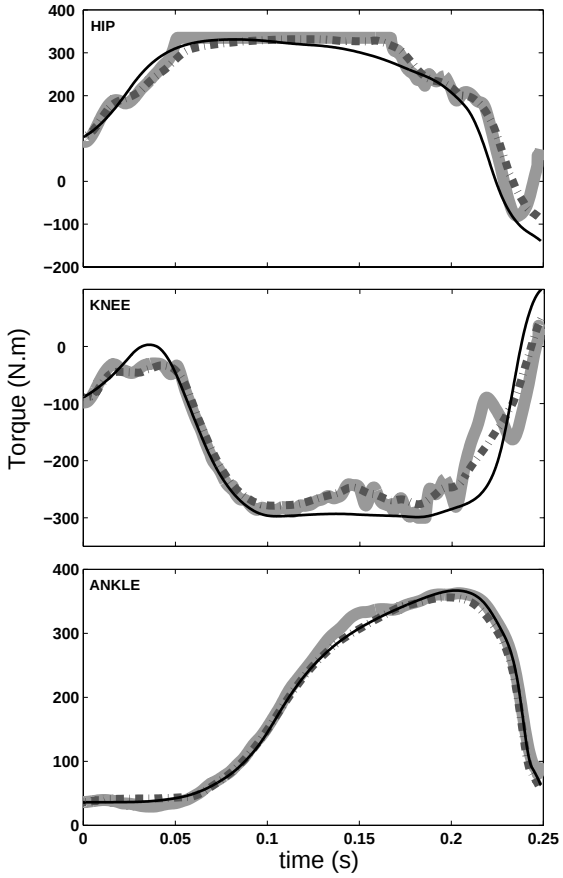

Figure 4.7: Neuromuscular torques for maximum height jump.
Individual joint torques for a maximum-height jump resulting from muscle forces computed by the neuromuscular tracker (NMT) compared to the actual torques predicted by parameter optimization (Actual). Joint torques obtained from the skeletal motion tracker (thick gray lines) are also shown (from Fig. 4.3)

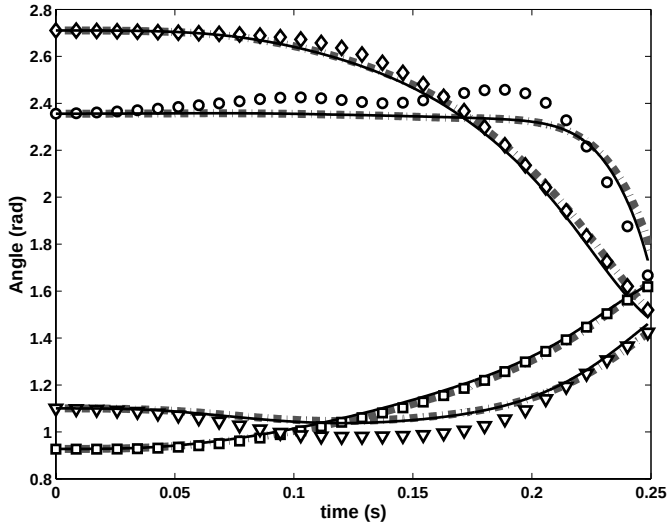

Figure 4.8: Neuromusculoskeletal simulation kinematics for maximum height jump. Segment angles resulting from the NMT simulation (NMT-thick dash-dot) compared to the actual performance (dark thin) and the input observations (HAT-square, thigh-diamond, shank-triangle, foot-circle)

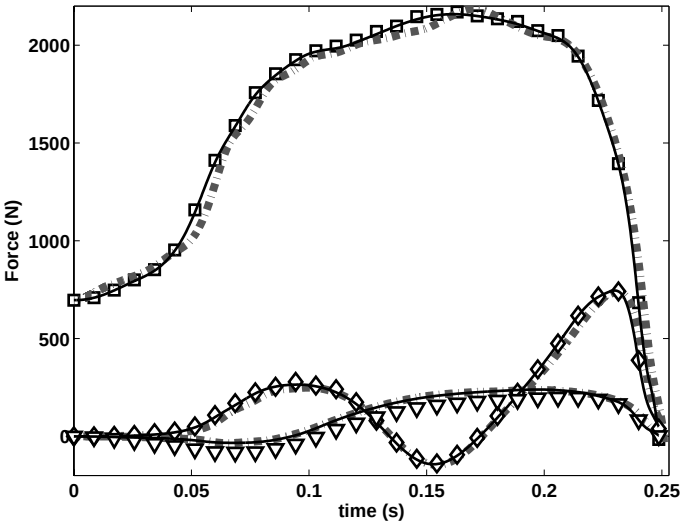

Figure 4.9: Neuromusculoskeletal simulation ground reaction forces for maximum height jump. Ground reaction forces resulting from the NMT simulation (NMT-thick dash-dot) compared to the actual performance (dark thin) and the input observations (vertical-square, fore-aft-diamond, moment-triangle)

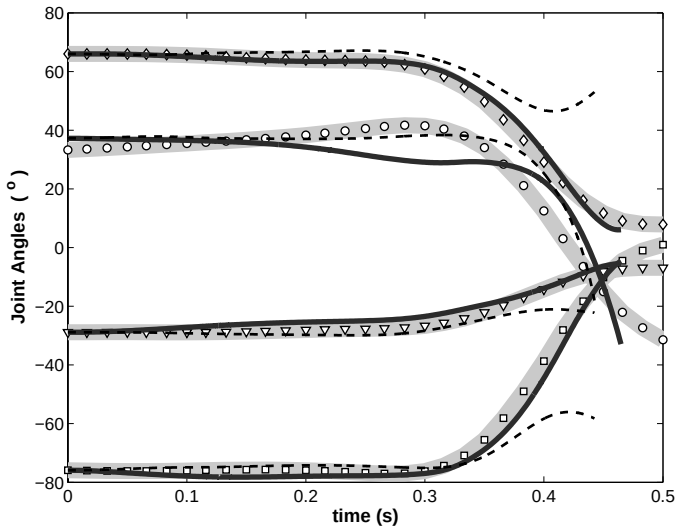

Figure 4.10: NMT kinematics of vertical jumping from experimental data.
Joint angles resulting from a forward simulation of the NMT-computed muscle forces (bold) compared to experimental results (shaded and identified by symbols: HAT-triangle; hip-diamond; knee-square, ankle-circle). Torques obtained from inverse dynamics were also applied to the model to produce a forward simulation (dashed lines).

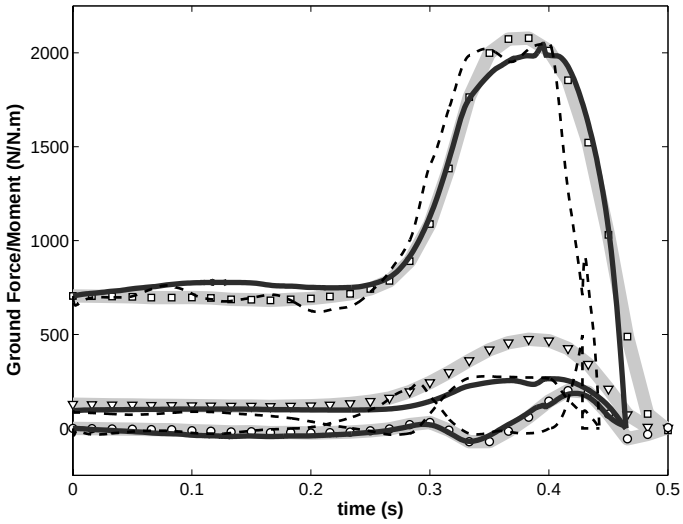

Figure 4.11: NMT ground reaction forces of vertical jumping from experimental data.
Ground reaction forces resulting from a forward simulation of the NMT-computed muscle controls (bold) compared to experimental results (shaded and identified by symbols: vertical square; fore-aft circle, moment triangle). Torques obtained from inverse dynamics were also applied to the model to produce a forward simulation (dashed lines).

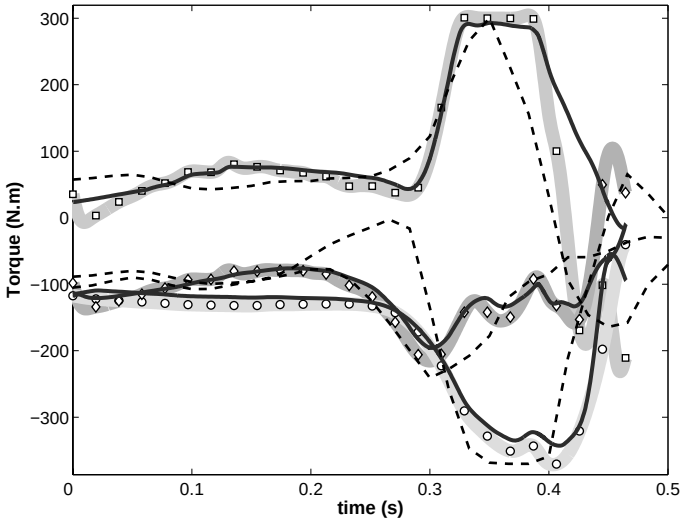

Figure 4.12: NMT torques for vertical jumping from experimental data.
Muscle torques obtained from the complete NMT method (bold lines) compared to results from Stage 1 only (shaded and identified by symbols: hip-diamond; knee-square, ankle-circle). The dotted lines are joint torques computed from inverse dynamics.

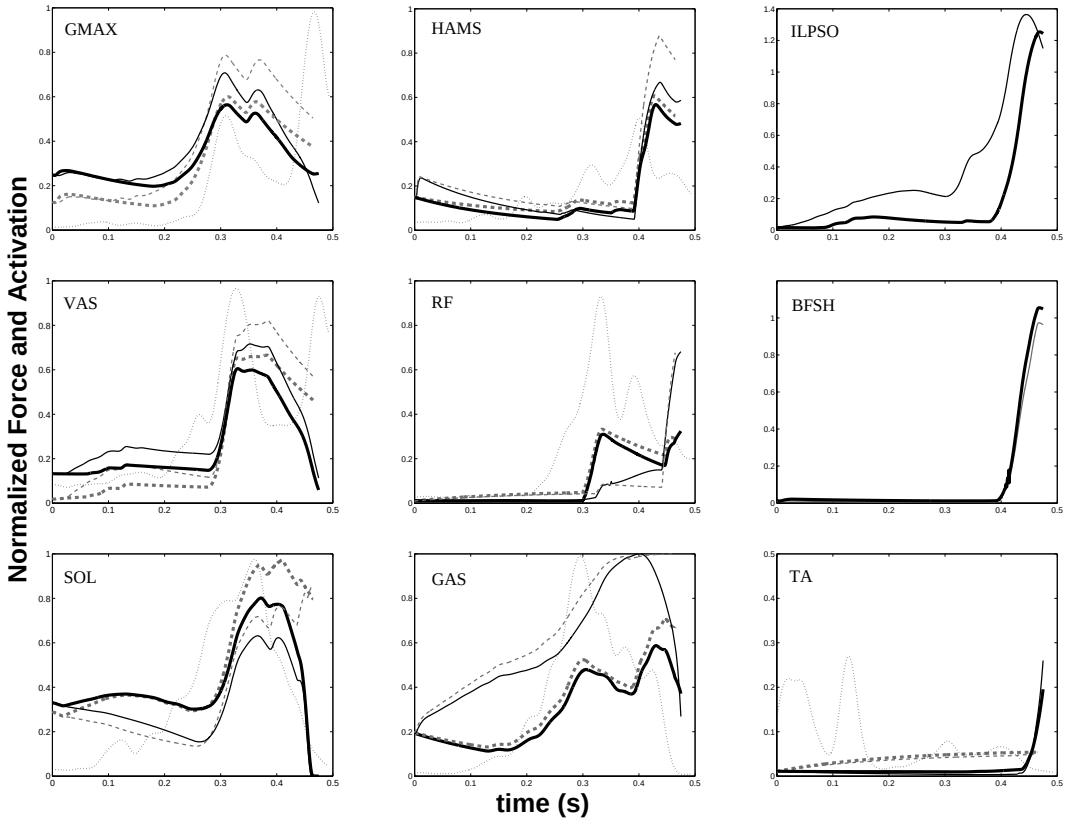

Figure 4.13: Estimated muscle activity and forces for vertical jumping from experimental data. Muscle activations and normalized muscle forces computed by the NMT method with EMG tracking (thick dashed and solid lines, respectively) compared to muscle activations and normalized muscle forces computed by the NMT method without EMG tracking (thin dashed and solid lines, respectively). Measured muscle EMG data from the subject are shown as dotted lines for measured muscles. Muscle forces were normalized by dividing by the maximum isometric force of each muscle.

Chapter 5

NMT Analysis for Human Gait

5.1 Introduction

Upright bipedal gait is one of the distinguishing characteristics of humans that separates us from the great apes and the rest of the animal kingdom. It is quintessentially one of the things that make us human. Unfortunately, gait disorders as a consequence of disease, such as diabetes; aging, where a large "boomer" generation is reaching retirement; and injury from recreation and vehicular accidents, are on the rise. At the same time that treatments from physiotherapy, orthopaedics, and pharmacology emerge, there remains several fundamental questions about the underlying mechanics of human gait. These include, but are not limited to, how muscles are coordinated to produce gait, what forces are generated by muscles and what are their contributions to joint loading and movement of the body?

Understanding the function of individual muscles is a very active area of biomechanics research spanning from the late 1930's to the present (*Elftman* (1939); *Bresler and Frankel* (1950); *Chow and Jacobson* (1971); *Townsend and Seireg* (1972); *Pedotti et al.* (1978); *Crowninshield and Brand* (1981); *Olney and Winter* (1985); *Davy and Audu* (1987); *White and Winter* (1993); *Taga* (1995); *Kepple et al.* (1997); *Anderson and Pandy* (2001a,b, 2003); *Neptune et al.* (2001, 2004); *Jonkers et al.* (2002, 2003); *Zajac et al.* (2002, 2003); *Pandy* (2003); *Thelen et al.* (2003); *Thelen and Anderson* (2006); *Higginson et al.* (2006); *Erdemir et al.* (2006); *Heintz and Gutierrez-Farewik* (2006)). The main challenges are in obtaining muscle forces that satisfy our understanding of skeletal motion (rigid-body dynamics) and muscle physiology and anatomy (musculoskeletal geometry) whilst satisfying our observations of the movement. The present methods of forward and inverse dynamics on their own are inadequate for one main reason: neither method can be used to verify if the model is, in fact, representative of the

subject. For example, it is possible to obtain smooth accurate looking torque profiles for stance from a three segment model (HAT, thigh, shank) using inverse dynamics with hip, knee, and ankle angles, and ground reaction forces (i.e. *Pandy and Berme* (1988b)) regardless of how the model interacts with the ground or the inertia of the system. Since inverse dynamics does not require consistency between the model dynamics and experimental data there is a potential for a disconnect between the subject and the model. Consequently, we must rely primarily on our measurements/estimates of parameters and model assumptions being accurate. Forward dynamics produce simulations that are consistent with the dynamics described by a model, but it does not provide a practical mechanism to test if the model is consistent with the subject and his/her data. Validation of forward dynamics solutions are performed post optimization by comparison to subject data, consequently days, weeks, or even months may be invested in obtaining an optimization solution for a model that may have deficiencies in its ability to reproduce subject performance.

Anderson (1999) developed a three dimensional, 23 degrees-of-freedom, 54 muscle musculoskeletal model of the human body with articulating lower limbs. It still represents the state of the art in whole body musculoskeletal modeling, and was used to generate a forward simulation of maximum height jumping (*Anderson and Pandy* (1999)) and a half cycle of human gait (*Anderson and Pandy* (2001a)) which had good agreement with experimental data. Unfortunately, the computational complexity and expense of performing a single optimization (i.e. 10,000 CPU hrs, *Anderson and Pandy* (2001a)) is prohibitive for the majority of clinical and research applications. The neuromusculoskeletal tracking (NMT) method (3) is applied to gait analysis using virtually the same model and experimental data collected from a single subject, in order to compute individual muscle forces and to compare the simulation results to experimental findings.

5.2 Methods

5.2.1 Experimental Treatment

Data were collected from one healthy male volunteer (age 24yrs, height 178 cm, mass 65kg) during normal self-selected gait at the University of Melbourne's Department of Mechanical and Manufacturing Engineering by Dr. Hyung Joo Kim. Thirty photo-reflective markers were placed on the subject corresponding to anatomical locations identified in Table 5.1. Ground reaction forces were collected from two force-plates to provide simultaneous and continuous ground reaction forces from toe-off of the contra-lateral (left) leg to heel-strike ipsi-lateral leg (right) representing 85% of a full gait cycle. Three trials of complete marker kinematics and ground reaction forces with the feet stepping fully on the force-plates were selected for analysis. Movement periods ranged from 0.83 to 0.87s with one trial having a period of 0.85s, which was selected as the "median" trial for tracking. The three trials were normalized in time to reflect the 85% of the gait cycle represented in the experimental data. In comparison with gait literature this represents 15 to 100% of the full gait cycle beginning and ending at ipsi-lateral heel-strike. Symmetry of gait was not assumed to mirror 50% of the trial to form a whole gait cycle as in earlier studies (*Anderson and Pandy* (2001a); *Neptune et al.* (2001); *Thelen and Anderson* (2006)) for the purpose of demonstrating the ability of tracking the complete period of available experimental data. Note the median trial for one subject was selected for tracking analysis, while the remaining trials (3) from the same subject were used to evaluate the variability of the experimental and to include one standard deviation (SD) data for comparison with tracking results.

5.2.1.1 Inverse Kinematics

Unfiltered spatial marker coordinates affixed to the subject were transformed to model kinematics using the following inverse kinematics techniques from *Seth* (2000), which are very similar to the two level optimization procedure described by *Reinbolt et al.* (2005). First, a static trial (~10 secs in duration) of the subject standing in place and with all markers in view was used to define segment

Table 5.1: Anatomical marker placements

Acronym	Description
C7	seventh cervical vertebra
SACR	sacral marker mid-way between the posterior superior iliac spines
R(L)SHO	right (left) shoulder marker on the acromio-clavicular joint
R(L)ASIS	right (left) anterior superior iliac spine
R(L)THAP	right (left) proximal anterior thigh marker
R(L)THAD	right (left) distal anterior thigh marker
R(L)THLD	right (left) distal lateral thigh marker
R(L)LEPI	right (left) lateral epicondyle knee marker
R(L)TIAP	right (left) proximal anterior tibial marker
R(L)TIAD	right (left) distal anterior tibial marker
R(L)MMAL	right (left) medial malleolus ankle marker
R(L)LMAL	right (left) lateral malleolus ankle marker
R(L)HEEL	right (left) proximal calcaneus
R(L)P1MT	right (left) proximal 1st metatarsal head
R(L)P5MT	right (left) proximal 5th metatarsal head
R(L)TOE	right (left) toe at the junction of 2nd and 3rd proximal metatarsals

lengths, joint center locations, and the virtual fixed locations of markers on the model, coined as "body points", that would enable the model's body points, $\rho(q)$, to match the global marker positions, $\hat{\rho}$, in a least-squares sense. The components of the body fixed vectors defining the skeletal geometry as well as the static model joint coordinates (angles and positions, q) that minimized the sum of squared errors with respect to the marker positions were determined by solving a curve-fitting least-squares problem. The optimization converged to a mean RMS error (across all markers) of just under 2 mm.

The second phase was to optimally posture the model at each frame of the marker motion captured during gait immediately following the static trial and with marker locations unchanged. Another least squares curve-fitting optimization was applied at each frame to determine the set of model (5.3) joint coordinates, q, that placed the body points corresponding to the markers as close as possible to the experimental marker positions during gait without having the feet penetrating the ground. In this regard the contact model, $S(q, \dot{q})$, was used as a penalty function from which experimental values of ground reaction forces were subtracted to enable some penetration of the foot for the supporting leg(s) during the gait cycle. The resulting joint coordinates, $\hat{q}$, postured the model with a mean RMS error in

marker positions of 5.8 mm. For comparison, neglecting the ground constraint resulted in a mean RMS error of 4.8 mm, indicating that non-rigid movement of the markers was the most significant source of differences between model and experiment. Therefore, the mean RMS error including ground constraints was considered adequate for the purposes of tracking and simulating the complete movement and muscle coordination of the subject during normal gait..

5.2.1.2 Consistency of Kinematics and Ground Reaction Force Data

A major problem for inverse methods including earlier tracking attempts, has been the issue of consistency between measured kinematics, ground reaction forces, and the multi-body dynamics model. Specifically, kinematics and ground reaction forces are not independent quantities and are related by the dynamics of the subject, which is represented by the model. Since ground reaction forces are responsible for accelerating the center of mass of the subject and the trajectory of the center of mass is dependent on the kinematics of the joints that link the model to the ground, the acceleration of the center of mass determined from kinematics should be equivalent to the acceleration of the center of mass calculated from ground reaction forces.

We can test the consistency (i.e. check if the ground reaction forces and kinematics tell us the same thing about center of mass movement) by determining the center-of-mass trajectory, ρ_{com}, from ground reaction forces and, conversely, ground reaction forces from the acceleration of the center of mass from differentiating the kinematics data. It was not surprising that integrating the acceleration of the center of mass as determined by dividing the GRFs by body mass (and in the vertical direction subtracting the acceleration due to gravity) yields a very close trajectory of the center of mass to that determined from the model when positioned by the experimental joint coordinates (Fig. 5.1). This shows that the model, experimental positions, and ground reaction forces are consistent, so there should be no consistency problem. Not true. If we differentiate the kinematics twice to estimate accelerations, which inverse dynamics relies upon heavily, we can compute the ground reaction forces necessary to

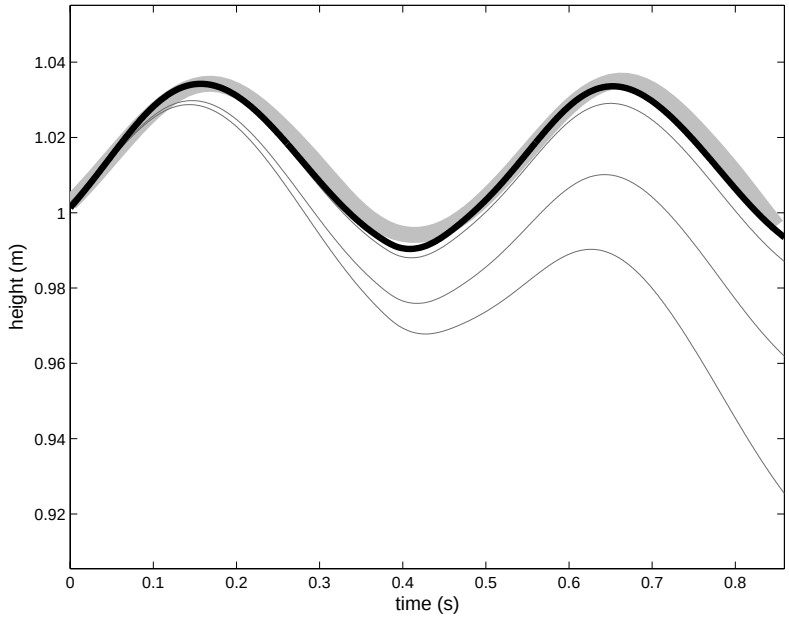

Figure 5.1: Vertical trajectory of model center of mass during gait.
Trajectory of center of mass was computed using joint kinematics determined from marker data (shaded) and also by integrating accelerations of the center of mass from ground reaction forces (bold). Thin lines depict integration of ground reaction forces with varying initial velocities where bold indicates the best match.

produce the resulting center of mass acceleration. In this case, ground reaction forces estimated from experimental acceleration data do not match up as well with experimental ground reaction forces (Fig. 5.2) and reveals the magnitude of errors introduced by differentiation, since position data was consistent with ground reaction forces (Fig 5.1). Similar findings were demonstrated long ago by *Thornton-Trump and Daher* (1975) but remains to be neglected by some inverse dynamics analyses today.

In an inverse dynamics analysis the differences in external forces (Fig. 5.2) result in residual forces to achieve force balance, which enables the model to follow the kinematics. The residual elimination algorithm (*Thelen and Anderson* (2006)) alters specified degrees of freedom (such as pelvis translation and back angles, which affect the the center-of-mass position the most) such that when differentiated the resultant accelerations match the ground reaction curve (i.e. Fig. 5.2) .

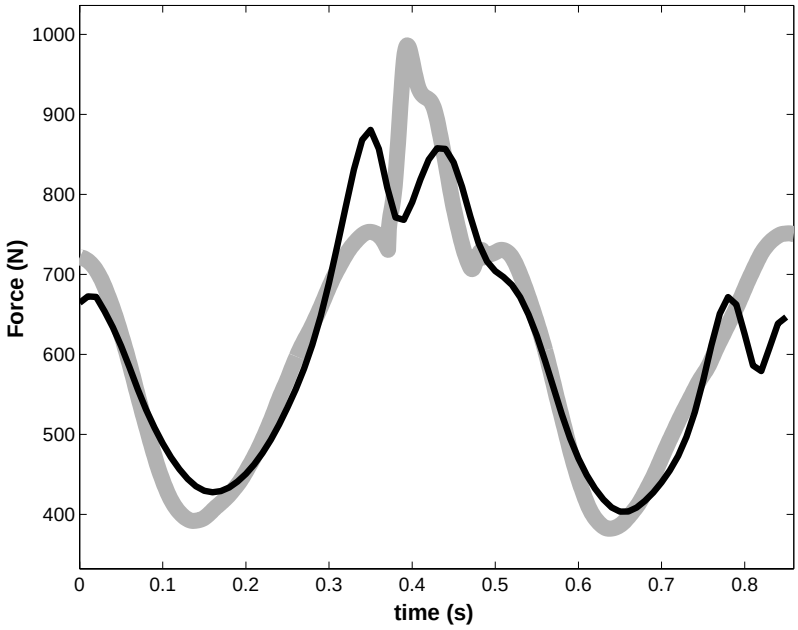

Figure 5.2: Vertical ground reaction forces estimated from center of mass accelerations. Vertical ground reaction forces obtained by accelerating the center of mass based on acceleration estimates from numerical differentiation (bold) compared to experimental ground reaction forces (shaded)

5.2.2 Musculoskeletal Model

The musculoskeletal model developed by *Anderson* (1999) used to simulate gait is briefly summarized herein (Fig 5.3). The equations of motion for the multi-body dynamics of the skeleton were implemented as FORTRAN subroutines, which were compiled and linked into the Simulink environment (MATLAB, The MathWorks Inc.). The contact dynamics and muscle model were similarly compiled and linked into Simulink in which the complete musculoskeletal simulation could be performed and the NMT stages could be implemented to control the model (i.e. Figs. 3.3 and 3.4).

5.2.2.1 Multi-body Skeletal Model

A generic version of the multi-body dynamical model by *Anderson* (1999) (Fig. 5.3) was developed that enabled segment lengths, masses, and inertia to be specified as well as the orientation of joint axes and local coordinates of body points as determined in section 5.2.1.1. Masses and inertia

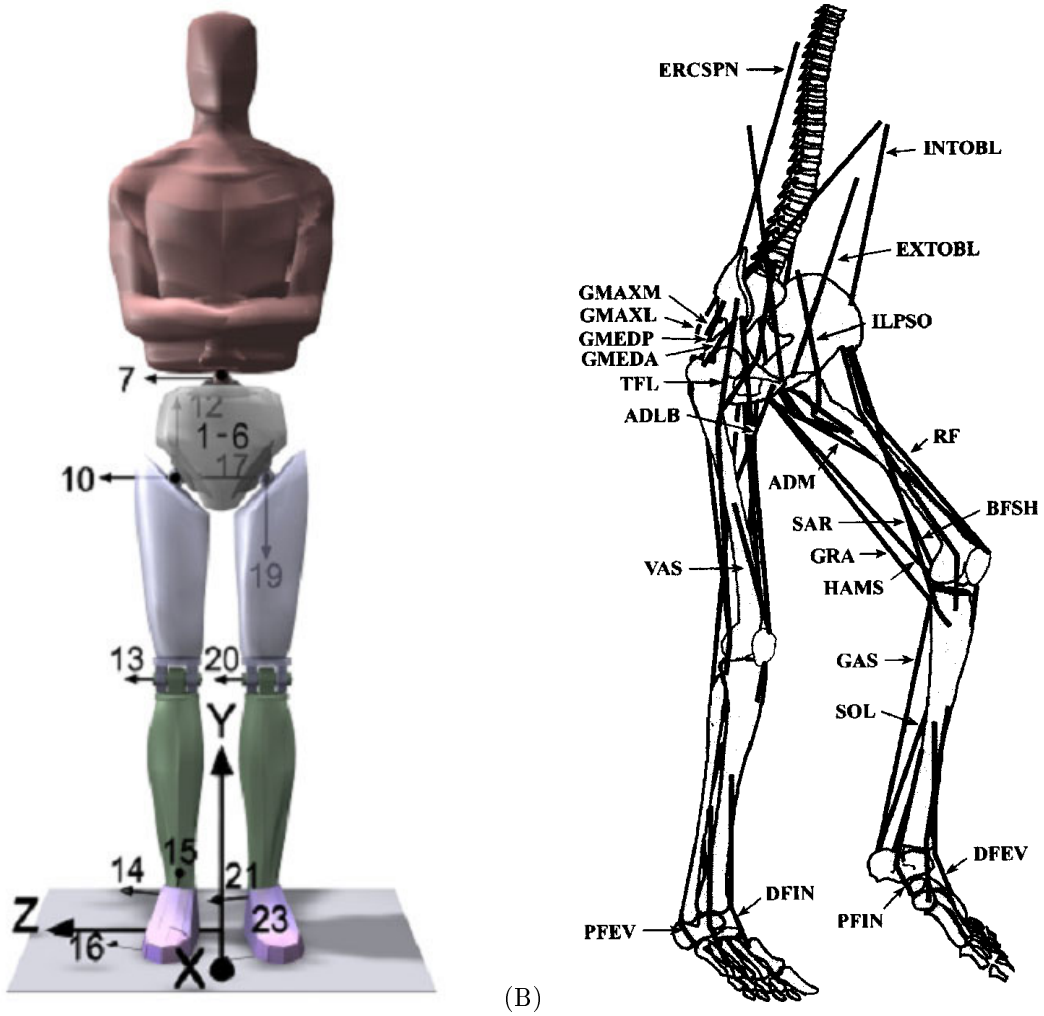

(A) (B)

Figure 5.3: Musculoskeletal model by *Anderson and Pandy* (2001a) used to simulate human walking. (A) Model of the body and its articulating segments. The first six-degrees-of-freedom were used to define the position and orientation of the pelvis relative to the ground. The remaining nine segments branch out as three open chains from the pelvis. The head, arms, and torso (HAT) were represented as a single rigid body that articulated with the pelvis via a three-dof (7-9) ball-and-socket back joint located at approximately the third lumbar vertebra. Each hip was modeled as a three-dof (10-12, 17-19) ball-and-socket joint, each knee as a one-dof (13, 20) hinge joint, each ankle-subtalar joint as a universal joint (14-15, 21-22) with a single joint center, and each metatarsal joint (16, 23) as a hinge joint. The directions of the knee, ankle, subtalar, and metatarsal joint axes were anatomical and based on in vivo and cadaveric measurements. (B) Muscles in the model. Abbreviations used for the muscles are as follows: (ERCSPN) erector spinae; (EXTOBL) external abdominal obliques; (INTOBL) internal abdominal obliques; (ILPSO) iliopsoas; (ADLB) adductor longus brevis; (ADM) adductor magnus; (GMEDA) anterior gluteus medius and anterior gluteus minimus; (GMEDP) posterior gluteus medius and posterior gluteus minimus; (GMAXM) medial gluteus maximus; (GMAXL) lateral gluteus maximus; (TFL) tensor fasciae latae; (SAR) sartorius; (GRA) gracilis; (HAMS) semimembranosus, semitendinosus, and biceps femoris long head; (RF) rectus femoris; (VAS) vastus medialis, vastus intermedius, and vastus lateralis; (BFSH) biceps femoris short head; (GAS) gastrocnemius; (SOL) soleus; (PFEV) other plantar flexors including peroneus brevis and peroneus longus; (DFEV) peroneus tertius and extensor digitorum; (DFIN) tibialis anterior and extensor hallucis longus; (PFIN) tibialis posterior, flexor digitorum longus, and flexor hallucis longus. Muscles included in the model but not shown in the diagram are: (PIRI) piriformis; (PECT) pectinius; (FDH) flexor digitorum longus/brevis and flexor hallucis longus/brevis and; (EDH) extensor digitorum longus/brevis and extensor hallucis longus/brevis.

were scaled from those by *Anderson* (1999) to a specific subject according to the ratio of the mass of the subject and the mass of the original model. This was considered justifiable, since the subject was a college aged male of similar height and mass as the subjects upon which the original model was based.

The equations of motion for the model were solved using SD/Fast (Parametric Technology Corporation) and the resulting FORTRAN codes were used to create a dynamically linked library (DLL) that returned the system mass matrix, M, and generalized force vector, $\Im$, due to centripetal and Coriolis effects that corresponded to the 23 degrees of freedom (joint coordinates, q) and their derivatives (generalized speeds, $\dot{q}$). Applied ligament, L, contact, S, and muscle torques were determined by their own models as separate functions/system (blocks), and assembled in Simulink to determine the complete system equations of motion:

$$\ddot{q} = {}^{-1}\{\Im(q,\dot{q}) + L(q,\dot{q}) + S(q,\dot{q}) + T \cdot \tau\} \tag{5.1}$$

5.2.2.2 Ligament Model

Ligaments as described by *Anderson* (1999) were implemented to penalize the model from exhibiting ranges of motion that were outside that observed in the subjects. Accordingly, we have relaxed the bounds on the toes and ankles since our subject exhibited greater range of motion than permitted by the original model. On the other hand, bounds were tightened on the range of motion of the back and the stiffness reduced, such that passive effects are experienced within the bounds of the range of motion of extension, lateral bending, and extension of the back. The reasoning for this to compensate for the fact that a single back joint does not exist and that unmodelled muscle and passive tissue are responsible for the relatively small range of motion of several vertebra that is exhibited as the total movement of the upper body. As concluded by *Anderson* (1999) passive and unmodelled muscles of the spine result in a more stable upper body that may require less active control of the obliques and erector spinae muscles to maintain an upright position. According to *Anderson* (1999) this may have

accounted for the greater activity of these muscles in the model when compared to the EMG of the same muscles in the subjects.

The original model also had insignificant damping (i.e. $D = 0.001\ \frac{N \cdot m \cdot s}{rad}$) at the joints, which was introduced primarily for the stability of numerical integration. Damping at the joints, however, contributes more significantly with experimental findings for knee extension ranging from 1 to 7 $\frac{N \cdot m \cdot s}{rad}$ depending on joint angle and joint torque *Zhang et al.* (1998). *Riener et al.* (1996) also included damping, but via the muscle model, introducing a linear damping proportional to the velocity of the muscle. They report factors of 0.01 to 0.03 $(\frac{s}{m})^{0.5}$, which is normalized to the muscle maximum isometric strength. If we consider the combined effects of the Vasti muscle group ($F_{max} = 6865N$, *Anderson* (1999)) as the primary knee extensors and a knee moment arm of 0.04 m (*Spoor et al.* (1990)) we obtain a rotational damping factor ranging from 0.0275 to 0.247 $\frac{N \cdot m \cdot s}{rad}$. To be more in line with these experimental findings, a constant rotational damping factor of D =0.25 $\frac{N \cdot m \cdot s}{rad}$ was selected for all joints in the present model, which remains relatively small compared to muscle moments but is not insignificant at high velocities.

5.2.2.3 Ground Contact Modeling for Human Gait

In an earlier study of maximum height jumping (4.3.2), the mechanism of imposing friction and slipping in the contact model by *Anderson and Pandy* (1999) (and *Anderson and Pandy* (2001a)) was found to be inappropriate for representing the "rolling-without-slipping" constraint when the foot moves in contact with the ground, and caused lingering horizontal plane forces. The problem was adequately resolved for jumping by allowing true slipping (i.e. horizontal forces go to zero). In gait, where the translations of the foot are more significant and the feet leave the ground and remake contact, horizontal springs were found to be cumbersome and inaccurate. Translations of the foot required the spring rest-lengths to be adjusted throughout the simulation according to the frictional limit (coefficient of friction multiplied by the vertical force) which meant the changes in rest-length of a spring could change abruptly, resulting in discontinuities in contact forces and severely impairing the quality of of numerical

Jacobians and thus impairing the tracker response during transition.

Besides the numerical difficulties, the application of horizontal springs is conceptually flawed. Rolling without slipping is a non-holonomic constraint dependent on the velocity of the point of contact in the horizontal plane. The position of contact, unlike a position constraint such as a pin joint, is not fixed and applying spring forces from a fixed reference (as defined by the rest length) makes little physical sense. Deformation of the sole of a shoe in the fore-aft and medio-lateral directions are a result of internal loads and a consequence of being between the ground reaction and the foot and is not due to inherent elasticity in surface contact. The same is true for the vertical direction, however, the constraint is position dependent since the foot cannot penetrate the ground, which is fixed. Springs are then convenient at both enforcing the position constraint and including the effects of shoe/foot compliance in a single formulation.

Multiple points are convenient because the distribution of forces result in a ground reaction moment, which would otherwise have to be imposed as an additional rotational constraint. Three points per contact surface is sufficient (with separate toes, there are two surfaces) as long as the surface is assumed to be flat and the center of pressure remains an interior point of the perimeter defined by the contact points. By varying the pressure on each contact point the center of pressure can move continuously to any interior location on the surface defined by three contact points. *Anderson* (1999) used a total of five points, with two points defining the metatarsal axis from medial to lateral borders of the foot, and so there are two common points for the separate toes and hind-foot segments (Fig. 5.4). These five points describe the underlying outline of the foot contact surface.

The horizontal constraints must be imposed (within the bounds of friction) directly upon the point(s) of contact based on their velocity. Having springs in the vertical direction enables two possible approaches of enforcing the rolling-without-slipping constraint. The first approach is to impose a nonholonomic kinematic constraint as a function of the velocity of the center of pressure evaluated

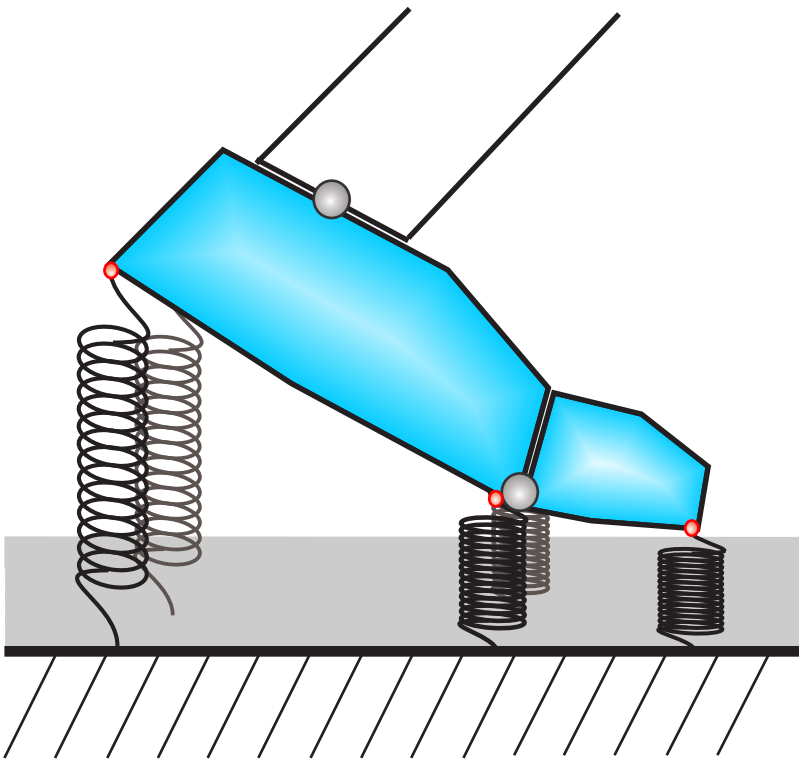

Figure 5.4: Five contact point model for foot and ground interaction.

at every instant from the distribution of vertical springs. The velocity of the center of pressure can be constrained to have zero velocity in the horizontal plane and Lagrange multipliers used to enforce the constraint, which would correspond to the fore-aft and medio-lateral ground reaction forces. The ground reaction moment about the vertical axis, however, would remain undetermined. To account for the vertical moment either the horizontal components of the ground reaction force have to be distributed amongst the contact points or an additional moment has to be applied, both of which are somewhat arbitrary.The second approach, is to formulate a resistive force at each contact point as a function of its horizontal velocity and the vertical force/position.

Gilchrist and Winter (1996) described a nonlinear spring-damper in the vertical direction and established horizontal plane forces proportional to the linear horizontal velocity of the contact point with a nonlinear damping coefficient (a polynomial of the vertical force), such that no damping was experienced when the vertical force was zero and a damping factor of 1 was applied when the vertical force reached or exceeded body weight. As such, the model does not simulate slipping when horizontal forces exceed the Coulomb friction limit. Enforcing Coulomb friction introduces discontinuities which again result in non-smooth derivatives, which is a problem for establishing the feedback linearization control law.

More recently. *Wojtyra* (2003) addressed this issue by adopting a pseudo-Coulomb model which introduces friction (or slipping) continuously via an *arctan* function, thereby enabling continuous derivatives over the "slipping" boundary. Furthermore, the model considers the total magnitude of the horizontal plane velocity for damping and slipping, unlike models such as *Anderson* (1999) that can allow slipping for an individual contact point and doing so along one component (direction) while experiencing friction in the other, which is unrealistic. Consequently, the contact model equations described by *Wojtyra* (2003) were applied in place of the original equations described by *Anderson* (1999).

The current contact model, $S(q, \dot{q})$, applies the three dimensional contact forces at each contact

point on the feet, and returns, the net fore-aft, vertical, and medio-lateral forces for the respective feet as well as the ground plane (fore-aft and medio-lateral) coordinates of the center of pressure as the outputs, s. When the foot is not in contact with the ground, the center of pressure coordinates default to zero. The current model also allows the elevation of the ground to be set externally, which is useful to simulate other tasks, such as stair climbing, but has more immediate uses in adjusting the ground elevation to correspond best with the experimental data. It was found that even when the foot was positioned such that it satisfied the foot markers with minimal error (~1mm) that the swing foot still registered significant ($>$ 25N) contact forces that acted to "drag" the swing leg. To avoid this problem without altering any experimental data, we allow the ground below the swing to be penetrated within a certain tolerance by effectively lowering the elevation of the ground under the swing foot. This lowering of the ground is a function of the transition times as detected by the center of pressure and vertical ground reaction force data, such that the ground height transitions smoothly fromΔh below the stance foot to the nominal ground height, H_0, at heel-strike. As contact is reestablished h rises according to an *arctan* function to the nominal ground height (Eq. 5.2).

$$h = H_0 - \begin{cases} \Delta h \left[\frac{1}{\pi} arctan(K_g(t - t_{in} - \Delta t)) + \frac{1}{2}\right] \\ \Delta h \left[\frac{1}{\pi} arctan(K_g(t_{out} + \Delta t) - t)) + \frac{1}{2}\right] \end{cases} \tag{5.2}$$

The gradual parameter, K_g, affects how quickly the height is adjusted to and from the nominal height, H_0, once contact is established (i.e. non-zero experimental vertical ground force) with the transition being more rapid with larger parameter values. For matching the available experimental gait data, $\Delta h = 0.02m$ and $K_g = 2000$, were found to virtually eliminate ($<$5N) scuffing forces from the contact model. A small offset, ($\Delta t = 0.01$secs) was used so that the nominal ground height was restored prior to heel strike and after toe-off so that the change in ground height does not interfere with the transition dynamics of the contact model.

5.2.2.4 Muscle Modeling and Muscle Action

The muscle contraction dynamics described by *Pandy et al.* (1990) and *Anderson* (1999) was cast into a form suitable for the NMT method (3.16) such that activation, a, and normalized muscle force, F^{MT}, were the states, x, of the muscle model.

$$\dot{x} = \left\{ \begin{array}{c} \mathcal{A}(x) + \beta(x) \cdot u \\ \\ \dot{F}^{MT}(x,\, l^{MT}(q), v^{MT}(q, \dot{q})) \end{array} \right\} \tag{5.3}$$

where the activation dynamics describe by $\mathcal{A}$ and β, are the first order linear dynamics described by *Zajac* (1989).

The action of the muscle was applied directly to the multi-body model via the muscle resultant joint moments by transforming muscle forces via a muscle moment arm matrix, $\Upsilon(q)$, such that

$$\tau = \Upsilon(q) \cdot F^{MT}(x)$$

The moment arms were obtained by splining the moment arm curves reported by *Anderson* (1999) as a function of the joint angles for which the muscles span. The moment-arm matrix was validated by applying the muscle forces from and comparing resultant torques to the values reported by *Anderson* (1999), which generated identical results for both vertical jumping and walking.

5.2.2.5 Model Initial Conditions for Forward Simulation

Accurate initial conditions are very important for the accurate simulation of the model where desired trajectories are to be replicated as closely as possible. For example, if the initial velocity of the model is off by 0.1m/s (specified by the pelvis horizontal speed), which is only 3% of the average fore-aft velocity of the pelvis, by the end of the simulation the model would deviate by some 8cm, resulting in large tracking errors for all the markers, given the ground reaction forces were reproduced identically. This was calculated by perturbing the initial fore-aft by 0.1 m/s and integrating the center of mass

acceleration according to the experimental ground reaction forces to obtain the velocity and position of the center of mass (as in Section 5.2.1.2). Although position errors can be reduced by deviating from the ground reaction forces to compensate, this works against the goal to also minimize differences in ground reaction forces. The best approach is to minimize errors in the initial conditions.

An optimization scheme was developed to systematically obtain more accurate initial conditions for model joint coordinates and velocities. The objective function (Eq. 5.4) was defined as the squared error differences between the model and experimental data at t = 0, in terms of the ground reaction forces, including center of pressure coordinates, joint angles, joint velocities and center of mass velocity. The experimental values for the initial velocity of the center of mass, $\dot{\hat{\rho}}_{com}\Big|_{t=0}$, were determined such that when used as the constants of integration and integrating the center of mass acceleration due to the experimental ground reaction forces, the trajectory of the center of mass, ρ_{com}, overlays that obtained by the marker position data, $\hat{\rho}_{com}$, as in Fig. 5.1.

The errors (Eq. 5.5) were scaled such that: 3N in the horizontal plane and 5N in the vertical ground force error accounted for one unit of error; center of pressure and pelvis translation errors were in mm; joint angle errors were in degrees; a pelvis velocity of 5 cm/s represented one unit of error, while errors in center of mass velocity were in cm/s (Eq. 5.6). This enabled the optimization algorithm to vary joint velocities in order to match ground reaction forces and center of mass trajectory while closely maintaining the initial joint coordinates obtained from the inverse kinematics process.

$$J = \sum (c_{ii})^2 \Big|_{t=0} \tag{5.4}$$

where the errors and scaling factors are:

$$e = \left\{ (\hat{s}_f - s_f),\ (\hat{s}_{cop} - s_{cop}),\ (\hat{q} - q),\ (\dot{\hat{q}} - \dot{q}),\ (\dot{\hat{\rho}}_{com} - \dot{\rho}_{com}) \right\} \tag{5.5}$$

$$c = \left\{ \begin{bmatrix} 0.33 \\ 0.20 \\ 0.33 \end{bmatrix}, \begin{bmatrix} 1000 \\ 1000 \end{bmatrix}, \begin{bmatrix} 1000 \\ \vdots_{3} \\ 180/\pi \\ \vdots_{23} \end{bmatrix}, \begin{bmatrix} 20 \\ \vdots_{3} \\ 5 \\ \vdots_{23} \end{bmatrix}, \begin{bmatrix} 100 \\ 100 \\ 100 \end{bmatrix} \right\} \tag{5.6}$$

subject to the contact dynamics, $s = S(q, \dot{q})$, marker kinematics as describe by body points, $\rho(q)$, and the center of mass kinematics, $\rho_{com}(q)$ and $\dot{\rho}_{com}(q, \dot{q})$ defined by the multi-body skeletal model.

5.2.3 The NMT Method

5.2.3.1 Skeletal Motion Tracking of Gait

Stage 1 of the NMT was enhanced to improve the quality of solutions in particular for tracking gait. One of the difficulties of tracking gait is the inherent instability of the system. Small deviations in joint kinematics can combine to have much broader effects in terms of the location of the center of mass and the location of the foot at heel-strike. In this regard, marker positions of key landmarks provide information about the global position of the body, which is critical in stable walking. The tracking of marker positions was included so that errors in joint angles could be tolerated as long as they did not adversely impact the overall location of landmarks. That is, deviations in the hip, knee and ankle angles can all be tolerated as long as heel strike still occurs at the correct location according to the marker and center-of-pressure data. Since the joint angles are themselves estimates (from inverse kinematics) adhering strictly to these angles is not accurate when marker positions represent the direct measurements.

Consequently, the direct tracking of measured marker positions with the model has two anticipated benefits: first, small deviations in angles are tolerated as long as marker positions remain close to experiment, and second, tracking markers of the upper body require the model to maintain an upright position, which is not guaranteed by tracking joint angles where small variations, for example in ankle inversion of the stance foot, greatly affect the position of the center of mass with respect to the feet and ground.

The tracking of marker positions is introduced in the same manner that ground reaction force tracking was included in the method of computed torques (Chapter 3). The positions of the markers, defined by the global position of body points, are functions of the current joint coordinates of the model:

$$\rho = \wp(q)$$

and to establish control over the second order skeletal dynamics (Eq. 5.1) these model outputs are differentiated twice. The formulation of the model using SD/Fast, enables us to obtain the position and velocity of any local point on a body in global coordinates given the current kinematic state, $Q = \{q, \dot{q}\}^T$. The Jacobian of the velocity of the marker points, $\dot{\rho}$, is used to obtain the feedback linearizing control law to obtain the control torques,

$$\tau_\rho = \left[\frac{\partial \dot{\rho}}{\partial Q} G\right]^{-1} \left\{\nu_\rho - \frac{\partial \dot{\rho}}{\partial Q} F\right\} \tag{5.7}$$

where $\tau_\rho$corresponds to estimates of the joint torques based purely from marker feed-back errors that define the control vector, ν_ρ and is appended to the system feedback linearizing control law (Eq. 3.10) to determine the torques in a least-squares sense.

The marker tracking control vector is determined by a second order linear feedback control law:

$$\nu_\rho = \ddot{\hat{\rho}} - 2\lambda_\rho \left(\dot{\hat{\rho}} - \dot{\rho}\right) - \lambda_\rho^2 \left(\hat{\rho} - \rho\right) \tag{5.8}$$

where $\hat{\rho}$ are the experimental positions of the markers and their derivatives (velocities and accelerations) are estimated by central difference numerical differentiation. The resulting feedback linearizing control law for skeletal dynamics requires solving:

$$\left[\begin{bmatrix} \frac{\partial \theta}{\partial Q}\left[\frac{\partial \theta}{\partial Q} F\right] \\ \frac{\partial s}{\partial Q} \\ \frac{\partial \dot{\rho}}{\partial Q} \end{bmatrix} G\right] \tau = \left\{\nu - \begin{bmatrix} \frac{\partial \theta}{\partial Q}\left[\frac{\partial \theta}{\partial Q} F\right] \\ \frac{\partial s}{\partial Q} \\ \frac{\partial \dot{\rho}}{\partial Q} \end{bmatrix} F\right\} \tag{5.9}$$

for the joint torques, τ, in Eq. 5.9 which is an overdetermined system of 123 equations (23 q's, 10 s's, and 30×3 ρ's) and 17 unknowns. This is solved in a weighted least squares sense with each equation corresponding to a particular experimental reference input.

Another aspect in tracking human gait, versus that of jumping, for example, is that gait is bilaterally asymmetric, and intermittent contact means ground contact data, particularly center of pressure data, is irrelevant during swing. Although zero ground forces contribute little to control during swing, they do not adversely affect control, since both model and experiment indicate zero and transitions to and from non-zero values are more or less continuous. On the other hand, center of pressure location is an undefined state (set to zero only as a default value for the model) when the foot is not in contact and is instantaneously defined as soon as contact forces are non-zero, resulting in a discontinuous signal. Discontinuities in model output result in undefined gradients in the region of transition.

Rather than break the gait cycle into multiple phases (i.e. ipsi-lateral support, double support, and contra-lateral support) to avoid discontinuities at transitions, an adaptive weighting scheme was adopted in order to gradually introduce center-of-pressure tracking as contact is established. Consequently, the weightings on center of pressure are scaled by the experimental vertical ground reaction force according to:

$$W_{cop} = \begin{cases} W_0 \left[\frac{1}{\pi} arctan(K_c(t - t_{in})) + \frac{1}{2}\right] \\ W_0 \left[\frac{1}{\pi} arctan(K_c(t_{out} - t)) + \frac{1}{2}\right] \end{cases} \tag{5.10}$$

where the desired weighting during contact is W_0; t_{in} and t_{out} are the transition times into $(W_0 : 0 \rightarrow 1)$ and out $(W_0 : 1 \rightarrow 0)$ of contact corresponding to the experimental data, and K_c determines the rate at which the transition occurs. A rapid transition with $K_c = 1000$ was used in this study.

5.2.3.2 Optimal Selection of Tracker Weightings

To verify that the accuracy of tracking were not purely a consequence of arbitrarily selected weightings, we also used optimization to determine the 37 skeletal motion tracking parameters (16 for joint kinematics, q, with legs (7) symmetrically weighted; 3 ground reaction forces and 2 center of

pressure coordinates, s, weighted equally for both feet; and 16 marker coordinate, ρ, weightings with the same values for each leg and for each (3D) component). A genetic algorithm (*Seth* (2000)) was employed where the evaluation of the fitness function (performance index) was performed by running the tracking simulation to determine the sum of mean squared (SMS) errors across all tracking references. The smaller the total SMS error the more 'fit' that individual solution. A population of 50 chromosomes (each a sequence of weighting parameters) was used and convergence was defined as a homogeneity factor of 0.5 (1/2 of the population is identical to the fittest individual) and 20 generations without a change of the fittest individual. A sequential quadratic programming method was used to further refine the weighting parameters to improve tracking accuracy.

Optimization of the 37 skeletal-motion weightings required a total of 67 generations for the genetic algorithm to converge. With a population of 50 individuals and an average of 120 secs per tracking simulation the computing time was in excess of 110 hours divided amongst two desktop computers (Pentium 4, 2.2 GHz). A sequential quadratic programming algorithm implemented by $MATLAB$'s *fminseach* function was applied using the genetic algorithm solution as the initial guess. The algorithm was terminated after 72 hours because the last 24 hours failed to produce a single decrease in tracking error. As with any nonlinear optimization problem of high dimensionality, it is very difficult to ascertain if a global optimum was achieved. *Seth* (2000) and *van Soest and Casius* (2003) have demonstrated, however, that the genetic algorithm is more robust than gradient based approaches. The resultant weightings for skeletal motion tracking are presented in Table 5.2.

5.2.3.3 Neuromuscular Tracking

The muscle model dynamics are recast in a form suitable for feedback linearization. Equation 5.3 becomes:

$$\dot{x} = A(x) + B(x)u \tag{5.11}$$

Table 5.2: Weightings for uniform, user selected and optimized skeletal motion tracker settings

Reference	Uniform	User	Optimized
pelvis fore-aft (q_1)	1	1	140.4
pelvis vertical (q_2)	1	20	570.0
pelvis medio-lateral (q_3)	1	50	669.7
pelvis abduction/add (q_4)	1	35	172.3
pelvis internal/ext (q_5)	1	80	155.0
pelvis extension (q_6)	1	40	175.0
back extension (q_7)	1	45	110.0
back abduction/add (q_8)	1	22	36.7
back internal/ext (q_9)	1	75	135.0
hip flexion ($q_{10,17}$)	1	22	73.5
hip adduction ($q_{11,18}$)	1	22	65.9
hip internal ($q_{12,19}$)	1	8	49.8
knee extension ($q_{13,20}$)	1	17	40.9
ankle dorsi-flexion ($q_{14,21}$)	1	7	202.1
ankle inversion ($q_{15,22}$)	1	3	8.9
metatarsal (toe) flexion ($q_{16,23}$)	1	1	9.2
fore-aft GRF ($s_{1,6}$)	1	12	135.2
vertical GRF ($s_{2,7}$)	1	20	171.3
medio-lateral GRF ($s_{3,8}$)	1	15	1051.1
fore-aft COP ($s_{4,9}$)	1	20	380.4
medio-lateral COP ($s_{5,10}$)	1	15	149.1
C7 (ρ_1)	1	10	257.8
SACR (ρ_2)	1	5	32.5
R(L)SHO ($\rho_{3,17}$)	1	30	72.1
R(L)ASIS ($\rho_{4,18}$)	1	10	76.1
R(L)THAP ($\rho_{5,19}$)	1	0	1.4
R(L)THAD ($\rho_{6,20}$)	1	13	59.2
R(L)THLD ($\rho_{7,21}$)	1	15	111.6
R(L)LEPI ($\rho_{8,22}$)	1	15	34.2
R(L)TIAP ($\rho_{9,23}$)	1	1	2.5
R(L)TIAD ($\rho_{10,24}$)	1	1	8.2
R(L)MMAL ($\rho_{11,25}$)	1	12	188.9
R(L)LMAL ($\rho_{12,26}$)	1	12	131.7
R(L)HEEL ($\rho_{13,27}$)	1	13	400.1
R(L)P1MT ($\rho_{14,28}$)	1	12	179.5
R(L)P5MT ($\rho_{15,29}$)	1	12	72.4
R(L)TOE ($\rho_{16,30}$)	1	2	49.8

$$f = x_2 \tag{5.12}$$

where $A = \left\{ \begin{array}{c} \mathcal{A} \\ \dot{F}^{MT} \end{array} \right\}$ and $B = \left\{ \begin{array}{c} \beta \\ 0 \end{array} \right\}$

Unlike the muscle model used to study maximum height jumping, the contraction dynamics by *Pandy et al.* (1990) implemented in the current model (*Anderson* (1999)) have muscle force as a state and its derivative is not an explicit function of the activation dynamics and therefore not an explicit function of the muscle excitations, u. If we try to establish the feedback linearizing control law by differentiating once,

$$\dot{f} = \dot{F}^{MT}(x)$$

we cannot solve for the excitations, u. The muscle model is second order and must be differentiated again to yield,

$$\ddot{f} = \frac{\partial \dot{F}^{MT}}{\partial x} \left[A + B \cdot u \right]$$

from which we can solve for u to obtain the the resultant feedback linearizing control law,

$$u = \left[\frac{\partial \dot{F}^{MT}}{\partial x} B \right]^{-1} \left\{ \eta - \frac{\partial \dot{F}^{MT}}{\partial x} A \right\} \tag{5.13}$$

and the corresponding linear system:

$$\ddot{f} = \eta \tag{5.14}$$

$$\tau_m = \Upsilon f \tag{5.15}$$

which is easily written in first order form,

$$\dot{F} = \begin{bmatrix} 0 & I \\ 0 & 0 \end{bmatrix} F + \begin{bmatrix} 0 \\ I \end{bmatrix} \eta \tag{5.16}$$

where $F = \{f, \dot{f}\}^T$and I is an $m \times m$ identity matrix.

The primary goal of the neuromuscular system is to produce the required torques to actuate the skeletal model; thus the first criterion is to match the torques from skeletal motion tracking. Second is to select forces in a manner that is physiologically relevant. Since the muscle forces, and their production rates are the states of the FBL system, it is possible to minimize the weighted sum of forces, which would be similar to that performed in static optimization, with one major difference, the total amount of force over the performance interval is minimized and not merely at any single instant. The cost functional for the linear system can therefore be written as,

$$J = \frac{1}{2} \int_0^{t_f} \left[\left(Cf - \begin{Bmatrix} \hat{\tau} \\ 0 \end{Bmatrix} \right)^T Q \left(Cf - \begin{Bmatrix} \hat{\tau} \\ 0 \end{Bmatrix} \right) + \eta^T R \eta \right] dt \tag{5.17}$$

where the output transform, $C = \begin{bmatrix} \Upsilon & 0 \\ I & 0 \end{bmatrix}$, results in the joint torques produce by the neuromuscular system as well as the individual muscle forces. The resultant torques are compared to the torques estimated by skeletal motion tracking, $\hat{\tau}$. Since the muscle forces are compared a zero reference, the secondary objective becomes to minimize the sum of squared muscle forces. Third, the amount of control input, η, can be minimized according to the weighting matrix, R. The cost functional, Eq. 5.17and linear system, Eq. 5.16 define a linear quadratic tracker, which is solved by the linear optimal control methods described in 3.4.

From the optimal solution for the control parameter, η, the individual muscle neural excitations, u, are determined by the feedback linearizing control law (Eq. 5.13) as inputs to the dynamic muscle model (Eqs. 5.11 and 5.12), which are integrated forward in time for the individual muscle activations and forces.

Table 5.3: Summary of skeletal motion tracking errors (average RMS)

Scheme	Pelvis Pos. (mm)	Body Ang. (^{O})	Leg Ang. (^{O})	GRFs (N)	COP (mm)	Marker (mm)
Uniform	11.7	8.0	6.0	20.4	13.3	15.8
User	12.2	2.5	5.9	14.8	18.7	16.1
Optimized	6.1	3.2	4.8	13.0	9.9	11.1

5.3 Gait Simulation Results

Neuromusculoskeletal tracking generated a forward dynamics simulation of human gait that was in good agreement with its corresponding experimental data representing the bilateral motion for 85% of the gait cycle based on user selected weightings. Skeletal motion tracking required 118 secs while neuromuscular tracking required 190 secs for a total computing time of just over 5 min to obtain dynamically generated muscle forces for 54 individual lower extremity muscles. Note that simulation data is presented from contra-lateral toe-off (cTO) to to ipsi-lateral heel-strike (HS), which corresponds to the complete set of bilateral experimental data available from two force-plates. We do not juxtapose the data from from the opposite leg to form a composite of 100% of the gait cycle since this assumes bilateral symmetry whereas we make no such assumption in tracking, which is unlike previous studies (i.e.*Anderson and Pandy* (2001a); *Neptune et al.* (2001); *Thelen and Anderson* (2006)). Other than for the purpose of simplifying an optimization problem or limitations on collection to one force-plate, assuming symmetry is unnecessary and undesirable in analyzing the majority of gait disorders.

Optimizing the weightings did reduce the overall tracker error over trial-and-error (user) selected weightings. Surprisingly, back and pelvis extension kinematics, showed greater discrepancy in the optimal solution, although leg kinematics, marker position and ground-reaction force tracking all improved. As expected, uniform weightings also produced a tracking simulation but produced gait motion with larger RMS errors in GRFs and joint angles (Table 5.3). Note, the body angle category consists of the three pelvis orientation angles and three back joint angles.

5.3.1 Kinematics

All three weighting schemes produced kinematics that had the appearance of normal gait, except that both the uniform and optimized weightings exhibited excessive hat (back) and pelvis extension nearing the end of the gait cycle (Figs. 5.7 and 5.6). Tracking with user selected weightings, however, maintained a more upright posture but experienced larger deviations in pelvis translation (Fig. 5.5). Results for the hip were similar for both user and optimized weightings, which closely resembled the subject profile (Fig. 5.8). The motion of the legs were also well characterized by user weightings, but optimized weightings caused the tracker to follow the subject angles more closely (Fig. 5.9). The exception being metatarsal flexion angle which required much greater flexion angles in the model approaching toe-off (at ~65% of gait cycle) with both user selected and optimized weightings .

5.3.2 Ground Reaction Forces

Ground reaction forces synthesized by the musculoskeletal model during tracking were very close to the subject with the average RMS error (Table 5.3) representing less than 2.5% of body-weight (Fig 5.10). The most significant discrepancy occurred at heel-strike of the contra-lateral (left) leg, where the initial positive inflection in the fore-aft force is missing in the simulated ground reaction forces (fore-aft, Fig. 5.10). Notably, the model also presents impact transients (sharp peaks) at heel-strike that were not present in the experimental data.

5.3.3 Joint Torques

Joint torques computed from the NMT analysis were compared with an inverse dynamics analysis. Inverse dynamics was performed using the weighted pseudoinverse method as described by *Kuo* (1998) since this is the same approach used by the feedback linearizing control module of the NMT method.

For hip flexion and adduction (Fig. 5.13) as well as knee and ankle extension (Fig. 5.14), the

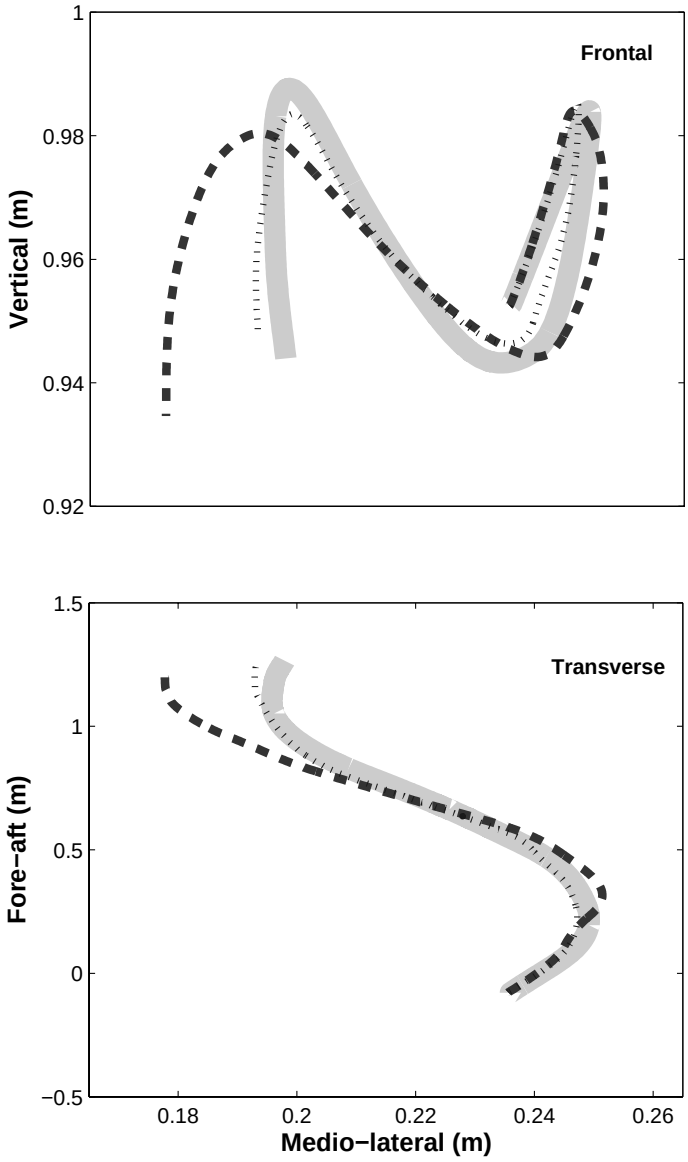

Figure 5.5: Model versus experimental pelvis translation.
Pelvis translation in the frontal plane and transverse plane of the model determined by NMT simulation for user (dashed) and optimally defined (dotted) tracker weightings. Results are compared to experiment (shaded) of subject trial being tracked.

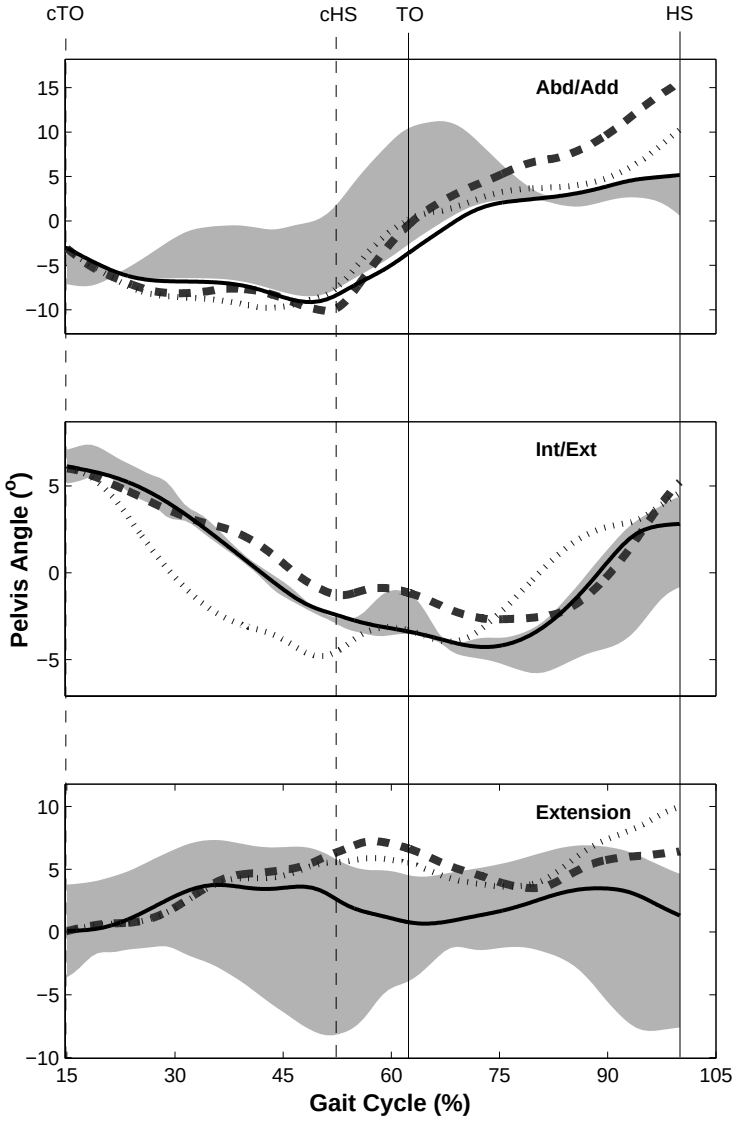

Figure 5.6: Model versus experimental pelvis orientation.
Pelvis extension, abduction and internal/external rotation angles determined by NMT simulation for user (dashed) and optimally defined (dotted) tracker weightings. Results are compared to the individual trial being tracked (thin solid) and +/- 1 SD variability (shaded) according to experiment.

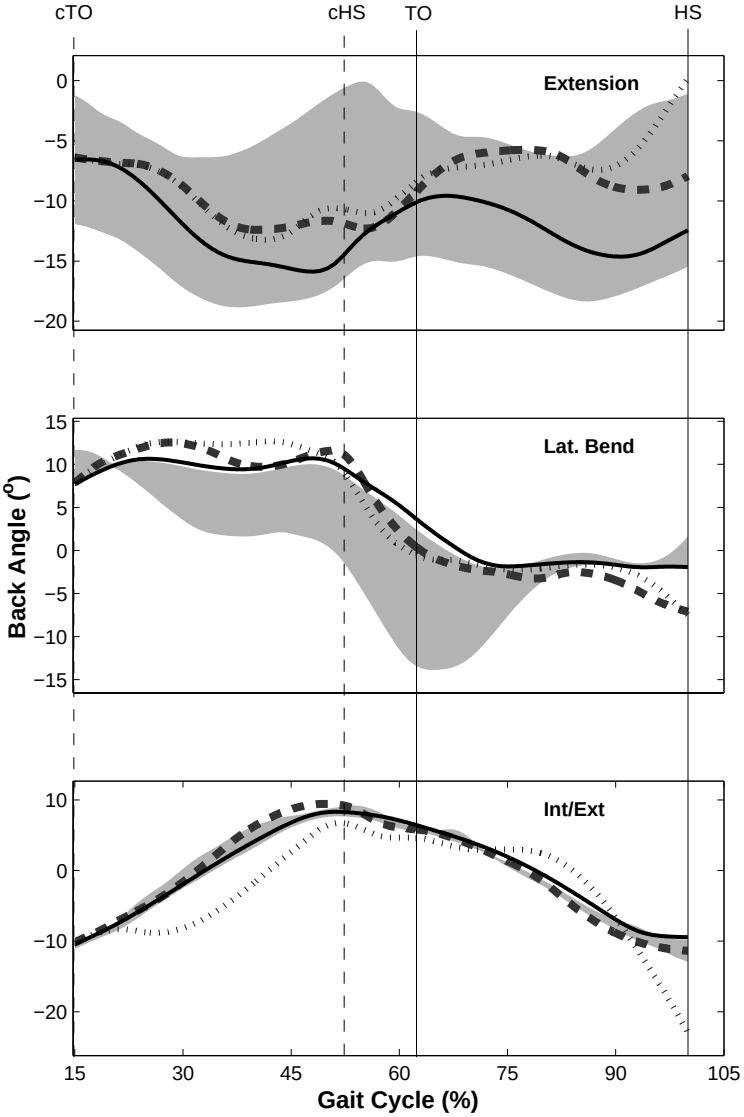

Figure 5.7: Model versus experimental back joint angles.
Back extension, lateral bending and internal/external rotation angles determined by NMT simulation for user (dashed) and optimally defined (dotted) tracker weightings. Results are compared to the individual trial being tracked (thin solid) and +/- 1 SD variability (shaded) according to experiment.

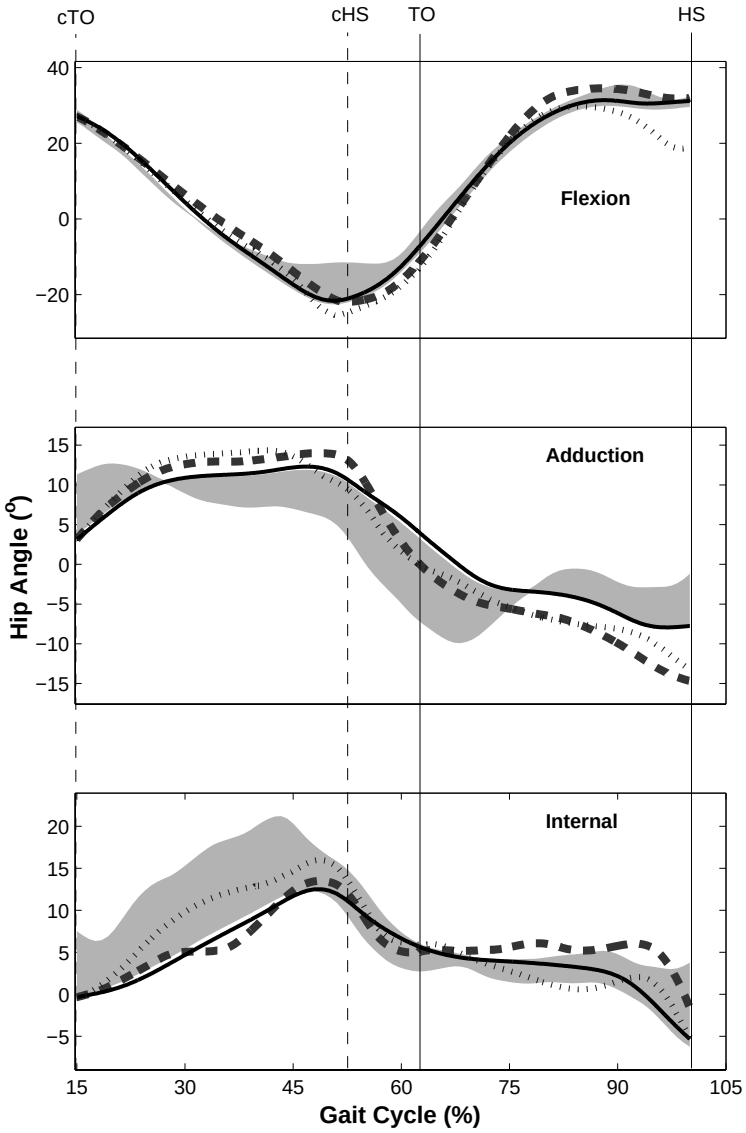

Figure 5.8: Model versus experimental hip joint angles.
Right hip flexion, abduction and internal/external rotation angles determined by NMT simulation for user (dashed) and optimally defined (dotted) tracker weightings. Results are compared to the individual trial being tracked (thin solid) and +/- 1 SD variability (shaded) according to experiment.

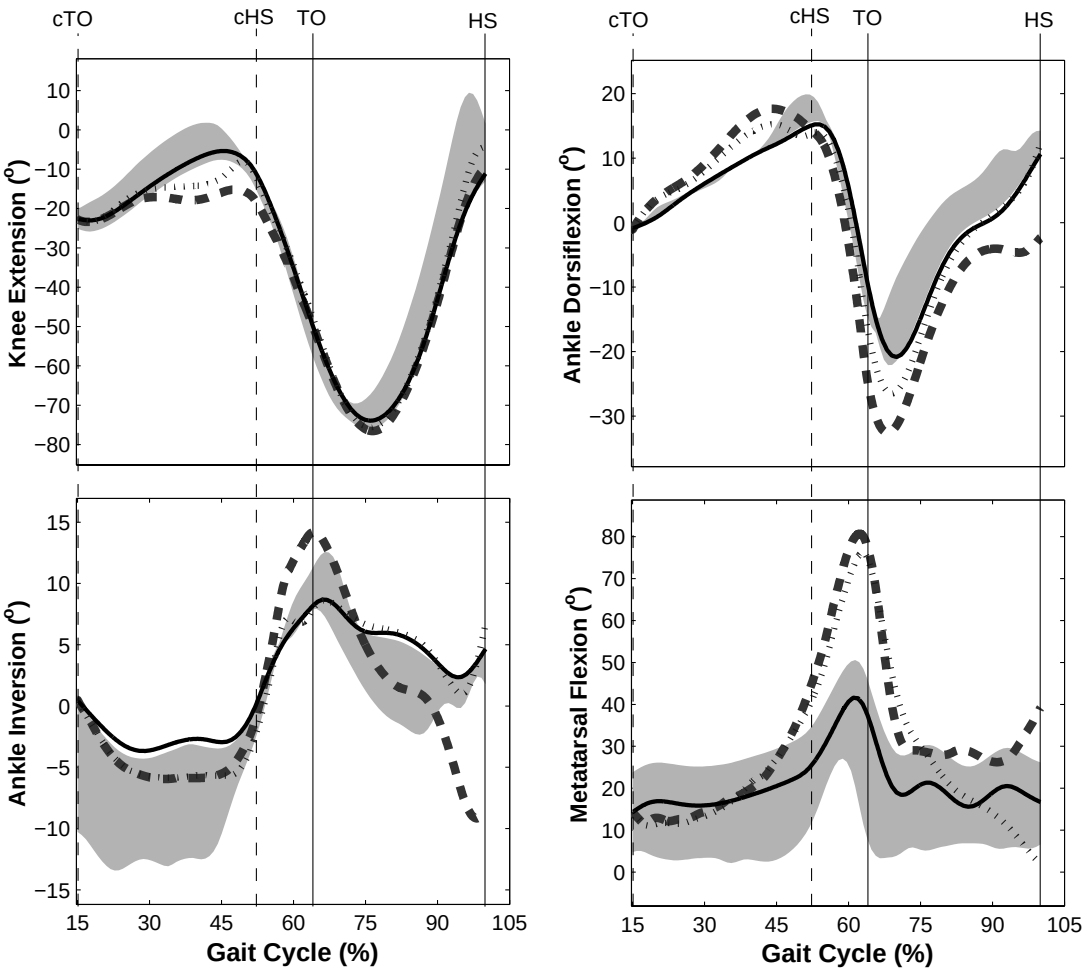

Figure 5.9: Model versus experimental angles of the lower leg.
Right leg knee extension, ankle dorsi-flexion, ankle inversion and metatarsal flexion angles determined by NMT simulation for user (dashed) and optimally defined (dotted) tracker weightings. Results are compared to the individual trial being tracked (thin solid) and +/- 1 SD variability (shaded) according to experiment.

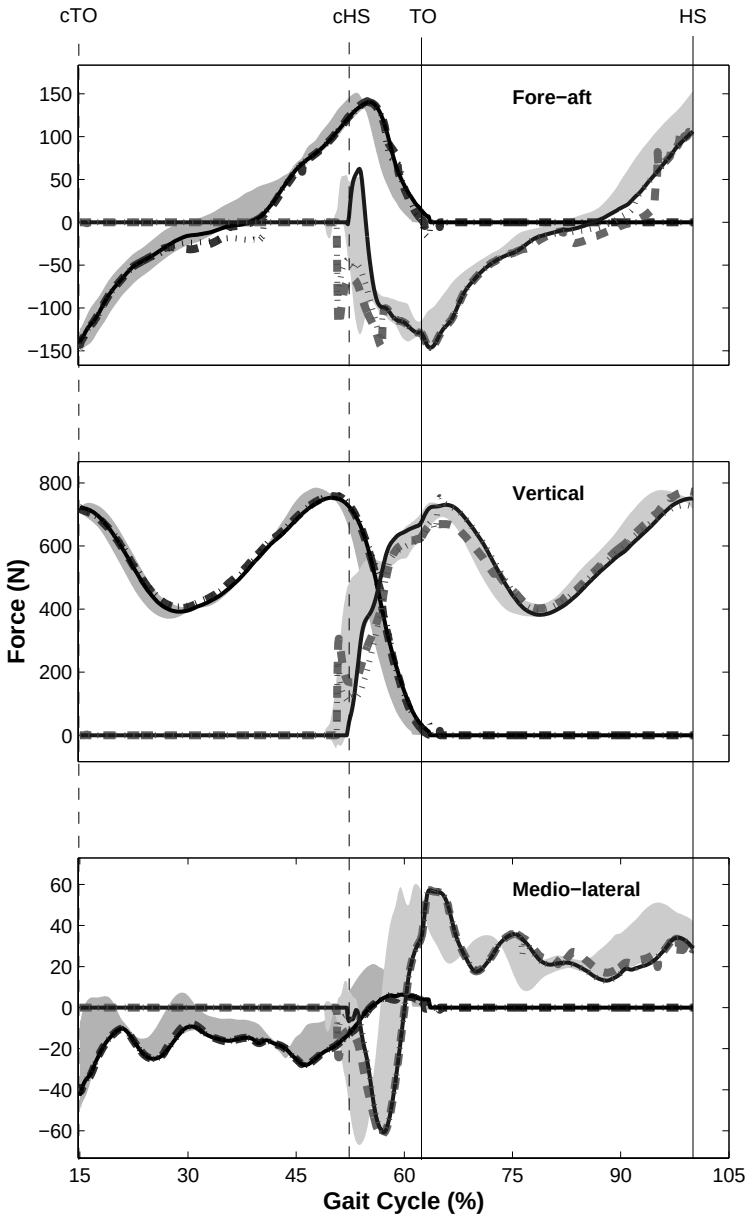

Figure 5.10: Model versus experimental ground reaction forces.
Fore-aft, vertical and medio-lateral ground reaction forces determined by NMT simulation for user (dashed) and optimally defined (dotted) tracker weightings. Results are compared to the individual trial being tracked (thin solid) and +/- 1 SD variability (shaded) according to experiment.

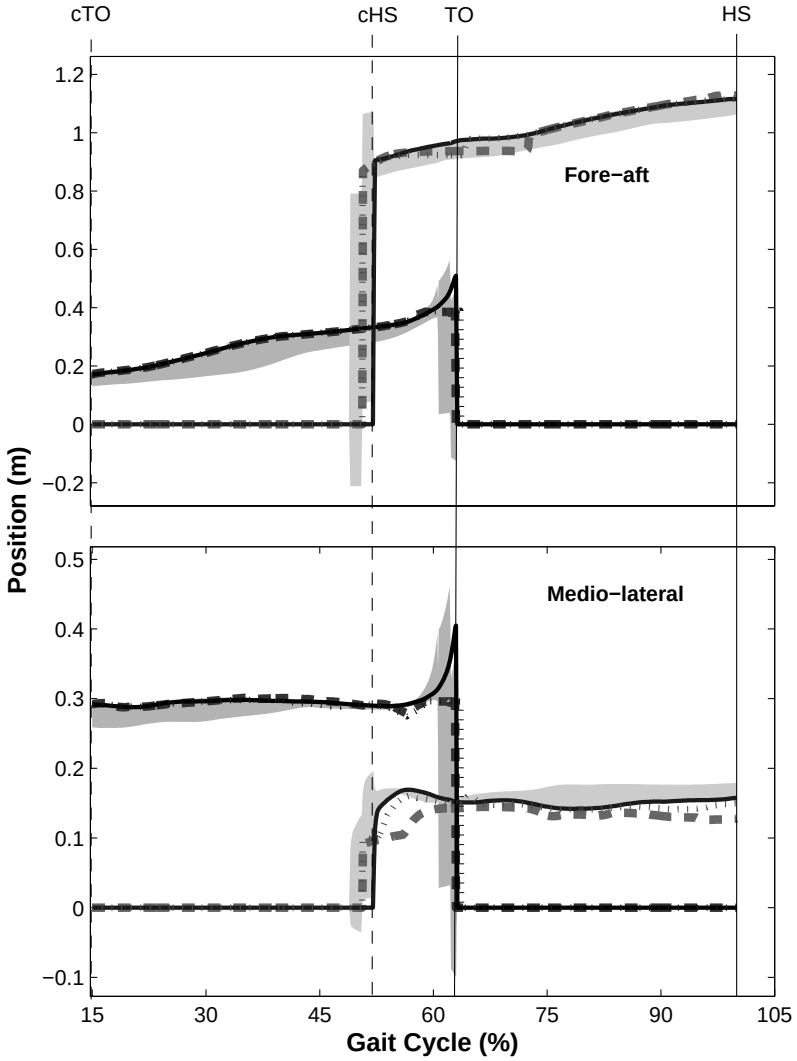

Figure 5.11: Model versus experimental center of pressure location.
Fore-aft and medio-lateral center of pressure location determined by NMT simulation for user (dashed) and optimally defined (dotted) tracker weightings. Results are compared to the individual trial being tracked (thin solid) and +/- 1 SD variability (shaded) according to experiment.

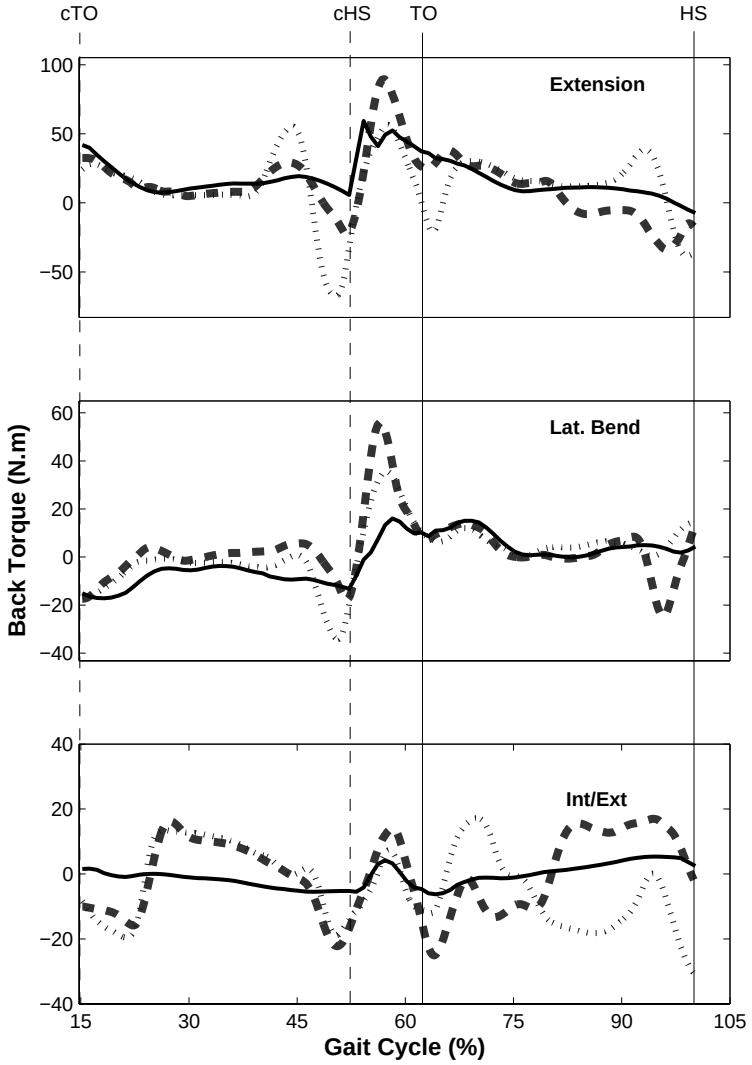

Figure 5.12: NMT versus inverse dynamics for back joint torques.
Back extension, lateral bending and internal/external rotation joint torques determined by NMT simulation for user (dashed) and optimally defined (dotted) tracker weightings are compared to results from an inverse dynamics analysis (thin solid).

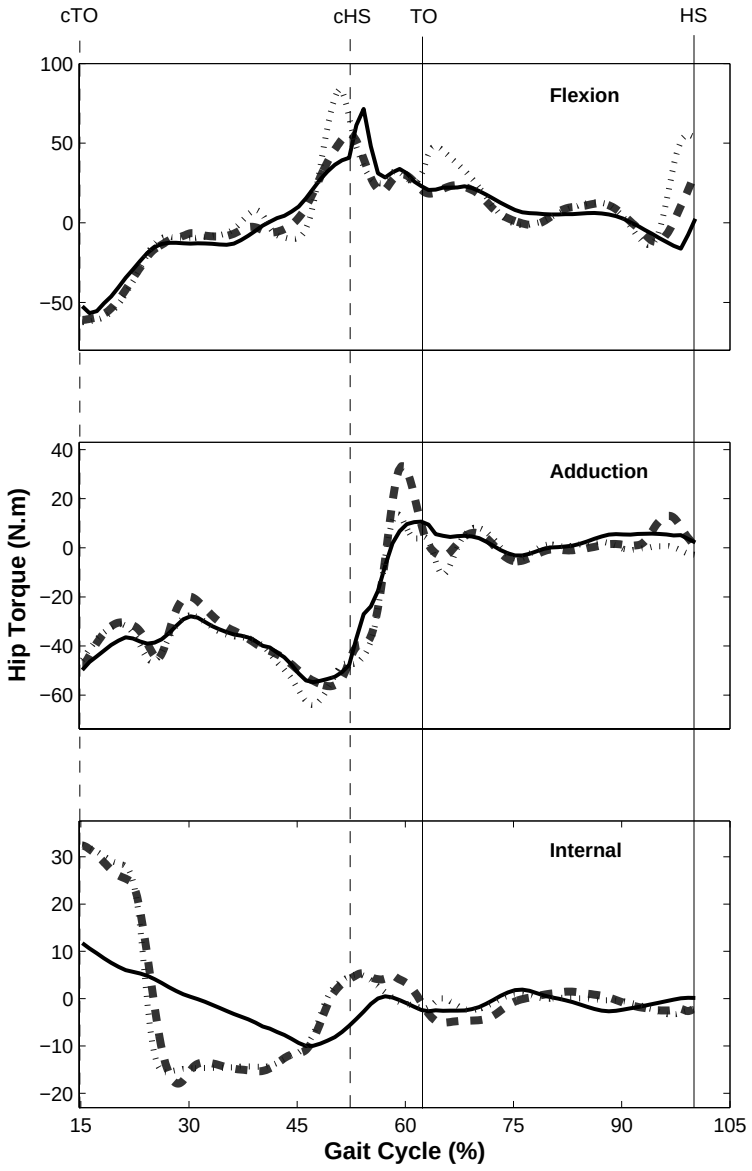

Figure 5.13: NMT versus inverse dynamics for hip joint torques.
Right hip flexion, abduction and internal/external rotation joint torques determined by NMT simulation for user (dashed) and optimally defined (dotted) tracker weightings are compared to results from an inverse dynamics analysis (thin solid).

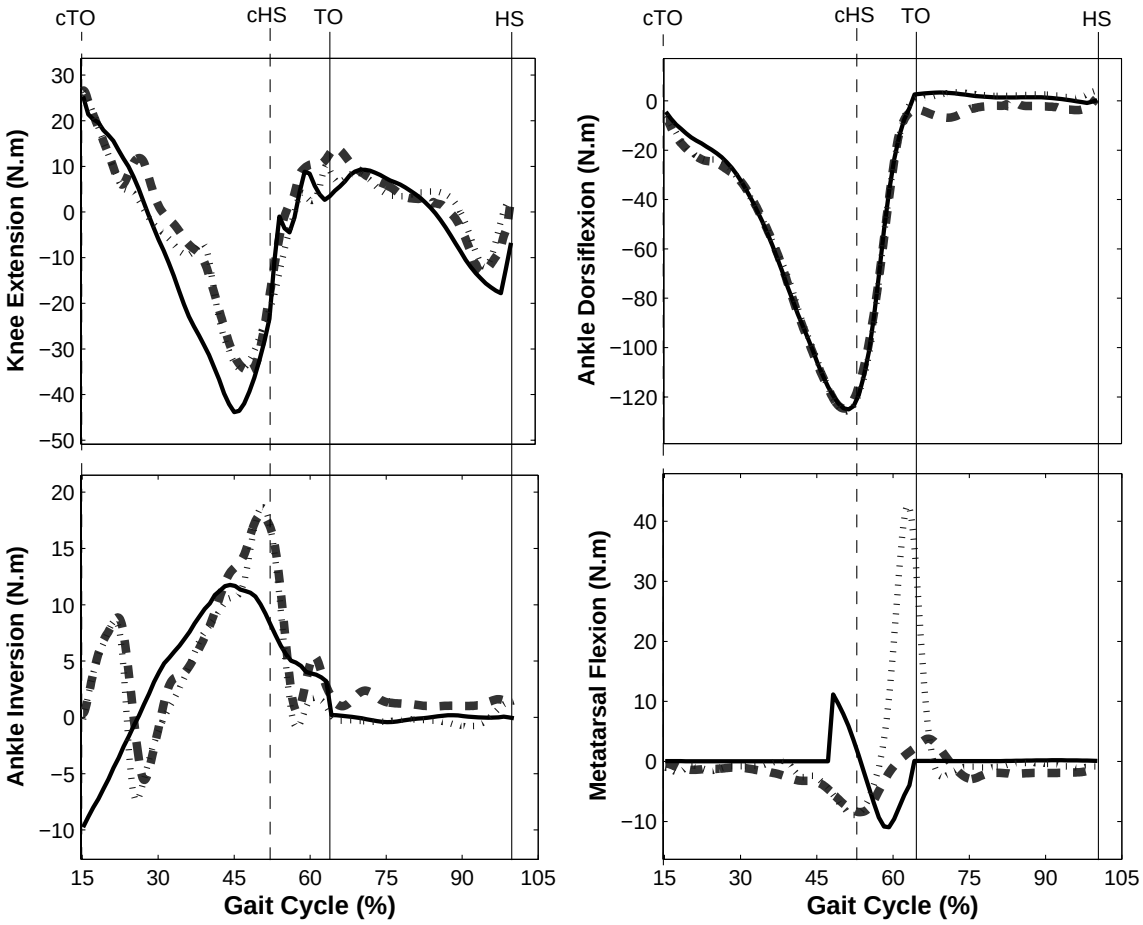

Figure 5.14: NMT versus inverse dynamics for lower leg joint torques.
Right leg knee extension, ankle dorsi-flexion, ankle inversion and metatarsal flexion joint torques determined by NMT simulation for user (dashed) and optimally defined (dotted) tracker weightings are compared to results from an inverse dynamics analysis (thin solid).

torques computed from inverse dynamics are comparable to the NMT solutions. The NMT and inverse dynamics solutions differ more significantly for the back (Fig. 5.12), hip internal rotation, and metatarsal joint torques. The differences in NMT computed back joint torques (Fig. 5.12) correspond with the differences in joint angle tracking of the back extension and internal/external rotation angles (Fig. 5.7).

5.3.4 Muscle Activity

The muscle activations of selected muscles from the musculoskeletal model are presented in Figures 5.15 and 5.16. These muscles represent a significant proportion (17 of the 27) of the muscles modeled and were selected for comparison and validation against the physiological activity of the subject EMG (Fig. 5.15) and against muscle activity recorded by EMG during normal walking as reported by *Winter* (1987) (Fig. 5.16). The EMG data by Winter were normalized by their peak voltage and then multiplied by the peak activation generated by the model for each muscle in order to place model and experimental data on the same amplitude scale so that the temporal patterns of activation could be examined more closely. EMG from the subject was normalized by peak voltage measurements during maximum voluntary isometric contraction trials prior to walking.

The stronger weight bearing and propulsive muscles such as gluteus medius, hamstrings, erector spinae, vasti, gastrocnemius and soleus, are in very good agreement with the physiological data. Other important muscles with less agreement include rectus femoris and adductor magnus.

For completeness muscle forces of major muscles generated by the NMT simulation are compared to those computed by large scale parameter optimization (LSPO) performed by *Anderson and Pandy* (2001a) with virtually identical models (except ground contact) and very similar subject data (Fig .5.17). It is interesting that muscle forces for muscles considered as propulsive, i.e. soleus, gastrocnemius and to a lesser extent vasti (*Neptune et al.* (2001)), are very similar in magnitude and timing, but force output by NMT is considerably broader in time. Significant differences are apparent in hip flexor (iliopsoas) and extensor (gluteus maximus) muscles, with the NMT estimated peak bi-articular hamstrings and rectus

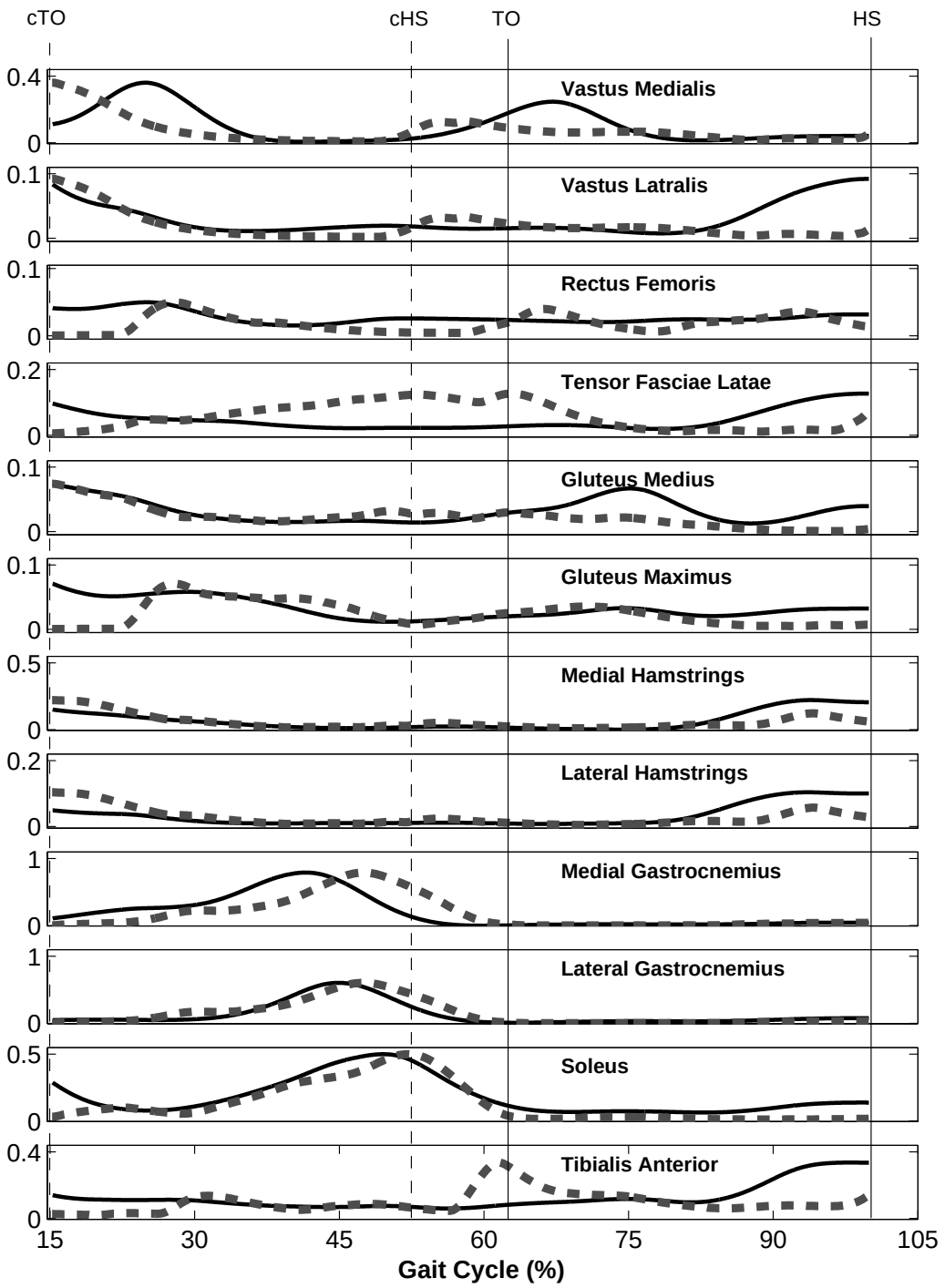

Figure 5.15: Model muscle activity versus subject EMG.
Simulated muscle activity estimated by the NMT method (dashed) compared to subject EMG for the trial being tracked (thin solid).

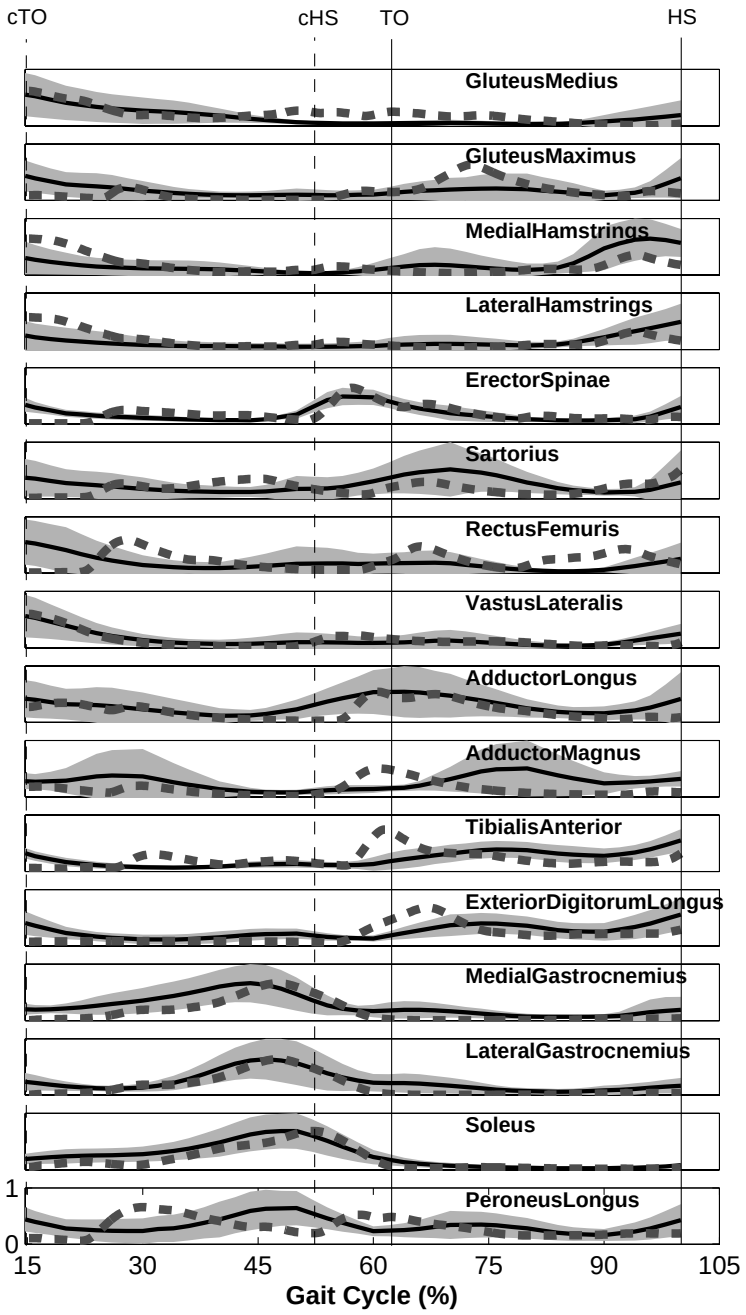

Figure 5.16: Model muscle activity versus EMG from *Winter* (1987).
Simulated muscle activity estimated by the NMT method (dashed) compared to mean (thin solid) and standard deviation (shaded region) of EMG measurements from healthy subjects tabulated by *Winter* (1987).

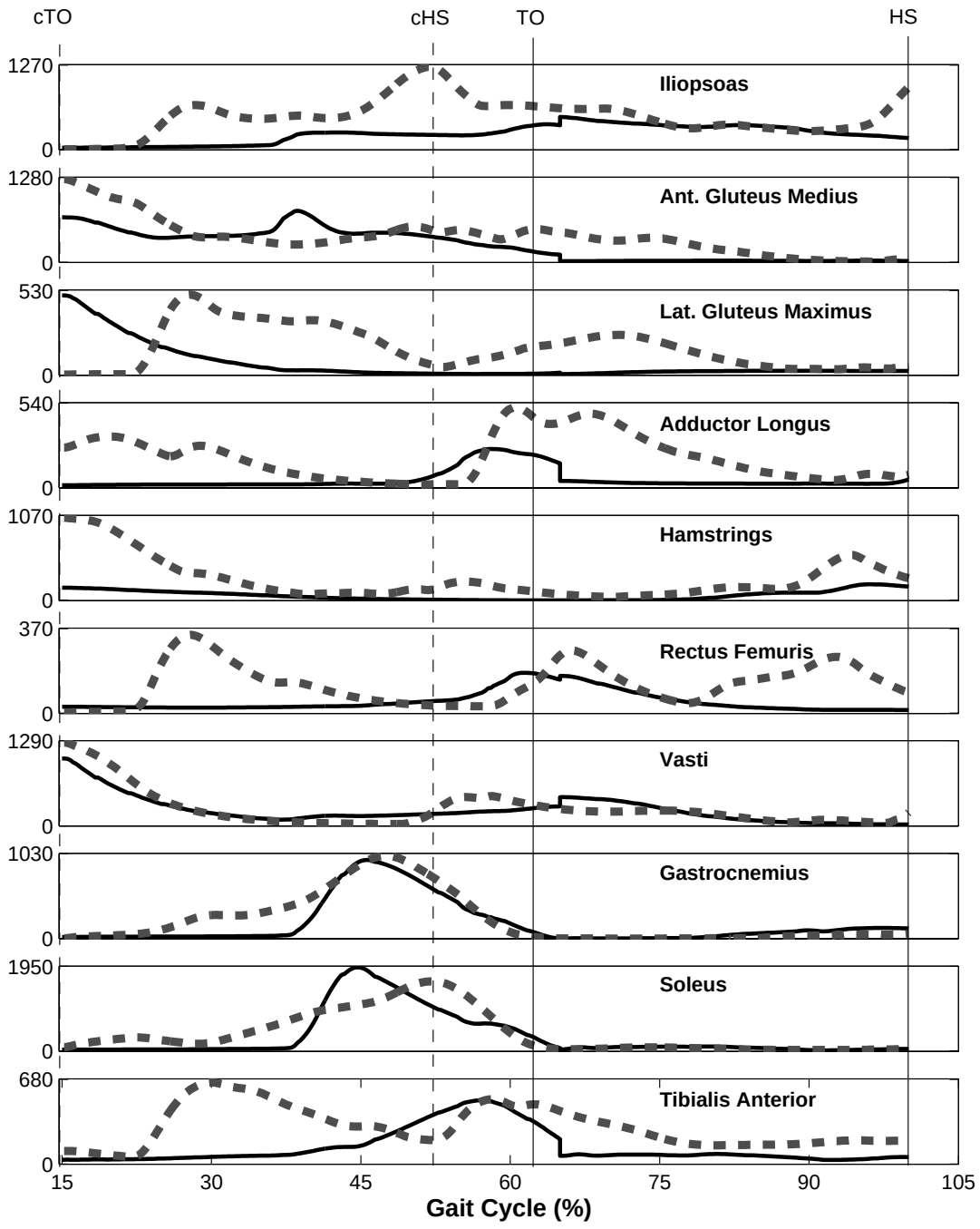

Figure 5.17: Model muscle forces versus those computed by *Anderson and Pandy* (2001a). Simulated muscle forces estimated by the NMT method (dashed) compared to mean (thin solid) compared to the muscle forces predicted by large scale parameter optimization approach by *Anderson and Pandy* (2001a).

femoris muscle forces also being larger than those predicted by LSPO.

5.4 Discussion

The objective of this study was to develop and apply a neuromusculoskeletal tracker to a state-of-the art musculoskeletal model in order to synthesize gait that replicated subject performance and to evaluate its feasibility as an analysis tool. The results clearly indicate that the NMT method is not only a viable approach but has significant advantages over earlier methodologies. The first major improvement is over optimization/forward dynamics methods in pure computing efficiency. Second, is improved simulation accuracy that is derived from the combination of kinematic marker tracking, ground force synthesis, and the evaluation of neuromuscular performance over the task period, which has not been demonstrated or is not possible with other tracking approaches. Thirdly, NMT provides a systematic approach to immediately test the accuracy of model parameters and dynamics directly against available experimental data.

It is important to stress that prior to this study only LSPO methods (*Anderson and Pandy* (2001a); *Neptune et al.* (2001); *Higginson et al.* (2006)) had been demonstrated to generate forward dynamics simulations of human gait that included both ground contact synthesis and a complete set of neuromuscular dynamics. Considering that the only three-dimensional forward dynamics simulation of gait yielding the control for more than two dozen individual lower extremity muscles (*Anderson and Pandy* (2001a), with virtually the same model) required over 10,000 CPU hours, the forward simulation generated by the NMT in about 5 minutes with superior accuracy especially in ground reaction forces is a major break through. The NMT approach represents a significant innovation in the state of the art of gait analysis and simulation capabilities for complex musculoskeletal models in general.

Although CMC (*Thelen and Anderson* (2006)) evaluates the torques necessary to satisfy the kinematics through a feedback corrected forward simulation, the ground contact forces are treated as external inputs irrespective of the actual kinematics of the model. Therefore, "perfect" ground forces

are applied to the model despite the kinematics of the feet, which is unrealistic. In the computation of individual muscle forces, CMC utilizes static optimization to decompose joint torques to allocate individual muscle activations, and is limited to instantaneous (time independent) performance indices. Both of these limitations are overcome by the NMT method.

It is also apparent that the NMT method demands better modeling in general. In particular, it forced us to revisit contact modeling and the results show, unequivocally, how a model can accurately generate ground reaction forces when that data is included in the tracking reference set. No other model or method has been able to produce as realistic ground contact profiles in all three directions. Not only are the forces very close to experiment (Fig. 5.10 compared to *Neptune et al.* (2001), excerpt Fig. 5.18) but so is the center-of-pressure location (Fig. 5.11), which provides additional reassurance that the model is accelerating in virtually the same manner as the human subject. This is critical for future studies of muscle function. In order to accurately ascertain what the role of individual muscles are during gait, it is critical that the same movement (i.e. acceleration of the center of mass) be observed in the model. It is difficult to have confidence in earlier studies of muscle function where models generated 40% (*Higginson et al.* (2006)) to 100% (*Neptune et al.* (2001, 2004)) greater ground reaction forces at heel-strike than the reference subject(s).

By tracking joint motion from an optimal inverse kinematics analysis plus raw marker positions and ground reaction forces simultaneously, the NMT method balances three goals that a control system must achieve in order to generate stable gait. First, limb segments must be coordinated such that they generate the locomotive pattern and these are described by the estimated joint angles from inverse kinematics. Second, it is insufficient that the legs move through some prescribed motion, if the system as a whole does not translate appropriately, in this regard tracking marker coordinates ensure that the desired global position of the system is being sought, as well as specific events, such as heel-strike occur in the correct place and time. Third, and perhaps most important, is that the system does not move in

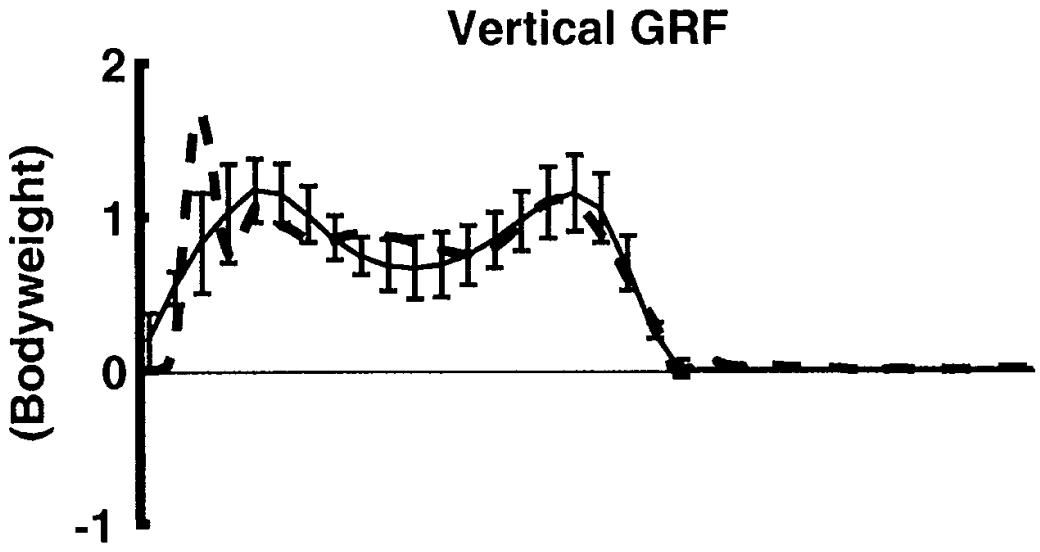

Figure 5.18: Vertical ground reaction force compared to experiment, presented by *Neptune et al.* (2001). Figure is an excerpt from *Neptune et al.* (2001). Simulated vertical ground reaction forces determined by a large scale parameter optimization to minimize differences between a forward dynamics simulation and experimental data. Results are compared to the mean of five subjects (solid) and +/- 2 SD (vertical bars) according to experiment.

isolation from its environment, and interactive forces support and accelerate the body so that movement of the center of mass can occur. Since the data provide considerable overlapping information, deviation from one reference (for example, back axial rotation) during simulation does not lead to divergent (unstable) behavior since other reference signals (like shoulder markers) can help to guide the overall behavior. This was found to be the case in earlier tracking attempts without marker position tracking, in particular, where relatively small deviations in joint angles combined to cause the model to fall over.

Because the NMT method requires the model to synthesize ground contact forces whilst tracking both experimental kinematics and ground reaction forces, simulation accuracy is ultimately limited by the accuracy of the model, since no residual forces or modification of the kinematic data is applied to enforce consistency with the model. Differences in model and human performance reflect differences in the model stemming from the distribution of mass, to rigid body, ideal joint assumptions and contact modeling. A methodology that produces simulated motion identical to experiment, given model/data assumptions and uncertainties, must in someway be compensating for differences. If a rigid model with ideal joints identically reproduces human behavior, does it mean the answers it provides are accurate? It depends on the degree of compensation/data manipulation that was required to achieve the similarity. Therefore, we believe that by not compensating for inherent differences, we can learn more about what is lacking or inaccurate in our model, allowing us to actively evolve the model. Unlike LSPO solutions, one can more readily ascertain that either the model is lacking in fidelity or detect errors in the processing of experimental data when the NMT fails to produce accurate results. Whereas with LSPO there are a host of potential culprits, such as: the optimization algorithm did not converge; the initial guess was not sufficiently accurate; and/or limitations/invalid assumptions in the model, etc ... which make it difficult to target specific model inaccuracies. By comparing the tracking solution for user and optimal weightings we have shown that the underlying differences of the simulations stem primarily from limitations of the model and that better weightings only help to further refine the simulation in a manner desirable to the user.

Weighted tracking is an innovation of the NMT method that improves simulation performance but also leads to the most significant difficulty of using the NMT method. Weightings enable us to favor some reference data or "channels" (i.e. ground forces over kinematics, individual markers, etc...) to leverage what the user deems more accurate data. Unfortunately, achieving the right balance of weightings becomes increasingly difficult with an increasing number of reference signals being tracked. For the tracking of gait, there were 37 independent weightings when right and left sides were weighted equally. In general, the tuning of weightings is straightforward and one can observe the consequence of weighting combinations in short order. Achieving a balance between the multiple criteria, however, can be a challenging and somewhat tedious task. Even so, it pales in comparison to the 810 initial control parameters (for a half gait cycle) that must be defined for the equivalent LSPO approach prior to running a computationally intensive optimization process.

Based on our analysis using a genetic algorithm combined with sequential quadratic programming to optimally "tune" weightings, the total increase in tracking precision does not warrant the greater computational cost and time required to perform the optimization. Especially since the increase in overall accuracy comes at the cost of increased errors in other features, such as back and pelvis extension angles in the current model.

The solutions from the NMT are not perfect and indeed there are some significant discrepancies in the kinematics that may cast doubt about the accuracy of results, the model and/or the efficacy of NMT method itself. In particular the angles associated with the pelvis ab/adduction and extension (Fig. 5.6) and to a greater extent the back extension and internal (axial) rotations, especially for optimal weightings (dotted lines, Fig. 5.7), are off the mark by the end of the cycle. Many attempts to correct the problem by adjusting weightings to highly penalize this error only lead to reduced accuracy of marker tracking and kinematics of the legs.

Examining the results more closely, one realizes that the model does not generate an initial

positive fore-aft reaction force at heel-strike of the contra-lateral leg (see fore-aft at cHS, Fig. 5.10) and, in fact, the model produces considerable negative forces, which means more braking occurs in the model than in the subject and so the center of mass of the model cannot translate as far forward as the subject for identical ground reaction forces beyond that point. The optimized weightings in minimizing the error of the overall joint and marker kinematics, consequently, over extends the back and pelvis which keeps the center of mass further back while the hips are kept forward to maximize the agreement of leg markers and continuing ground reaction forces. That is, the large back extension angles are a direct consequence of poor fore-aft force tracking at heel-strike. The model is unable to generate large enough aft velocity of the heel to elicit a positive reaction force and braking ensues immediately. Although the behavior of the model is not unrealistic, it does indicate some difficulty of the model to produce the adequate fore-aft force. Smaller but significant errors are also seen in the transition from braking (negative) to propulsion (positive) fore-aft force through mid-stance (at 30 and 90% of gait cycle, Fig. 5.10, fore-aft), with the transition occurring uniformly in the subject and more abruptly in the model. These errors can be due to inaccurate foot kinematics that cause the model to under estimate the heel velocity at contact and/or how rolling is realized in the contact model and perhaps its parameters. The parameters for the model were taken from *Wojtyra* (2003) who selected stiffness, damping, and friction parameters that agreed with earlier experiments, but these may differ with the subject and footwear, and so represent approximations of our subject. Nonetheless, for the majority of the cycle, the parameters appear to be adequate for ground force tracking, and so it is more likely that the treatment of rolling by the contact model requires additional attention. We can say with a high degree of certainty, given the quality of the tracking results, besides some difficulties of the model to produce the same fore-aft force, that the NMT methodology is not the source of discrepancy, especially since motion tracking recovers after points of transition. In fact, it is the use of the NMT method that is enabling us to make these inquiries about the cause of discrepancies that will lead to refinements to the model and to better represent test subjects in the future.

The accuracy of the ground reaction forces and the kinematics of the legs by the simulation implies that the actuation of the model is correct and, therefore, the net muscle moments are accurate. It is questionable to compare forward simulations to (or to track) joint powers computed from experiment using inverse dynamics methods (i.e. *Neptune et al.* (2001)) primarily because inverse dynamics relies heavily on error prone acceleration estimates, which was why one opts to use forward simulations to begin with. Second, joint velocities are also error prone, so the product of joint moments from inverse dynamics and estimated velocities acts to amplify noise. Therefore, tracking joint powers would have the effect of reducing the accuracy of the tracking simulation.

The accuracy of muscle moments is therefore established by the model's ability to track ground reaction forces and joint angles closely and not its similarity with inverse dynamics results. It was somewhat surprising to see how closely the torques from inverse dynamics resembled the NMT generated torques, particularly of the hip, knee and ankle in the sagittal plane (Figs. 5.13 and 5.14). The differences in back and non-sagittal plane forces, we believe, are attributed to the dynamical constraints in NMT to synthesize ground-reaction-force and center-of pressure outputs that match the experimental data. In this regard HAT motion, ankle-inversion and metatarsal flexion have a significant influence due to the concentration of mass in the HAT and the direct ground contact of the foot and toes. We do not believe the similarity with inverse dynamics strengthens the case for the accuracy of the net joint moments, although it maybe reassuring to some readers.

The accuracy of muscle forces then rests on how realistically the moments are synthesized and contributed to by the individual muscles. For the stronger muscles of the lower extremity the modeled muscle activity does in fact closely resemble the physiological activity of the muscles indicated by both the EMG of the subject (Fig. 5.15) and a normal group according to *Winter* (1987) (Fig. 5.16). In particular, the muscles that have been identified by earlier studies (*Neptune et al.* (2001); *Anderson and Pandy* (2003); *Jonkers et al.* (2003)) to play key roles in the support and forward propulsion of the

body, namely: soleus, gastrocnemius, vasti, hamstrings, gluteus medius (in 3D) and erector spinae have very good agreement with the EMG data. Soleus, gastrocnemius, and vasti correspond well in force magnitude and timing to the predictions by *Anderson and Pandy* (2001a) (Fig. 5.17). The broader and more gradual increase in gastrocnemius and soleus force generated by NMT, however, is in better agreement with the EMG data of the subject and Winter's normal group. Large discrepancies in force are seen for muscles involved with the trunk, such as iliopsoas and erector spinae as well as the biarticular muscles acting at the hip and knee. In this regard, we believe the NMT is more accurate due to the better agreement with EMG data (e.g. erector spinae, Fig. 5.16). However, we also believe the NMT solution is exhibiting higher activity of trunk muscles as a response to impact and transition errors in contact (see cHS to TO in extension and lateral bending torques, Fig. 5.12).

In summary, the NMT method provides a new approach to musculoskeletal simulation that effectively exploits information contained in experimental data. In gait and other locomotor tasks (i.e. running, jumping, etc...), where ground reaction forces are responsible for moving the body, NMT is particularly powerful in synthesizing those reaction forces according to contact dynamics. More accurate force-plate and certain marker data can also be weighted more heavily when that data is known to be more reliable. The result is a computationally efficient method for the forward simulation of complex musculoskeletal models that yields the activity and forces of individual muscles in a matter of minutes, without excluding complex aspects of ground contact or neuromuscular dynamics. Because all model dynamics are included, the NMT is well suited for validating the musculoskeletal model as a whole. As was the case in the current study, the NMT method required improvements to the contact model in order for tracking to work. In hindsight, the shortcomings of the original contact model seem obvious, but without having a simulation environment to test cause and effect directly, those issues would not have come to our attention as readily. Therefore, the NMT method may make its most immediate and significant contribution as a validation tool in the pursuit of neuromusculoskeletal models of higher fidelity.

Chapter 6

Conclusions and Future Directions

6.1 Conclusions

We have successsfully developed and demonstrated a new Neuromuscular Tracking (NMT) method for generating forward dynamics simulations of human gait that is more representative of individual subject performance than previous techniques. The NMT successfully satisfied the full dynamics of the musculoskeletal system including contact synthesis, which has been ignored by other tracking methodologies. Furthermore, individual muscle forces were computed dynamically with a savings of at least 3 orders of magnitude in computational costs over a large-scale parameter optimization (LSPO) approach. Muscle forces for human gait were computed in 5 min using NMT, which is 4 orders of magnitude less processing time on a desktop PC than the similar LSPO solution on a 32 processor supercomputer (*Anderson and Pandy* (2001a)). Unlike the LSPO approach, NMT also does not require an initial guess of the controls, which is another important time saving advantage.

As expected perfect tracking was not achieved, however, NMT itself proved to be an excellent validation tool, which demanded modifications to the model in order to more closely match its human counterpart. For example, contact modeling was revisited several times, initially to enable unfettered lift-off in jumping and then later to allow the model to produce similar ground reaction forces as observed during gait. Unlike earlier tracking approaches, the NMT is the only method that enables the model to dynamically compromise between ground reaction forces and kinematics that includes experimental marker coordinates during tracking. Accordingly, experimental data is leveraged to its fullest extent. In human locomotor tasks, where ground reaction forces are responsible for the global translation of the body as a whole, synthesis and close replication of ground reaction forces is essential for the validity

of all forces in the model, including muscle forces. In fact, the benchmark study, analyzing noise contaminated model kinematics, showed that perfect tracking of "experimental" kinematics alone does not mean an accurate representation of the actual motion was achieved. This is because noise and processing errors inherent in the kinematic data significantly impair acceleration estimates. Since joint kinematics are determined from markers coordinates, it makes greater sense to compare simulation accuracy directly against those measurements. The NMT takes this seriously and therefore includes marker tracking directly, which no forward dynamics method has addressed before. Since ground reaction forces are more accurate measurements, they should be leveraged to improve model behavior, which is precisely what the NMT method allows. It is critical that the ground reaction forces be reproduced in any model/simulation that is supposed to represent human locomotor performance. It is unclear how models that do not accurately reproduce experimental ground reaction forces can produce similar joint kinematics and translation of the center of mass.

As models become more complex in order to better represent human performance and individual subjects, the NMT method is well suited to provide correspondingly more accurate simulations in a timely fashion. This is unlike LSPO where additional muscles directly increase the size of the optimization problem and the computing resources required increase in proportion to the exponent of the number of unknowns. In contrast, the computation time of the NMT method is only related to the integration of system and controller dynamics, which increases predominantly in proportion to the square of the number of states in the linearized neuromuscular system (i.e. dimension of the Ricatti matrix equation). Therefore, the relative computational savings will increase with the number of muscles being controlled.

Another important advantage is that the NMT method can continue to produce movement patterns as long as the corresponding experimental data is available. Therefore, asymmetries or gait anomalies associated with a disorder can be observed, tracked and simulated over multiple cycles (as long as there are force-plates) to more accurately capture the dynamics of the disorder that may not be

apparent in a single stride. Parameter optimizations require increasing the number of unknowns as the performance period increases, whereas the weightings for the NMT method are applicable for all time.

Although the primary interest of the author is to study human performance in hopes to treat and/or assist those suffering from mobility disorders, this treatise deals heavily with the methodological details required to model and simulate human gait. The reason for this is that the methods and models available to date have not sufficiently demonstrated their ability to represent human gait or, if they have, the time required to produce this behavior has been intractable. Therefore, applying these methods would be either inaccurate or impractical for understanding muscle function and considering treatments in a clinical setting. As an engineer, it is important for me to see that the models and tools used to understand human performance not only accurately reflect human behavior in general but can represent the performance of the individual subject/patient according to all experimental measurements that are available for clinical assessment. In this regard, Neuromusculoskeletal Tracking begins to establish a framework for directly comparing model and human performance on practical timescale. This has been a long over due first step in establishing confidence in musculoskeletal models in the analysis of human performance.

6.2 Limitations

The most significant limitation of the NMT method is its reliance on experimental data in order to generate realistic simulations. As a tracker, the NMT method has limited predictive power compared to solving the optimal control problem based purely on a task based performance index. As a consequence, the quality of the NMT simulation is highly dependent on the quality of the experimental data being tracked. For this reason, higher quality/accuracy data such as force-plate recordings and specific marker positions are recommended as tracking references opposed to relying solely on inverse kinematics analyses.

The greatest difficulty of apply the NMT approach is in selecting motion-tracking weightings that

meet the multiple objectives of the task of tracking many joint angles, marker positions, ground reaction forces and center of pressure coordinates, which can be overwhelming. Although it has advantages over the non-weighted (i.e. uniform weighting) approach in terms of tracking reliable references more closely, it can lead to exceedingly poor tracking of lower weighted signals that ultimately lead to errors in all model outputs, and therefore, obtaining a good overall solution becomes a kind of balancing act. For example, metatarsal flexion is difficult to measure with accuracy because of the proximity of the markers on the toes and feet. Therefore, lowering the relative weighting on toes is practical compared to knee extension, for example. But as metatarsal flexion is weighted less, the satisfaction of toe marker kinematics and center-of-pressure increase their influence over the metatarsal joint, and if center-of-pressure is dominant over marker error, the model will flex and extend the joint in any way it can to affect the tracking of the center-of-pressure. This leads to "curling" of the toes to move the center-of-pressure forward during mid-stance and improves center-of-pressure tracking initially but more adversely affects the ankle and knee and ultimately the total accuracy is diminished as the simulation continues. Applying optimization is a systematic approach to find a set weightings that minimize the overall error, but it may have some unfavorable trade-offs. In tracking gait, for example, larger errors in back and pelvis kinematics were obtained in order to reduce the total error by tightening the tracking performance of the legs. It is important to note that while finding an appropriate set of weightings (i.e. 37 values) might be tedious, when compared to the alternative of finding the individual muscle control nodes (i.e., 54 x 15 = 810) as parameters, selecting weightings still remains a much smaller problem than finding viable initial conditions for the LSPO or direct collocation approaches.

The success of NMT as a control scheme depends on whether the desired state is reachable from the current state (the position and velocity of the joints). Control is determined by an instantaneous linear approximation of the system via feedback linearization (FBL). Therefore, if the model and experimental states deviate from one another, then the FBL approximation of the system becomes less valid and control is effectively lost. Consequently, the NMT is highly sensitive to initial conditions and the

ability of the model to achieve all the configurations (states with specific outputs, such as registering body weight in the contact model during quiet standing) described by the experimental data. At present, the NMT method does not control to avoid instability in the model and, in fact, if a desired state is in an unstable region, NMT will follow it "over a cliff" at which point no amount of control can correct the model. Consequently, another limitation of the NMT approach, and of most gait simulation approaches in general, is the lack stability control.

6.3 Future Directions

In the future there are several issues that should be addressed to improve tracking performance in general and gait simulations in particular. First, by far the most difficult aspect of tracking has been the synthesis and tracking of ground reaction forces and center-of-pressure coordinates with a continuous tracker when the tracking reference contains discontinuities. Attempts were made to limit the detrimental effects of discontinuities, such as those in center-of-pressure, on tracking performance. Unfortunately, as was observed during the tracking of gait, the inability of the model/controller to track closely through transition regions results in errors in contact forces, particularly in the fore-aft direction, which affected the acceleration of the center of mass and therefore the kinematic performance of the model as a whole. Therefore, it is imperative that contact models that capture some of the geometric aspects (i.e. contours) of the sole be explored. Models should be tested with known kinematics as inputs and compared with measured outputs using a tracking approach. Such a detailed analysis is vital not only to obtain a valid model of contact, but will be necessary to establish a protocol to determine the parameters of the contact model to best match the experimental/subject data we wish to replicate with the model.

Second, it is possible to integrate both stages of the NMT method simultaneously, feeding muscle forces/torques from the neuromuscular stage directly into the skeletal-motion stage. This is straightforward to implement without an optimal LQT for the neuromuscular system, however if minimum effort

(or any other time dependent objective) is required, then a method that combines optimal control (i.e. from an LQT) and error feedback must be developed. In this way the tracker behaves like a virtual "cerebellum" to the model by comparing a desired motor plan from experimental data and the optimal LQT output (i.e. optimal/desired response) against the actual torques and motion generated by the model.

Related to the complete integrated muscle control, is the important issue of balance/stability control in gait. Stability control can be introduced as an additional feedback term (like marker positions) that describes the position and velocity of the center of mass with respect to the outline (perimeter) of the base of support defined by the boundaries of the feet and how that support perimeter is moving in time. Accordingly, tracker weightings (for this reference) are scaled up as the center of mass approaches or passes the perimeter. In this case, the tracking reference can be the horizontal plane coordinates of the pelvis, such that it tries to move the center-of-mass directly over the pelvis. It may prove very enlightening to see how robust this relatively simple control scheme could be at keeping the model upright in tracking many continuous cycles of gait.

Ultimately, we hope to give rise to a framework for studying neuromotor control at the system level that encourages the inclusion of physiologically based feedback mechanisms such as the muscle spindle and the Golgi tendon apparatus as observers of model internal states and outputs instead of the ideal case of direct feedback of all model states and outputs. In this context tracker weightings may evolve to have a more physiological interpretation relating to neural weightings assigned to the many efferent (feedback) and, possibly, afferent (neural drive) neuromotor pathways. This would provide a way to test sensorimotor deficiencies, thought to be the cause of many movement disorders, directly upon a model in order to understand the effect of specific deficiencies as well as explore ideas/mechanisms for compensating for those deficiencies.

Bibliography

Anderson, F. C., A dynamic optimization solution for a complete cycle of gait, Phd, University of Texas at Austin, Austin, TX, 1999.

Anderson, F. C., and M. G. Pandy, Storage and utilization of elastic strain energy during jumping, *Journal of Biomechanics*, *26*, 1413–1427, 1993.

Anderson, F. C., and M. G. Pandy, A dynamic optimization solution for vertical jumping in three dimensions, *Computer Methods in Biomechanics and Biomedical Engineering*, *2*, 201–231, 1999.

Anderson, F. C., and M. G. Pandy, Dynamic optimization of human walking, *Journal of Biomechanical Engineering*, *123*, 381–90, 2001a.

Anderson, F. C., and M. G. Pandy, Static and dynamic optimization solutions are practically equivalent, *Journal of Biomechanics*, *34*, 153–61, 2001b.

Anderson, F. C., and M. G. Pandy, Individual muscle contributions to support in normal walking, *Gait and Posture*, *17*, 159–69, 2003.

Benoit, D. L., D. K. Ramsey, M. Lamontagne, L. Xu, P. Wretenberg, and P. Renstro¨m, Effect of skin movement artifact on knee kinematics during gait and cutting motions measured in vivo, *Gait and Posture*, *24*, 152–164, 2006.

Bobbert, M. F., and G. J. van Ingen-Schenau, Coordination in vertical jumping, *Journal of Biomechanics*, *21*, 249–262, 1988.

Bobrow, J. E., S. Dubowsky, and J. Gibson, Time-optimal control of robotic manipulators along a specified path, *International Journal of Robotics Research*, *4*, 3–17, 1985.

Bresler, B., and J. P. Frankel, The forces and moments in the leg during level walking, *Transactions of the ASME*, pp. 27–36, 1950.

Bryson, A. E., and Y.-C. Ho, *Applied Optimal Control*, Ginn and Company, Waltham, Massachusetts, 1969.

Buchanan, T. S., D. G. Lloyd, K. Manal, and T. F. Besier, Neuromusculoskeletal modeling: estimation of muscle forces and joint moments and movements from measurements of neural command, *Journal of Applied Biomechanics*, *20*, 367–395, 2004.

Buchanan, T. S., D. G. Lloyd, K. Manal, and T. F. Besier, Estimation of muscle forces using a forward-inverse dynamics model, *Medicine and Science in Sports and Exercise*, *37*, 1911–1916, 2005.

Cahouet, V., M. Luc, and A. David, Static optimal estimation of joint accelerations for inverse dynamics problem solution, *Journal of Biomechanics*, *35*, 1507–1513, 2002.

Cholewicki, J., S. M. McGill, and R. W. Norman, Comparison of muscles forces and joint load from an optimization and emg assited lumbar spine model: Towards development of a hybrid approach, *Journal of Biomechanics*, *28*, 321–331, 1995.

Chow, C. K., and D. H. Jacobson, Studies of human locomotion via optimal programming, *Mathematical Biosciences*, *10*, 239–306, 1971.

Cook, R. E., I. Schneider, M. E. Hazlewood, S. J. Hillman, and J. E. Robb, Gait analysis alters decision-making in cerebral palsy., *J Pediatr Orthop.*, *23*, 292–5, 2003.

Crispin, J. C., and J. Alcocer-Varela, Rheumatologic manifestations of diabetes mellitus, *The American Journal of Medicine*, *114*, 753–7, 2003.

Croce, U. D., P. O. Riley, J. L. Lelas, and D. C. Kerrigan, A refined view of the determinants of gait, *Gait and Posture*, *14*, 79–84, 2001.

Crowninshield, R. D., and R. A. Brand, A physiologically based criterion of muscle force prediction in locomotion, *Journal of Biomechanics*, *14*, 793–801, 1981.

Davy, D. T., and M. L. Audu, A dynamic optimization technique for predicting muscle forces in the swing phase of gait, *Journal of Biomechanics*, *20*, 187–201, 1987.

Delp, S. L., Surgery simulation: A computer graphics system to analyze and design musculoskeletal reconstructions of the lower limb, Ph.d. thesis, Stanford University, Stanford, CA, 1990.

Delp, S. L., and J. P. Loan, A graphics-based software system to develop and analyze models of musculoskeletal structures, *Journal of Biomechanics*, *25*, 21–34, 1995.

Duchene, J., and F. Goubel, Surface electromyogram during voluntary contraction: processing tools and relation to physiological events., *Critical reviews in biomedical engineering*, *21*, 313–397, 1993.

Elftman, H., The function of muscles in locomotion, *American Journal of Physiology*, *125*, 357–366, 1939.

Erdemir, A., S. McLean, W. Herzog, and A. J. van den Bogert, Model-based estimation of muscle forces exerted during movements, *Clinical Biomechanics*, p. in press, 2006.

Favre, P., R. Sheikh, S. F. Fucentese, and H. A. Jacob, An algorithm for estimation of shoulder muscle forces for clinical use, *Clinical Biomechanics*, *20*, 822–833, 2005.

Freeman, M., and V. Pinskerova, The movement of the normal tibio-femoral joint, *Journal of Biomechanics*, *38*, 197–208, 2005.

Gard, S. A., and D. S. Childress, The effect of pelvic list on the vertical displacement of the trunk during normal walking, *Gait and Posture*, *5*, 233–8, 1997.

Gilchrist, L. A., and D. A. Winter, A two-part, viscoelastic foot model for use in gait simulations, *Journal of Biomechanics*, *29*, 795–798, 1996.

Glantz, S. A., A three-element description for muscle with viscoelastic passive elements, *Journal of Biomechanics*, *10*, 5–20, 1977.

Goh, C. J., and K. L. Teo, Control parameterization: a unified approach to optimal control problems with general constraints, *Automatica*, *24*, 3–18, 1988.

Granata, K. P., P. E. Lee, and T. C. Franklin, Co-contraction recruitment and spinal load during isometric trunk flexion and extension, *Clinical Biomechanics*, *20*, 1029–1037, 2005.

G.Rau, E.Schulte, and C.Disselhorst-Klug, From cell to movement: to what answers does emg really contribute?, *Journal of Electromyography and Kinesiology*, *14*, 611–617, 2004.

Hatze, H., A myocybernetic control model of skeletal muscle, *Biological Cybernetics*, *25*, 103–119, 1977.

Heintz, S., and E. M. Gutierrez-Farewik, Static optimization of muscle forces during gait in comparison to previous emg-to-force processing approach, *Gait and Posture*, p. in press, 2006.

Heller, M. O., G. Bergmann, G. Deuretzbacher, L. Dorselen, M. Pohl, L. Claes, N. P. Haas, and G. N. Duda, Musculo-skeletal loading conditions at the hip during walking and stair climbing, *Journal of Biomechanics*, *34*, 883–893, 2001.

Higginson, J., F. Zajac, R. Neptune, S. Kautz, and S. Delp, Muscle contributions to support during gait in an individual with post-stroke hemiparesis, *Journal of Biomechanics*, *39*, 1769–1777, 2006.

Hill, A. V., The heat of shortening and the dynamic constants of muscle, in *Proceedings of the Royal Society of Biology*, vol. 126, pp. 136–195, 1938.

Hof, A. L., An explicit expression for the moment in multibody systems, *Journal of Biomechanics*, *25*, 1209–1211, 1992.

Holland, J. H., *Adapatation in Natural and Artificial Systems*, MIT Press, 1992.

Huang, Q.-H., Y.-P. Zheng, R. Li, and M.-H. Lu, 3-d measurement of body tissues based on ultrasound images with 3-d spatial information, *Ultrasound in Medicine and Biology*, *31*, 1607–1615, 2005.

Ingber, L., Simulated annealing: Practice versus theory, *Mathematical and Computer Modelling*, *18*, 29–57, 1993.

injury report forms, W., Web-based injury statistics query and reporting system (wisqars), *web-report*, National Center for Injury Prevention and Control, 2000, http://www.cdc.gov/ncipc/default.htm.

Jonkers, I., A. Spaepen, G. Papaioannou, and C. Stewart, An emg-based, muscle driven forward simulation of single support phase of gait, *Journal of Biomechanics*, *35*, 609–19, 2002.

Jonkers, I., C. Stewart, and A. Spaepen, The study of muscle action during single support and swing phase of gait: clinical relevance of forward simulation techniques, *Gait and Posture*, *17*, 97–105, 2003.

Kaplan, M. L., and J. H. Heegard, Predictive algorithms for neuromuscular control of human locomotion, *Journal of Biomechanics*, *34*, 1077–83, 2001.

Kepple, T. M., K. L. Siegel, and S. J. Stanhope, Relative contributions of the lower extremity joint moments to forward progression and support during gait, *Gait and Posture*, *6*, 1–8, 1997.

Kerrigan, D. C., Aesthetics of walking, *Journal of Rehabilitation Research and Development*, *38*, 9–10, 2001.

Kuo, A. D., A least-squares estimation approach to improving the precision of inverse dynamics computations, *Journal of Biomechanical Engineering*, *120*, 148–159, 1998.

Lee, G., and F. E. Pollo, Technology overview: The gait analysis laboratory, *Journal of Clinical Engineering*, *Spring*, 2001.

Lewis, F. L., and V. L. Symros, *Optimal Control*, 2 ed., John Wiley & Sons, Inc., New York, 1995.

Lloyd, D. G., and T. F. Besier, An emg-driven musculoskeletal model to estimate muscle forces and knee joint moments in vivo, *Journal of Biomechanics*, *36*, 765–776, 2003.

McConville, J. T., C. E. Clauser, T. D. Churchill, J. Cuzzi, and I. Kaleps, Anthropometric relationships of body and body segment moments of inertia, *Tech. rep.*, Wright-Patterson AFB, Air Force Aerospace Medical Research Laboratory, Ohio, 1980.

McGill, S., D. Juker, and P. Kropf, Appropriately placed surface emg electrodes reflect deep muscle activity (psoas, quadratus lumborum, abdominal wall) in the lumbar spine, *Journal of Biomechanics*, *29*, 1503–1507, 1996.

Menegaldo, L. L., A. de Toledo Fleury, and H. I. Weber, A 'cheap' optimal control approach to estimate muscle forces in musculoskeletal systems, *Journal of Biomechanics*, *39*, 1787–1795, 2006.

Neptune, R. R., S. A. Kautz, and F. E. Zajac, Contributions of the individual ankle plantar flexors to support, forward progression and swing initiation during walking, *Journal of Biomechanics*, *34*, 1387–98, 2001.

Neptune, R. R., F. E. Zajac, and S. A. Kautz, Muscle force redistributes segmental power for body progression during walking, *Gait and Posture*, *19*, 194–205, 2004.

Olney, S. J., and D. A. Winter, Predictions of knee and ankle moments from emg and kinematic data, *Journal of Biomechanics*, *18*, 9–20, 1985.

Osborne, J. R., W. P. Abraham, and M. D. Forte, Magnetic resonance imaging of knee menisci: diagnostic interpretation and pitfalls, *Operative Techniques in Orthopaedics*, *5*, 10–19, 1995.

Pandy, M. G., Computer modeling and simulation of human movement, *Annual Review of Biomedical Engineering*, *3*, 245–273, 2001.

Pandy, M. G., Simple and complex models for studying muscle function in walking, *Philosophical transactions of the Royal Society of London. B*, *358*, 1501–1509, 2003.

Pandy, M. G., and N. Berme, Synthesis of human walking: a planar model for single support, *Journal of Biomechanics*, *21*, 1053–1060, 1988a.

Pandy, M. G., and N. Berme, A numerical method for simulating the dynamics of human walking, *Journal of Biomechanics*, *21*, 1043–1051, 1988b.

Pandy, M. G., F. E. Zajac, E. Sim, and W. S. Levine, An optimal control model for maximum-height human jumping, *Journal of Biomechanics*, *23*, 1185–1198, 1990.

Pandy, M. G., F. C. Anderson, and D. G. Hull, A parameter optimization approach for the optimal control of large-scale musculoskeletal systems, *ASME Journal of Biomechanical Engineering*, *114*, 343–363, 1992.

Pandy, M. G., B. A. Garner, and F. C. Anderson, Optimal control of non-ballistic muscular movements: A constraint-based performance criterion for rising from a chair, *Journal of Biomechanical Engineering*, *117*, 16–26, 1995.

Patla, A. E., B. S. Hudgins, P. A. Parker, and R. N. Scott, Myolectric signal as a quantitative measure of muscle mechanical output, *Medical and Biological Engineering and Computing*, *20*, 319–328, 1982.

Pedotti, A., V. V. Krishnan, and L. Stark, Optimization of muscle-force sequencing in human locomotion, *Mathematical Biosciences*, *38*, 57–76, 1978.

Penrod, D. D., D. T. Davy, and D. P. Singh, An optimization approach to tendon force analysis, *Journal of Biomechanics*, *7*, 123–129, 1974.

Powell, M. J. D., Algorithms for functions that use lagrangian functions, *Math. Prog.*, *14*, 224–248, 1978.

Reinbolt, J. A., J. F. Schutte, B. J. Fregly, B. I. Koh, R. T. Haftka, A. D. George, and K. H. Mitchell, Determination of patient-specific multi-joint kinematic models through two-level optimization, *Journal of Biomechanics*, *38*, 621–626, 2005.

Riener, R., J. Quintern, , and G. Schmidt, Biomechanical model of the human knee evaluated by neuromuscular stimulation, *Journal of Biomechanics*, *29*, 1157–1167, 1996.

Risher, D. W., L. M. Shutte, and C. F. Runge, The use of inverse dynamics solutions in direct dynamics simulations, *Journal of Biomechanical Engineering*, *119*, 417–422, 1997.

Runge, C. F., F. E. Zajac, J. H. J. Allum, D. W. Risher, A. E. Bryson, and F. Honegger, Estimating net joint torques from kinesiological data using optimal linear system theory, *IEEE Transactions on Biomedical Engineering*, *42*, 1158–1164, 1995.

Sangeux, M., F. Marin, F. Charleux, L. Du¨rselen, and M. H. B. Tho, Quantification of the 3d relative movement of external marker sets vs. bones based on magnetic resonance imaging, *Clinical Biomechanics*, *21*, 984–991, 2006.

Saunders, J. B., V. T. Inman, and H. D. Eberhart, The major determinants in normal and pathological gait, *Journal of Bone and Joint Surgery*, *35A*, 543–558, 1953.

Seth, A., A predictive control method for human upper-limb motion: Graph-theoretic modelling, dynamic optimization, and experimental investigations, Master's thesis, Uinversity of Waterloo, Waterloo, Ontario, Canada, 2000.

Seth, A., J. J. McPhee, and M. G. Pandy, Multi-joint coordination of vertical arm movement, *Journal of Applied Bionics and Biomechanics*, *1*, 45–56, 2003.

Slotine, J.-J., and W. Li, *Applied Nonlinear Control*, Prentice-Hall, Inc., New Jersey, 1991, basis for the ideas of non-linear optimal tracker using the feedback linearization technique.

Spong, M. W., and M. Vidyasagar, *Robot Dynamics and Control*, John Wiley & Sons, Toronto, 1989.

Spoor, C. W., J. L. van Leeuwen, C. G. M. Meskers, A. F. Titulaer, and A. Huson, Estimation of instantaneous moment arms of lower-leg muscles, *Journal of Biomechanics*, *23*, 1247–1259, 1990.

Srinivas, M., and L. M. Patnaik, Genetic algorithms: A survey, *Computer*, pp. 17–26, 1994.

Stalenhoef, P. A., J. P. M. Diederiks, J. Knottnerus, A. D. M. Kester, and H. F. J. M. Crebolder, A risk model for the prediction of recurrent falls in community-dwelling elderly: A prospective cohort study, *Journal of Clinical Epidemiology*, *55*, 1088–94, 2002.

Staudenmann, D., J. R. Potvin, I. Kingma, D. F. Stegeman, and J. H. van Dieën, Effects of emg processing on biomechanical models of muscle joint systems: Sensitivity of trunk muscle moments, spinal forces, and stability, *Journal of Biomechanics*, p. in press, 2006.

Storen, S., and T. Hertzberg, The sequential linear quadratic programming algorithm for solving dynamic optimization problems - a review., *Computers and Chemical Engineering*, *19*, S495–S500, 1995.

Taga, G., A model of neuro-musculo-skeletal system for human locomotion, *Biological Cybernetics*, *73*, 97–111, 1995.

Thelen, D. G., and F. C. Anderson, Using computed muscle control to generate forward dynamic simulations of human walking from experimental data, *Journal of Biomechanics*, *39*, 1107–1115, 2006.

Thelen, D. G., F. C. Anderson, and S. L. Delp, Generating dynamic simulations of movement using computed muscle control, *Journal of Biomechanics*, *36*, 321–328, 2003.

Thornton-Trump, A. B., and R. Daher, The prediction of reaction forces from gait data, *Journal of Biomechanics*, *8*, 173–178, 1975.

Townsend, M. A., and A. Seireg, The synthesis of bipedal locomotion, *Journal of Biomechanics*, *5*, 71–83, 1972.

van Drongelen, S., L. van der Woude, T. Janssen, E. Angenot, E. Chadwick, and H. Veeger, Glenohumeral joint loading in tetraplegia during weight relief lifting: A simulation study, *Clinical Biomechanics*, *21*, 128–137, 2006.

van Soest, A. J., A. L. Schwab, M. F. Bobbert, and G. J. van Ingen Schenau, The influence of the biarticularity of the gastrocnemius muscle on vertical-jumping performance, *Journal of Biomechanics*, *26*, 1–8, 1993.

van Soest, A. J. K., and L. J. R. R. Casius, The merits of a parallel genetic algorithm in solving hard optimization problems, *Journal of Biomechanical Engineering*, *125*, 141–46, 2003.

Watelain, E., J. Froger, F. Barbier, G. Lensel, M. Rousseaux, F. X. Lepoutre, and T. A., Comparison of clinical gait analysis strategies by french neurologists, physiatrists and physiotherapists., *J Rehabil Med.*, *35*, 8–14, 2003.

Waters, R. L., and S. Mulroy, The energy expenditure of normal and pathological gait, *Gait and Posture*, *9*, 207–231, 1999.

White, S. C., and D. A. Winter, Predicting muscle forces in gait from emg signals and musculotendon kinematics, *Journal of Electromyography and Kinesiology*, *4*, 217–231, 1993.

Winter, D. A., *The Biomechanics and Motor Control of Human Gait*, University of Waterloo Press, Waterloo, Canada, 1987.

Winter, D. A., *Biomechanics and Motor Control of Human Movement. Wiley, New York, NY.*, Wiley, New York, NY, 1990.

Winters, J. M., Hill-based muscle models: a systems engineering perspective, in *Multiple Muscle Systems: Biomechanics and Movement Organization*, edited by J. M. Winters and S.-Y. Woo, chap. 5, Springer-Verlag, 1990.

Winters, J. M., and L. Stark, Muscle models: what is gained and what is lost by varying model complexity, *Biological Cybernetics*, *55*, 403–420, 1987.

Wojtyra, M., Multibody simulation of human walking, *Mechanics Based Design of Structures and Machines*, *31*, 357–379, 2003.

Yamaguchi, G. T., Performing whole-body simulations of gait with 3-d, dynamic musculoskeletal models, in *Multiple Muscle Systems: Biomechanics and Movement Organization*, edited by J. M. Winters and S.-Y. Woo, chap. 43, Springer-Verlag, 1990.

Yamaguchi, G. T., D. W. Moran, and J. Si, A computationally efficient method for solving the redundant problem in biomechanics, *Journal of Biomechanics*, *28*, 999–1005, 1995.

Zajac, F. E., Muscle and tendon: properties, models, scaling, and application to biomechanics and motor control, *Critical Reviews in Biomedical Engineering*, *17*, 359–411, 1989.

Zajac, F. E., and M. E. Gordon, Determining muscle's force and action in multi-articular movement, *Exrercise Sport Science Review*, *17*, 187–230, 1989.

Zajac, F. E., R. R. Neptune, and S. A. Kautz, Biomechanics and muscle coordination of human walking. part i: introduction to concepts, power transfer, dynamics and simulations, *Gait and Posture*, *16*, 215–32, 2002.

Zajac, F. E., R. R. Neptune, and S. A. Kautz, Biomechanics and muscle coordination of human walking. part ii: lessons from dynamical simulations and clinical implications, *Gait and Posture*, *17*, 1–17, 2003.

Zajac, F. E., R. R. Neptune, and S. A. Kautz, Authors' response to "comments on 'biomechanics and muscle coordination of human walking: parts i and ii'", *Gait and Posture*, *19*, 208–209, 2004.

Zhang, L.-Q., G. Nuber, J. Butler, M. Bowen, and W. Z. Rymer, In vivo human knee joint dynamic properties as functions of muscle contraction and joint position, *Journal of Biomechanics*, *31*, 71–76, 1998.

VITA

Ajay Seth was born in Montreal, Quebec, Canada on July 5, 1973. Ajay entered Centennial High School in Greenfield Park, Quebec, in 1985 and completed his secondary education at Marianopolis College, Montreal, in 1992. Ajay entered the University of Waterloo in Fall 1992 and graduated with an Honors Bachelor of Applied Science degree in Systems Design Engineering in May 1997, after completing the cooperative engineering program that combined eight academic semesters with six work terms in industry. During this time, Ajay worked for a diverse range of industries from small start-up companies, such as Visible Genetics Inc. in Toronto, to large multi-national engineering companies, like CAE Electronics in Montreal, as well as government agencies having spent two work terms at the Canadian Space Agency.

Ajay began his graduate education in Systems Design Engineering at the University of Waterloo, under the supervision of professors John McPhee and Richard Wells (Kinesiology) in Fall 1997. Here he explored methods of predicting muscle function in the human upper extremity using a computational model and earned his Master of Applied Science degree in Spring 2000. In February that year Ajay had joined Visible Genetics Inc., Toronto, as a full-time software/algorithms developer. In 2002, Ajay entered the PhD program in the Department of Biomedical Engineering at the University of Texas at Austin to pursue research in computational biomechanics under the guidance of professor Marcus Pandy.

Permanent Address:

Ajay Seth, 8 University Circle, St. Catharines, Ontario, Canada. H2H 4B4

This dissertation was typed by the author using LyX – a freely available GUI for LaTeX.